

Electronic Thesis and Dissertation Repository

---

8-23-2022 2:00 PM

## Configuration and Sizing of Small Modular Reactor with Thermal Energy Storage within a Microgrid for Off-grid Communities

Michael W. C. Davis, *The University of Western Ontario*

Supervisor: Jiang, Jing, *The University of Western Ontario*

A thesis submitted in partial fulfillment of the requirements for the Master of Engineering Science degree in Electrical and Computer Engineering

© Michael W. C. Davis 2022

Follow this and additional works at: <https://ir.lib.uwo.ca/etd>



Part of the [Nuclear Engineering Commons](#), and the [Power and Energy Commons](#)

---

### Recommended Citation

Davis, Michael W. C., "Configuration and Sizing of Small Modular Reactor with Thermal Energy Storage within a Microgrid for Off-grid Communities" (2022). *Electronic Thesis and Dissertation Repository*. 8830. <https://ir.lib.uwo.ca/etd/8830>

This Dissertation/Thesis is brought to you for free and open access by Scholarship@Western. It has been accepted for inclusion in Electronic Thesis and Dissertation Repository by an authorized administrator of Scholarship@Western. For more information, please contact [wlsadmin@uwo.ca](mailto:wlsadmin@uwo.ca).

## Abstract

Many off-grid communities in Canada rely on diesel generators for their electricity needs. This is not only expensive but also produces significant greenhouse gas emissions. Small modular reactors (SMRs) have been proposed to replace diesel generators and can be combined with photovoltaic (PV) sources to form a microgrid. However, fluctuations in loads and PV create challenges for SMRs. Integrating a thermal energy storage (TES) system with the SMR can increase the flexibility of the power system to operate more effectively. This thesis first examines methodologies to determine suitable configurations of such a microgrid. Through analysis of the system components and the patterns of PV and demand, techniques for component sizing and operational modes of the combined SMR and TES system are developed. A case study has demonstrated the SMR size can be reduced when integrating TES so that the overall microgrid can operate more effectively and improve the SMR economics.

## Keywords

Microgrid, microgrid sizing, renewable generation, small modular reactor, thermal energy storage, off-grid communities

## Summary for Lay Audience

The Canadian electrical grid provides reliable electricity to cities and most communities across the country. However, there are nearly 300 off-grid communities far from the electrical grid that must produce their own electricity. Many off-grid communities currently provide their own electrical supply using diesel generators that produce significant greenhouse gas emissions, which is harmful to people and the environment. A goal is to reduce emissions by replacing diesel generators with small modular nuclear reactors and adding renewable energy resources, including solar power. Small modular nuclear reactors have been proposed to complement solar power to meet the needs of off-grid communities. However, these small modular nuclear reactors can have issues complementing solar power and can have high installation costs. The thesis investigates adding heat storage with the nuclear reactor to address these issues. A significant problem to address is how to determine the appropriate sizing of the system components. Characteristics of the electrical demand and renewable resource profiles must be analyzed to determine appropriate sizing for the small modular nuclear reactors, renewable resources, and storage devices. Through a case study of a benchmark community, this work has demonstrated that the power rating of the nuclear reactor can be reduced when integrating heat storage. This can allow the overall system to operate more effectively and can make the small nuclear reactor more cost effective.

## Acknowledgments

I wish to express my sincerest gratitude to my supervisor, Dr. Jing Jiang, for all the mentoring, guidance, and continuous care throughout my research. This work would not have been possible without his ongoing support.

I am also thankful for all the members of the Control Instrumentation and Electrical Systems (CIES) research group of the University of Western Ontario. Especially, Dr. Adeel Sabir for his warm welcome into the lab and care when I was developing my research topic, Dr. Michaelson for his expertise, guidance, and assistance through my thesis writing, and Dr. Ataul Bari for his assistance within the lab group.

I am deeply thankful to my parents. I cannot accurately describe how much they have done and continue to do for me. Without them, I simply could not have accomplished anything.

To my partner Rochelle Furtado, I appreciate you in every way. You have been with me every step of the way through this process. Either listening to me trying to figure out my research or putting a smile on my face after a tough day, you are always there for me, and I thank you for that.

# Table of Contents

Abstract.....	ii
Summary for Lay Audience.....	iii
Acknowledgments.....	iv
Table of Contents.....	v
List of Tables.....	viii
List of Figures.....	x
List of Appendices.....	xiii
List of Symbols.....	xiv
List of Abbreviations.....	xvii
Chapter 1.....	1
1 Introduction.....	1
1.1 Current Situation, Issues, and Motivations for Research.....	2
1.2 Research Objectives, Methodologies and Scope.....	4
1.2.1 Research Objectives.....	5
1.2.2 Scope and Methodologies.....	5
1.2.3 Contributions of Thesis.....	7
1.3 Organization of Thesis.....	7
Chapter 2.....	8
2 Background and Literature Review.....	8
2.1 Information and Description of Off-grid Communities.....	8
2.1.1 Power Needs and Renewable Resource Potential in Off-grid Communities.....	9
2.1.2 Current Power Systems.....	11
2.1.3 Microgrids.....	13
2.1.4 Small Modular Reactors.....	16

2.2	Energy Storage within Microgrids.....	17
2.2.1	Types, Description and Characteristics of Thermal Energy Storage.....	19
2.2.2	Thermal Storage Mechanisms.....	22
2.3	Considerations for SMR Integration into Microgrids.....	25
2.4	Integration of SMRs with TES .....	28
2.5	Selection and Description of SMR Type .....	32
2.5.2	High Temperature Gas-Cooled Reactors with TES.....	37
Chapter 3	.....	39
3	Configuration and Analysis of Microgrid with SMR and Thermal Energy Storage ...	39
3.1	Description of System Components.....	39
3.1.1	Demand Profile .....	40
3.1.2	Renewable Generation Characteristics .....	46
3.1.3	SMR as a Controllable Source.....	50
3.1.4	Electrical Energy Storage .....	51
3.1.5	Integration of TES with SMR.....	52
3.2	Determination of TES Configuration and Materials for Integration with HTGR	54
3.3	SMR-TES Design Description and Model .....	56
3.3.1	Description of the System and Key Parameters.....	58
3.3.2	Design Calculations .....	61
3.4	Methodology of Analysis.....	64
3.4.1	Modelling and Analysis under Steady-state Conditions.....	64
3.4.2	Economic Considerations .....	66
3.4.3	Dynamical Analysis .....	67
Chapter 4	.....	72
4	Components Sizing Under Different Configurations.....	72
4.1	Sizing Problem for the Overall Microgrid .....	72

4.2 Methodology for Component Sizing .....	74
4.3 Analysis of SMR Integrated into a Microgrid .....	76
4.4 Analysis of SMR-TES Integrated into a Microgrid.....	79
4.4.1 SMR-TES Simulations for Sizing Assessment of TES .....	82
4.4.2 Methodology for Sizing SMR-TES System .....	86
Chapter 5.....	93
5 A Case Study.....	93
5.1 Community Electricity Profile.....	93
5.2 Single SMR Sizing Problem .....	96
5.2.1 Steady-State Analysis .....	96
5.2.2 Dynamical Analysis .....	103
5.2.3 Dynamic PV and SMR Considerations.....	117
5.3 Solutions to Sizing Problem.....	118
Chapter 6.....	121
6 Conclusions .....	121
6.1 Summary.....	121
6.2 Conclusions.....	121
6.3 Suggestions for Future Work .....	123
References.....	124
Appendices.....	133

## List of Tables

Table 2-1 KLFN Diesel Generator Parameters [17] .....	13
Table 2-2 Description of energy storage performance parameters [24] .....	18
Table 2-3 Properties of common sensible heat storage materials .....	20
Table 2-4 Properties of two commonly used thermal oils [26] .....	21
Table 2-5 Properties of commonly used molten salts [27] .....	22
Table 2-6 Off-grid SMR designs under development in Canada .....	32
Table 2-7 Selected on-grid and off-grid HTGRs under development .....	36
Table 2-8 HTR-10 design data at 100% and 30% full power .....	36
Table 2-9 The manipulated and controlled variables of X Energy Xe-100 during load-following operations [55] .....	37
Table 3-1 Core and primary loop design parameters .....	58
Table 3-2 Thermal energy storage intermediate loop design parameters .....	60
Table 3-3 Power cycle design parameters .....	61
Table 3-4 Breakdown of TES costs .....	67
Table 4-1 Input parameters for the community .....	72
Table 4-2 Relationship between core sizing and TES characteristics .....	85
Table 5-1 Electricity profile of a community .....	94
Table 5-2 Results of steady-state analysis with integration of PV .....	101
Table 5-3 Effect of SMR ramp rates on EES requirements .....	110
Table 5-4 EES requirements based on SMR response delays .....	118

Table 5-5 Sizing solution results.....	118
Table A-1 Conditions of steam/water around power cycle .....	133
Table A-2 Thermodynamic properties at states around power cycle .....	134

# List of Figures

Figure 2-1 Power System Line Diagram for KLFN Community [11].....	12
Figure 2-2 (a) Thermal solar power plant with two-tank direct and (b) Two-tank indirect thermal energy storage.....	23
Figure 2-3 Thermal solar power plant with thermocline thermal energy storage system .....	24
Figure 2-4 LWR system configuration for load-following through by-passing steam from the main steam header.....	30
Figure 2-5 LWR system configuration with TES integrated within the steam cycle .....	31
Figure 2-6 Diagram of High Temperature Gas-cooled Reactor with a steam cycle.....	34
Figure 3-1 Simplified schematic for off-grid microgrid.....	40
Figure 3-2 (a) Example of the annual power demand of a remote community and (b) Load curves to define limits on the demand .....	41
Figure 3-3 Typical timeseries demand represented by a timeseries mean bounded by variance within lower and upper limits .....	44
Figure 3-4 PV potential from PVWatts Calculator showing range of daily trends in summer and winter seasonal limits.....	47
Figure 3-5 Solar irradiance dataset measurements for a volatile day .....	48
Figure 3-6 Comparison of PV model with PVWatts calculator .....	50
Figure 3-7 Simplified microgrid schematic including the SMR integrated with thermal energy storage.....	53
Figure 3-8. Description of HTGR system configuration with power cycle and thermal energy storage integration into a two-tank indirect intermediate loop .....	56
Figure 3-9 Simplified schematic of SMR- TES model.....	57

Figure 3-10 Simulink modelling block diagrams for (a) Demand and (b) PV generation ..... 69

Figure 3-11 Simulink model for (a) Determination SMR operation based on the net demand, and (b) EES operation to determine EES requirements..... 70

Figure 4-1 Sizing methodology flowchart ..... 74

Figure 4-2 Typical demand and PV production at a remote community with associated net demand for (a) Summer and (b) Winter..... 78

Figure 4-3 Performance of SMR-TES system to follow demand based on power and energy calculations with (a) Demand and SMR power, (b) TES power and (c) TES energy ..... 84

Figure 4-4 SMR-TES system operation from SMR core and BOP sizing to determine system operation and required TES storage capacity with (a) demand, (b) SMR core and SMR-TES output, (c) steam mass flow rate, (d) hot and cold tank mass flow rates and (e) hot and cold tank storage levels..... 90

Figure 5-1 Input community demand profiles in winter month..... 94

Figure 5-2 (a) Seasonal variations in the daily PV profiles between summer and winter and (b) Defined range of PV output profiles in the winter month..... 95

Figure 5-3 Key parameters of SMR-TES operation with proper component sizing with (a) SMR output, (b) Hot tank inlet and outlet mass flow and (c) Cold and hot tank levels..... 99

Figure 5-4 Required SMR operation in summer months when PV output exceeds demand 103

Figure 5-5 Simulations of actual and required SMR system response with 500kW installed PV ..... 106

Figure 5-6 (a) Power of EES and (b) Energy capacity of EES for one day with 500kW installed PV ..... 107

Figure 5-7 (a) EES capacity requirements and (b) EES maximum power required for different amounts of installed PV capacity and SMR ramp rates ..... 109

Figure 5-8 Effect of the required EES capacity from varying the SMR-TES ramp rate under 3 different PV capacities .....	111
Figure 5-9 Effect of maximum EES capacity from varying the SMR-TES ramp rate for (a) Charging and (b) Discharging under 3 different PV capacities .....	111
Figure 5-10 Required EES power with 3,500 kW PV installed at (a) 10%/min and (b) 20%/min SMR ramp rate .....	112
Figure 5-11 (a) Required EES capacity and (b) Maximum power during summer months when PV output is below demand .....	113
Figure 5-12 (a) SMR actual versus net when instantaneous PV production exceeds instantaneous demand at 3500 kWe PV installed and (b) Selected timeframe from (a) .....	115
Figure 5-13 Operation of system when PV exceeds load with (a) Net demand, (b) Power of SMR and PV compared to load and (c) Required power from EES.....	117
Figure A-1 Steam power cycle schematic .....	133

## List of Appendices

Appendix A: Steam Cycle. This appendix presents the model calculations for the steam power cycle. ....	133
Appendix B: Simulations. This appendix presents the calculations and process for the steady-state and dynamical simulations .....	138

## List of Symbols

$c_{P,he}, c_{P,ms}$	Specific heat capacity of helium, and specific heat of molten salt (kJ/(kg· °C))
$C_{SMR}$	Lifecycle SMR system cost (M\$)
$C_{CORE}, C_{BOP}, C_{TES}$	Lifecycle capital costs for SMR core, BOP, and TES components (M\$)
$E_{EES}$	Amount of electrical storage (kWh)
$E_{EES}^{size}$	Installed EES capacity from sizing (kWh)
$G$	Incident solar irradiance (W/m <sup>2</sup> )
$\bar{G}$	Maximum timeseries of solar irradiance profile (W/m <sup>2</sup> )
$k$	Timestep index variable
$L$	Magnitude of power required for the community (kW)
$L_{avg}$	Average demand (kW)
$L_{max}$	Maximum annual demand (kW)
$\underline{L}, \bar{L}$	Lower and upper bounds of demand (kW)
$L_W^l$ and $L_S^l$	Winter and summer demand intervals (kW)
$m_{HT}, m_{CT}$	Mass of molten salt in hot tank and cold tank (metric tons)
$m_{TES}^{size}$	Mass of molten salt from sizing (metric tons)
$\dot{m}_{CT,in}, \dot{m}_{CT,out}$	Mass flow rates into and out of cold tank (kg/s)
$\dot{m}_{HT,in}, \dot{m}_{HT,out}$	Mass flow rates into and out of hot tank (kg/s)

$\dot{m}_{he}, \dot{m}_{steam}$	Helium mass flow rate and steam mass flow rate (kg/s)
$P_{EES}$	Power of the EES system (kW)
$P_{net}$	Net power demand (kW)
$\underline{P}_{net}, \overline{P}_{net}$	Lower and upper bounds on net demand (kW)
$P_{PV}$	Power generation from the PV system (kW)
$\underline{P}_{PV}, \overline{P}_{PV}$	Lower and upper limits of PV output (kW)
$P_{PV}^{size}$	Installed PV capacity from sizing (kW)
$P_{SMR}$	Power generation from an SMR (kW)
$P_{out}$	SMR system electrical output power (kW)
$P_{SMR}^{size}, P_{BOP}^{size}$	SMR core and BOP sizing (kW)
$p_{he}, p_{steam}$	Helium coolant pressure and steam turbine inlet pressure (MPa)
$Q_{SMR}$	SMR core heat production rate (kW <sub>th</sub> )
$Q_{he:ms}, q_{he:ms}$	Heat transfer rate from helium coolant to molten salt (kW <sub>th</sub> ) and specific heat transfer (kJ/kg)
$Q_{ms:steam}, q_{ms:steam}$	Total heat transfer rate from molten salt to steam (kW) and specific heat transfer (kJ/kg)
$SOC$	State of charge of electrical storage system (%)
$T_{HT}, T_{CT}$	Hot tank and cold tank temperatures (°C)
$T_{in}, T_{out}$	Helium inlet and outlet temperatures (°C)

$T_{fw}$	Power cycle feed-water temperature (°C)
$T_{steam}$	Steam turbine inlet temperature (°C)
$w_{pump}$	Input work done by the feedwater pump (kJ/kg)
$w_{turb}$	Output work done by the steam in the turbine (kJ/kg)
$\alpha$	Load stochastic perturbation factor (%)
$\delta_S$	Normal random variable for load variability (kW)
$\eta_{PV}, \eta_{EES}$	Efficiency of PV system, and of EES system
$\sigma_D$	Variation in the daily demand limits (%)
$\sigma_S$	Timestep variation parameter (kW)
$\sigma_Y$	Variation in daily peak demand throughout the year (%)

## List of Abbreviations

BOP	Balance Of Plant
CNSC	Canadian Nuclear Safety Commission
CSP	Concentrated Solar Power
EES	Electrical Energy Storage
EMS	Energy Management System
EUR	European Utilities Requirements
FP	Full Power
HPR	Heat-Pipe Reactor
HTF	Heat Transfer Fluid
HTGR	High Temperature Gas-cooled Reactor
KLFN	Kasabonika Lake First Nation
LFR	Lead-cooled Fast Reactor
LWR	Light Water Reactor
NPP	Nuclear Power Plant
O&M	Operations and Maintenance
PV	PhotoVoltaic
SMR	Small Modular Reactor
SOC	State Of Charge

TES	Thermal Energy Storage
TRL	Technology Readiness Level

# Chapter 1

## 1 Introduction

The electrical power grid in Canada consists of connected networks of electricity generation sources, transmission lines, and distribution systems to deliver electricity to cities and most communities. These electrical networks supply reliable electricity to most Canadians at reasonable rates but do not supply many off-grid communities due to the excessive cost of transmission infrastructure. Many off-grid communities provide their own electrical supply by using diesel generators because they are simple to install and operate, and have a low capital cost [1]. However, diesel generator-based power systems are problematic from an environmental perspective. Diesel generators produce substantial greenhouse gas emissions during operation. Further, diesel generators have limited reliability and maneuverability. The constant fuel supply required to operate the diesel generators can be difficult to sustain and can be expensive.

The desire to reduce emissions and shift to clean renewable energy sources has resulted in more and more photovoltaic (PV) and wind power generation systems being introduced in these communities. However, renewable energy is not dispatchable and cannot easily displace diesel based generation. Energy systems in the form of microgrids need controllable sources for reliable operation. These controllable sources are required to operate flexibly to meet variations in demand along with variability and intermittence from renewable resources.

In 2018, the Canadian Small Modular Reactor (SMR) Roadmap was created, which outlined a path to explore the role of SMRs to meet energy demands and reduce greenhouse gas emissions while contributing to innovation and economic development [2]. This roadmap has identified off-grid communities as target applications for SMRs to replace diesel gen-sets. SMRs offer two significant advantages: elimination of the need of a constant fuel supply by using reactors that can operate for extended periods without refueling, and the potential of flexible generation that can allow for integration with renewable resources [3].

## 1.1 Current Situation, Issues, and Motivations for Research

A representative off-grid community in Canada could be a northern Ontario community with a population of thousands that currently relies on diesel gen-sets to meet their electricity needs. This community would have large seasonal and daily variations in electricity demand along with significant variability due to the relatively small community size with primarily residential loads. The northern latitude would result in significant seasonal and daily variations in renewable resources with considerable variability and intermittence.

### **Motivations**

Current diesel generator based power systems have many technical, economic, and environmental issues for the off-grid communities they serve. Most significant is the large amounts of greenhouse gas and particulate emissions and high electricity costs. Many of the current diesel generators are nearing their life expectancy, which creates the opportunity to replace these diesel generators with alternative power sources.

Within these microgrids, flexible generation sources and storage are required to satisfy the requirements of an off-grid community. The combination of controllable sources and storage must complement the renewable generation to meet the demand while accounting for all variability. Because battery storage is currently one of the costlier options for adding flexibility to the grid, there are more economical options to cope with renewable resources in such a microgrid [4].

SMRs are a potentially viable power source that can be used in combination with renewable energy sources in the form of microgrids. One current issue with SMRs is the expected high costs and especially high capital costs. Another issue is that while SMRs have the potential for flexible operation, this is generally not the preferred operation mode using current load-following methods. SMRs operating in flexible modes through core power maneuvers can cause core instabilities and thermal stresses on core components [5]. One way to overcome the above issues is to incorporate energy storage systems. In principle, storage can take three forms: electrical, mechanical, and thermal.

Since nuclear reactors directly produce thermal energy before it is converted into electricity, thermal energy storage (TES) can be directly coupled to SMRs.

### **Potential Advantages of Integrating SMRs with Thermal Energy Storage**

Small modular reactors with thermal energy storage have the potential to replace diesel generators to form a suitable microgrid. There are the following advantages:

- Adding TES can potentially reduce transients in the reactor core by instead adjusting the TES and the balance of plant (BOP) including the power cycle to meet any changes in demand and renewable generation.
- The flexibility of the SMR-TES can be increased by allowing the core to operate at constant power while adjusting the TES and BOP to achieve load-following operation.
- The power rating of the SMR core can be reduced by adding TES and oversizing the BOP system to generate peaking output during periods of high demand.
- The total SMR-TES costs can be minimized by reducing SMR core power rating with very small added TES costs.
- The size and capacity of other storage systems, such as battery storage can be reduced.

SMRs are a potential solution as the main component in microgrids to meet the needs of off-grid communities by coupling with TES and enabling the integration of renewable generation. However, SMRs are currently under development and have not yet been demonstrated. Further, these advantages of integrating SMRs with thermal energy storage units has not yet been proven in the context of microgrids. For this innovative concept of integrating an SMR system with a thermal energy storage system, more investigations are needed. A significant problem is the determination of the suitable configuration and sizing of these microgrid components for off-grid communities [6]. Characteristics of the

load and renewable resource profiles must be analyzed to determine appropriate sizing for the SMR, renewable resources, and storage devices [6].

### **Existing Issues**

There are still a lot of investigations that need to be done to answer the following questions:

- How the unique microgrid characteristics of off-grid communities determine the SMR requirements?
- How TES can be utilized to meet the microgrid requirements?
- What is the optimal sizing of SMR and TES?
- What is the economic viability when adding TES costs to improve SMR flexibility and increase the SMR utilization?

The motivation for the current research is to answer the above questions through modelling, simulation, and optimization.

## **1.2 Research Objectives, Methodologies and Scope**

The above advantages of integrating SMRs with thermal energy storage has not yet been proven in the context of microgrids for off-grid communities. In order to address the above issues, specific problems need to be solved that include:

- What type of SMR, and TES materials and configurations would work for near-term deployment for off-grid communities?
- Given typical load profiles of an off-grid community, and characteristics of renewable energy resources, what would be the desired performance requirements on SMRs with TES and without TES?
- How can the SMR-TES system be configured and operated (SMR core, TES, and BOP) effectively in a microgrid?

- How to determine the size of the reactor core power level, the size of TES storage and that of the BOP?
- What are the ‘optimal’ configuration for a combined SMRs and TES?
- How much renewable generation can be accommodated in such a configuration?
- What additional amounts of electrical storage is required?

### 1.2.1 Research Objectives

- Determine requirements of an SMR system in a microgrid based on load profiles and renewable energy characteristics representative of an off-grid community in Canada.
- Conceptual design description of an SMR with thermal energy storage and steam power cycle for a chosen SMR type and thermal energy storage configuration.
- Analyze the SMR system to account for variability and intermittence of renewable generation and load variations to determine additional storage requirements for this microgrid.
- Determine configuration, sizing, and operation of SMR with TES as the main generation source within this microgrid.
- Determine the amount of PV energy that can be included in this microgrid.
- Determine the amount of electrical energy storage that is required.

### 1.2.2 Scope and Methodologies

The scope of this investigation includes:

- The research focuses on SMRs with TES in a microgrid as the controllable generation source to supply to off-grid communities.

- A benchmark off-grid community is described and defined in terms of a number of descriptive parameters.
- PV will be the only type of renewable generation source explored in this thesis, since it has been used in northern communities in Canada. Wind is also a viable renewable energy source in these off-grid communities but will not be considered in this work.
- The power from PV systems should be chosen as the first source for consumption.
- Battery storage will be used since it is the most common small-scale storage system.
- The focus of the sizing and the operation of the system will be on meeting system power balance. System frequency and voltage control are not considered.
- For sizing, the maximal power demand from the of-grid community should be met, and no demand response strategies are considered.
- The SMR system to meet both electrical and thermal loads in a cogeneration mode within the off-grid community are not explicitly considered. The effect of such loads on to the overall system can be investigated simply through aggregated total loads.

The following techniques will be used in this research:

- Survey of power needs and renewable resource potential of typical off-grid communities through literature review.
- Model the load-profile and seasonality.
- Examine technologies of TES and BESS and their associated pros/cons.
- Analyze and select the type of SMRs for the given scenarios.

- Formulate sizing problems by considering the size of renewable energy resources, and the dynamic behaviors of SMRs and TES systems.
- Carry out sizing and demonstrate the solution process by using the benchmark off-grid community as a case study.

### 1.2.3 Contributions of Thesis

This thesis has made three major contributions:

- Conceptual design of an SMR with a thermal energy storage system for near-term off-grid community deployment.
- Technical evaluation through sizing of the microgrid components that include an SMR integrated with TES as the main controllable source, with economic considerations that improve SMR costs.
- Integration of SMR technologies with TES has been demonstrated to enhance technological and economic capability to serve the needs of off-grid communities.
- Demonstration that the SMR core power rating can be reduced when adding TES while still meeting peak demands of community.

## 1.3 Organization of Thesis

The remainder of the thesis is organized as follows. Relevant literature on off-grid communities in Canada including current diesel generator based power systems, and microgrids including small modular reactors, thermal energy storage, and photovoltaic generation have been reviewed in Chapter 2. Analysis of the microgrid configuration and modelling have been discussed in Chapter 3. In Chapter 4, the sizing methodology and analysis has been presented. Chapter 5 presents a case study to demonstrate the sizing problem through steady-state and dynamic analysis in a benchmark community. Finally, the work has been concluded with a summary and some highlights of suggested future work in Chapter 6. Two Appendices are included to provide a description of the steady-state and dynamic modelling processes.

## Chapter 2

### 2 Background and Literature Review

In this chapter, some background information is presented first for off-grid communities and their current power systems. Additionally, background information is given on the development of alternative power systems in the form of microgrids including small modular reactors, thermal energy storage and photovoltaic generation.

#### 2.1 Information and Description of Off-grid Communities

There are nearly 300 off-grid communities in Canada with a total population estimated at more than 190,000 [7]. These communities primarily rely on diesel generation for their electricity needs [7]. Many of these communities are in northern Ontario and the territories (Nunavut, Yukon, and Northwest Territories), and there are also similar communities in Alaska. The populations of these communities range from hundreds to thousands [7]. Energy usage in these communities is primarily residential but larger communities can also have significant portions from commercial and industrial activities [8]. An illustrative example of a small off-grid community in northern Ontario is Kasabonika Lake First Nation (KLFN), with a population of approximately 1,000 people [9]. The community annual demand varied between 200 kW to 850 kW in 2014, with a total annual energy demand of approximately 4.2 GWh [9], [10]. Over time the community demand has increased and the peak demand has reached to 900 kW in the winter [11].

These off-grid power systems have unique challenges due to the limited capacities of their electrical generators, and cannot rely on any external sources for support or back-up [12]. Most off-grid communities that use diesel generator based power systems are typically operated by regional utilities such Hydro One for Ontario [9]. Due to the remote nature and dispersion of communities across the country, grid connections to these communities can have prohibitive costs. The cost estimated at connecting 17 off-grid communities in Ontario to the power grid is estimated to be as high as 1.83 billion dollars [13]. It is estimated that 1500 km of new transmission line would have to be installed

[13]. Comparatively, it is estimated that the current cost of diesel generation for these communities is a total of 43 M\$ per year [13].

### **Issues with Diesel-based Power Systems**

Diesel generators produce significant amounts of greenhouse gas and particulate emissions that is very harmful to the communities and the environment. The KLFN community consumed 1.2 million liters of diesel fuel in one year, resulting in 3,400 metric tons of CO<sub>2</sub> emissions [14]. Diesel is expensive, and that leads to high electricity costs. At a diesel price of \$1.80/L the annual fuel cost for this community would be 2.16 M\$, with additional annual operations and maintenance (O&M) costs of 1.8 M\$ [9]. These high costs can result in an unsubsidized price for electricity in remote regions of Canada as much as 1.3 \$/kWh [9]. Diesel fuel supply is also difficult to sustain in remote regions due to large storage volume requirements, and often has to be delivered by plane or via winter roads only [9], [12]. Diesel generators have finite ramp rates to vary their electrical output and often cannot operate below 30-50% of their rated output. Operating at lower load levels reduces fuel efficiency [12]. Many of the diesel generators in the current fleet are aging and nearing life expectancies and many communities are in need of diesel generator upgrades or replacements. This creates an opportunity for replacement with other sources such as SMRs [2].

## **2.1.1 Power Needs and Renewable Resource Potential in Off-grid Communities**

### **Communities in Canada and their Electricity Needs**

There are many remote communities in Canada that are geographically dispersed and have widely varying characteristics of load and renewable generation potential. Electrical demand can vary greatly among communities due to varying sizes, geographical location, specific social-economic conditions, and current power system configurations. Surveys of off-grid communities in Canada have been completed in [7], [15] that describe community population, annual electrical demand, renewable resource potential, and current power systems including installed diesel and renewable resource capacity.

Community population and annual electricity demand vary greatly. Many of the communities have populations from 230 to 2,280 but some can have up to 6,000. The majority of the communities annual electricity demand is between 1,430 MWh/yr to 11,290 MWh/yr, but the maximum is 128,732 MWh/yr [15]. Only the total annual electrical energy consumption is available for many of these remote communities, with very little information available on any trends.

### **Renewable Resource Potential of Photovoltaics**

Renewable sources are desirable in off-grid communities to reduce emissions. Some communities use hydropower because it can be a reliable and cost-effective source. However, it is dependent on geographic conditions and is only used on large scale to provide electricity to a number of communities in Quebec, NWT and the Yukon [7]. Renewable generation in the form of wind and PV are being used more and more in many communities. Wind and PV generation can be attractive option specifically in northern Ontario.

PV is a favored source due to its reliable operation and lower installation and O&M costs per kW as compared with small wind turbines [9]. PV systems have experienced a continual cost decrease over time due to innovation and utilization of more PV systems. PV has advantages including long lifetimes of often more than 20 years, no moving parts, minimal operations and maintenance costs, and modular system design which allows for easy expansion [16].

Solar resources in northern Ontario are found to be sufficient to employ PV based power generation. The measured average direct solar radiation in the range of 2.81-3.81 kWh/(m<sup>2</sup>·day) is generally constant at similar latitudes in the region [15]. In other regions including the territories correspond to 70-90% of the annual potential of more southern locations such as Ottawa, Ontario [12].

However, like the variability and uncertainty in specific community demand, there are also variability and uncertainty in power production from renewable resources for off-grid communities. The biggest limitations of renewable resource potentials in northern

locations are the large seasonal variations. At high latitudes, the availability is more concentrated in summer months and is much less in winter months [12]. PV systems exhibit intermittence, where the actual output is often less than the rated maximum output due to weather or other conditions. Intermittence is related to PV variability and is defined as the random changes in the PV output over time. Variability and intermittence become more significant as the renewable penetration amount increases, and this issue currently only allows for small amounts to be added. This is a major reason why renewable generation is used only in a limited number of communities.

### 2.1.2 Current Power Systems

In current off-grid power systems, there are typically 3 or more diesel generators that are oversized to account for the differences in average and peak loads. Common practice is to choose generators with different ratings to limit running some at partial loads that can reduce fuel efficiency. Typically, one diesel generator operates while a second is kept on standby to be able to quickly operate if required [9]. A third diesel generator is typically kept as a backup to ensure system reliability. A typical diesel configuration for the KLFN community first had 400 kW, 600 kW, and 1,000 kW units that were sized based on the ranges of demand [9], [10]. A 1,500 kW diesel generator has since been added while the 400 kW generator has been removed [11]. Once the peak demand reaches 90% of the maximum rating of the largest diesel generator, the community is placed into load restrictions until additional generation sources can be added. In this community there are three 10 kW wind turbines and a 30 kW wind turbine that have been installed [11], along with 12.4 kW roof top PV [17].

The dispatch strategy includes running one diesel generator at a time except for brief overlap when switching generators [11]. Once a given generator reaches 90% of its rated power capacity and continues providing a power higher than 90% of its rated power for 2 minutes, the next larger generator is turned on and the smaller one is then shut down [11]. When the load demand falls below 80% of the rated output of the next smaller generator and stays in that condition for 15 minutes, then the smaller unit will turn on and supply the load, while the larger unit will be turned off [11]. This is done in order to operate within allowable limits and to operate at the highest fuel efficiency for a given load [14].

The specific electrical parameters of the power system can vary in communities. This can be dependent on a number of factors including the community size. A single line diagram representing the KLFN community power system can be seen in Figure 2-1. Here the items labelled store (STR), school (SCL), police station (PLC), nursery station (NRS), and water treatment plant (WTP) represent commercial demands, along with the community residential demands. The wind turbines are connected to nodes 2 and 3 and the rooftop PV is connected to node 7 [17]. The corresponding diesel generator parameters are summarized in Table 2-1. It is seen that the diesel generators can operate between 40%-100% of their rated power with 10%/min ramp rate limits. The diesel generators operate at 600V, with 4.16 kW distribution for 120V/240V community loads [11].

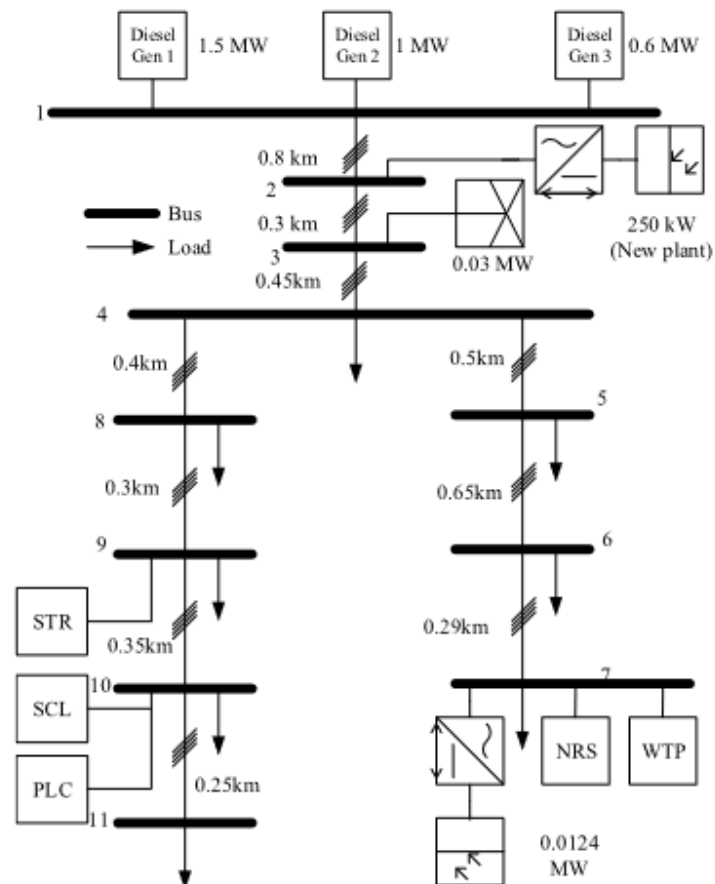


**Figure 2-1 Power System Line Diagram for KLFN Community [11]**

**Table 2-1 KLFN Diesel Generator Parameters [17]**

<b>Parameter</b>	<b>Diesel Gen 1</b>	<b>Diesel Gen 2</b>	<b>Diesel Gen 3</b>
Power Rating (kW)	1,500	1,000	600
Operating Range (kW)	1500-600	1,000-400	600-240
Voltage (V)	600	600	600
Ramp Rate (kW/min)	150	100	60

### 2.1.3 Microgrids

To enhanced beyond the current power systems, a microgrid can be defined as a smaller version of a large power system containing distributed generators, energy storage, loads, and its own control system [18]. The replacement of a diesel-based power system with an enhanced microgrid has been the preferred method that incorporates the use of renewable generation [18]. A significant purpose of the development of microgrids is to meet the load demands at the highest quality and reliability at a reasonable costs [11]. Compared to grid connected systems, the operation and control of off-grid microgrids is much more challenging and requires strategies for system power balance [11].

In a microgrid there are three levels of control functions including primary, secondary, and tertiary. Primary control is the fastest control level that operates based on local measurements that is responsible for voltage and frequency control as well as power sharing and balancing [11]. For synchronous generators, this is done by the voltage regulator and governor, that are under the influence of inertia of the machine [11]. Secondary control level corresponds to an energy management system (EMS) that has the role of ensuring reliable, secure and economic operation of the microgrid by monitoring and managing power flow, by scheduling the commitment and power dispatch of each unit to match generation to load, and ensures that system constraints are not violated [18], [19]. Tertiary control is the highest control level and determines the long term optimal set points [11].

The main variables participating in the control of operation of a microgrid are voltage, frequency, and power. Changes in demand affect the frequency and voltage of the microgrid which must be compensated by the generation and storage units to ensure they

remain within acceptable limits. When fast fluctuations in the load cause frequency deviations, the deviations must be reduced through adjusting generator outputs and kept within desired limits by restoring the system back to the nominal frequency. Primary frequency control should be able to act fast and provide the required service within a few seconds after a disturbance [11]. Secondary frequency control needs to be activated within a few minutes to respond to the changes in load and restore the system frequency [11]. These can be referred to as load-following modes. In current diesel generator based systems, the synchronous machines perform this control [11]. Integrating SMRs into microgrids is unclear and there has not been any considerable operation and control strategies developed. For this reason, the microgrid sizing and coordination for system power balance will be considered in this work. The microgrid control should be considered as future extension to this work.

The performance of regulation and load following services is greatly impacted by integration of intermittent and highly fluctuating renewable sources. This is most significant in off-grid cases where the characteristics and limited sizes and number of generation sources limits the system inertia. Renewable generation cannot easily replace diesel generation without large amounts of installed capacity and storage, which would be very expensive and technically challenging. The contribution of diesel generators in load-following operations is limited by their sizes and ramping capabilities [11].

### **Existing Work**

There has been considerable research in integration of wind and PV systems for remote communities and specifically in Canada. For example, many studies have focused on the KLFN community including [9], [10], [14], [20]. These studies have included renewable generation development, system sizing, and long-term planning. Many of the relevant studies in the literature are related to the sizing of power systems for various off-grid communities in Canada. Some studies have used site specific data including [1] for a site in Manitoba, Canada. The HOMER software was used to consider diesel generators, wind turbines and batteries to meet a peak demand of 537 kW and a daily energy consumption of 8,000 kWh/day [1]. The finding from the HOMER calculator was that an

enhanced diesel system, as well as a wind-diesel system can reduce the electricity cost and emissions compared to using the existing diesel generators alone. However, these optimized systems would not eliminate emissions and the optimized case only reduces annual emissions by approximately 30%. The HOMER software has also been used to model synthetic demand and renewable generation production when complete community information is not available. Another study [21] uses HOMER for a site with peak demand of 772 kW and a daily energy consumption of 8,000 kWh/day considering wind and PV generation. When comparing cases of different renewables amount ranging from 0% to 100%, it is found that increasing the renewable penetration amount increases the cost of electricity compared to a diesel-battery case, even with an emissions tax added [21]. A fully renewable case requires large amounts of generation sources and storage and can also result in significant excess electricity generation [21]. However, it is concluded that low penetration renewable systems can have comparable costs to the diesel-battery case.

It is found that existing diesel based systems are problematic and are desired to be replaced or enhanced. Adding renewable generation to these systems can lower the costs and can reduce required operation of the diesel generators to reduce emissions [9]. However, these systems can have issues with diesel generators operating at lower efficiencies and excess renewable generation does not further reduce operation costs. A limiting factor in the implementation of renewable generation is that existing diesel generation can be challenging to operate in a flexible way to account for renewable variability. This can be more significant at large renewable amounts.

In general, diesel-renewable, or fully renewable systems have the potential to be a viable option for these communities that may be the most cost-effective solution. However, they have not yet been completely proven, and there is still a lot of work needed towards these enhanced microgrids for off-grid applications for remote communities. Small modular reactor (SMR) based microgrids represent an alternative option that utilizes a controllable source that can perform complimentary operation to the renewable generation. Many of the environmental and technical issues of diesel generator based

systems have the potential to be eliminated when including SMRs and this warrants further investigations.

#### 2.1.4 Small Modular Reactors

SMRs are a revolutionary advancement from traditional nuclear power plants (NPPs). They utilize advanced design features and have an electrical output of less than 300 MW [22]. SMRs with power ratings between 2 and 10 MW are under development for off-grid communities [6]. Modules can be standardized, and mass produced from a factory. These modules can be transported by rail, barge, or road directly to the site for installation [8]. This can further reduce cost and time of construction.

SMRs are built on the knowledge gained from previous NPPs and utilize inherent and passive safety features [23]. Inherent safety eliminates hazards through design choices based on fundamental physical principles [23]. An example of this is the selection of fuels with a negative temperature coefficient so that the core reactivity decreases when temperature increases [23]. Passive safety is provided compared to active safety systems that require poised systems and external power sources. An example of a passive safety system is the decay heat removal after shutdown, that can be accomplished by coolant natural circulation instead of the requirement of shutdown cooling pumps [23]. These enhanced safety features can result in a lower core damage frequency and requires a smaller exclusion zone compared to current reactors. Any nuclear safety analysis is within a separate field and is outside the scope of this work.

The most significant advantages of SMRs include:

- SMRs are planned to have increased flexibility by utilizing multiple modules in a system. Individual modules are planned to have quicker ramp rates and the ability to operate over a larger power range.
- SMRs can have very long refueling intervals, e.g. no refueling over a 20-year lifetime [8].

- Some designs use non-water coolants, which can produce a high-temperature output that increases plant efficiencies and allows for efficient heat storage and process heat production.

## 2.2 Energy Storage within Microgrids

Energy storage is an important component for reliable operation of microgrids. It becomes more important as the share of renewable energy resources grows. Energy storage is used for load-following, accounting for variability, and providing capacity reserves.

The types of storage applicable to microgrids are dependent on the generation sources used. The fundamental division between energy sources is whether they produce heat or electricity [4]. In this analysis, our primary generation sources are SMRs and PV. Solar power directly produces electricity, so the method of storage of PV generation is limited to electrical storage. Nuclear energy first produces heat that is then converted to electricity, which allows for storage either in the form of heat or electricity. Therefore, the main types of energy storage considered here are thermal energy storage (TES) and electrical energy storage (EES) in the form of generic batteries. To compare different types of energy storage, there are several performance parameters that can be used to determine the suitability for a given application, as shown in Table 2-2.

### **Description of the Types of Energy Storage for Use within Microgrids**

**Battery Energy Storage.** Batteries operate through electrochemical reactions with different chemical species and store electrical energy. Batteries can have diverse characteristics due to the types of battery technologies. Since batteries directly store electrical energy, they can have very rapid response times on the scale of milliseconds to absorb or deliver energy. Battery systems are flexible and can be sized and configured to meet required discharge times along with energy and power capacities. Some major drawbacks of battery storage are high costs, limited round-trip efficiencies, and

significant storage degradation, which limits storage time to typically under 4 hours in these applications [4].

**Table 2-2 Description of energy storage performance parameters [24]**

<b>Performance Parameter</b>	<b>Description</b>
Energy capacity	The amount of energy stored (kWh)
Power capacity	The rate of charging and discharging of storage (kW)
Discharge time	The amount of time required to discharge the rated capacity (s)
Response time	The time between when power is requested and when power is delivered from the storage (s)
Storage degradation rate	The rate at which losses occur in the storage device
Round-trip efficiency	The ratio of energy discharged to the energy charged within the storage device
Cycle life and lifetime	Number of times that the storage device can be charged/discharged, and the total time until the device cannot operate effectively at the rated capacity
Cost	Includes capital cost (\$/kW or \$/kWh) and operating and maintenance costs (\$/year)
Energy/power density	Energy/power capacity per unit volume of the storage device

**Thermal Energy Storage.** Fundamentally, heat is considered to be of a lower quality than other forms of energy and can have more flexibility in its usage [4]. Thermal energy storage can be coupled with generation units that first produce thermal energy before converting it into electricity through a power cycle. Large thermal reservoirs can store thermal energy and utilize it later when desired. Adding TES to a generation unit can enhance load-following by acting as a buffer between the heat source and the power cycle. TES systems can have large energy and power capacities and low costs by utilizing simple storage mediums [4]. Adequately insulated storage units can have small degradation rates. Storage efficiencies are dependent on storage temperature and temperature swings, but can be significantly higher than electrical storage efficiencies. The lifetimes of the systems are very long, with almost no cyclic fatigue. TES systems have slower response times as compared to electrical storage due to thermal lags, but can have long discharge times.

Thermal energy storage has been used for on-grid concentrated solar power (CSP) plants that convert solar thermal energy into heat that drives a steam power cycle. CSP plants are dependent on the energy from incident solar radiation and have their power output reduced when a disturbance is introduced, such as cloud covering, that results in less available energy to be converted into electricity [25]. Heat storage is used to buffer changes in solar radiation and to produce constant output during nighttime when there is no sunlight. When implementing TES, the power cycle can be controlled independently from the heat production by manipulating the flow rates of the storage tanks [25]. Thermal oils and molten salts have been used as media for thermal energy storage in CSP plants that store energy in large, insulated tanks. Beyond the required storage performance parameters of a thermal energy storage system from Table 2-2, the materials must possess suitable thermophysical properties including [24]:

- High operating temperature range, high specific heat, and high thermal conductivity.
- Low viscosity, low volume change, low vapour pressure, low cost, high thermal stability, and easy availability.

### 2.2.1 Types, Description and Characteristics of Thermal Energy Storage

The most common types of TES include sensible heat and latent heat storage, depending on if the energy is stored in a raised temperature or in the phase change of a material, respectively. In general, sensible heat storage is simpler and has higher technology readiness level (TRL), and will be the focus in this thesis.

Latent heat storage systems store heat in the latent heat of a material during a constant temperature process like the solid-liquid phase change [26]. The thermal energy stored during this process can be expressed as:

$$H = m * L \tag{2.1}$$

where  $H$  represents the amount of thermal energy stored in kJ,  $m$  is the mass of material in kg, and  $L$  is the specific latent heat of the material in kJ/kg. The temperature of the

material is constant during discharge for latent heat but is limited to the phase change temperature. Latent heat is typically much larger than the associated sensible heat, but latent heat storage materials typically have poor thermal conductivity and higher costs.

Sensible heat storage systems store heat energy in the specific heat capacity of a material through a temperature change that can be expressed by:

$$H = m * c_p * \Delta T \quad (2.2)$$

where  $c_p$  is the specific heat capacity of the material in  $\text{kJ}/(\text{kg} \cdot ^\circ\text{C})$  and  $\Delta T$  is the rise in temperature during the charging process in  $^\circ\text{C}$ . Sensible heat storage systems are more technologically advanced than latent heat storage systems by avoiding phase changes and can have higher efficiencies and lower heat loss rates. Common sensible heat storage materials include water, thermal oils, molten salts, liquid metals, and earth materials with the properties summarized in Table 2-3 [26].

**Table 2-3 Properties of common sensible heat storage materials**

<b>Material</b>	<b>Operating Temperature Range (<math>^\circ\text{C}</math>)</b>	<b>Specific Heat (<math>\text{kJ}/(\text{kg} \cdot ^\circ\text{C})</math>)</b>	<b>Thermal conductivity (<math>\text{W}/(\text{m} \cdot ^\circ\text{C})</math>)</b>	<b>Heat Transfer Coefficient (<math>\text{W}/(\text{m}^2 \cdot ^\circ\text{C})</math>)</b>
Water and Steam	< 350	4.2	~0.1	800-4,000
Thermal Oils	12-400	2.0	0.1	1,000-3,500
Molten Salts	200-600	1.5	0.5	3,600-6,700
Liquid Metals (Sodium)	100-880	1.3	64.9	18,000 - 28,500

**Water and Steam.** Water and steam are common materials for energy storage due to their simplicity. The advantages of water are availability and low cost, with high specific heat and low viscosity [26]. In many advanced nuclear reactors with high outlet temperatures, the use of steam storage is limited. Due to the relatively low boiling temperature, steam may only be stored within the power cycle within accumulators.

**Thermal Oils.** Thermal oils are organic fluids with good heat transfer capability, with higher operating temperature ranges than water, but are typically limited to below  $400\ ^\circ\text{C}$ .

Thermal oils have low thermal conductivity, low specific heat, and a moderate heat transfer coefficient. Two commonly used thermal oils are Therminol VP-1 and Dowtherm with properties summarized in Table 2-4.

**Table 2-4 Properties of two commonly used thermal oils [26]**

<b>Composition</b>	<b>Operating Temperature Range (°C)</b>	<b>Kinematic Viscosity (mPa·s)</b>	<b>Density (g/cm<sup>3</sup>)</b>	<b>Heat Capacity (kJ/(kg· °C))</b>
Therminol VP-1	12-400	2.48	0.904	2.08
Dowtherm	12-400	2.56	0.897	2.51

**Molten Salts.** When the temperature of the system exceeds the thermal oil temperature limit, molten salts are the preferred heat transfer fluid and storage medium. Pure salts or salt eutectics with melting points around 250°C are considered for sensible heat storage, but this must be maintained to avoid freezing. High temperature ranges along with adequate thermo-physical properties have made molten salts desirable as the storage material in many advanced nuclear reactor designs. They have a high boiling point, typically above 560°C, with a very low vapor pressure that allows operation at atmospheric pressure. They have a high heat transfer coefficient, and a high thermal conductivity, but a low specific heat. There are many kinds of molten salts that are summarized in Table 2-5. Many of the thermo-physical properties are similar, but there can be significant differences in the operating temperature limits. The most common salt used in CSP plants is Solar Salt, which is a mixture of potassium nitrate and sodium nitrate (60% KNO<sub>3</sub> and 40% NaNO<sub>3</sub>). Many of the other salts are under development.

**Liquid Metals.** Some liquid metals proposed as advanced reactor coolants also possess characteristics suitable for storage, including sodium and lead [19]. Some metals and their alloys possess unique characteristics, e.g. low melting points close to or below ambient temperature, yet have a very high boiling point that avoids phase change issues. Liquid metals possess outstanding heat transfer characteristics including a very high thermal conductivity and heat transfer coefficient. However, liquid metals are very expensive and are prone to corrosion. In addition, sodium is a fire risk in air and lead-bismuth eutectic is toxic.

**Table 2-5 Properties of commonly used molten salts [27]**

<b>Composition</b>	<b>Operating Temperature Range (°C)</b>	<b>Viscosity (mPa·s)</b>	<b>Density (g/cm<sup>3</sup>)</b>	<b>Heat Capacity (kJ/(kg· °C))</b>	<b>Cost (\$/kg)</b>
Solar Salt	220-600	3.2	~1.8	~1.5	0.50
Hitec	142-535	3.1	~1.9	1.56	0.93
LiNaK carbonates	400-850	4.3	1.8	~1.4-1.5	~1.2-1.3
LiNaK fluorides	454-700	N/A	1.9	1.89	>2.0
ZnNaK chlorides	204-850	4.0	~2.0	0.81	<1.0
MgNaK chlorides	380-800	4.0	~1.6	~1.0	<0.5

**Solid Media Energy Storage.** Solid media storage systems offer a form of sensible thermal energy storage for high temperature applications. Common solid materials used for thermal energy storage include concrete, bricks, and rocks that are inexpensive, environmentally friendly, and easy to handle and manipulate. With a solid media storage, a heat transfer fluid is used to transfer energy to the thermal energy storage, typically through a heat exchanger [24].

### 2.2.2 Thermal Storage Mechanisms

A popular thermal energy storage system uses tank systems containing heat transfer fluids (HTF) to store heat. The system may consist of one or two insulated tanks.

**Two-Tank Direct.** An example of a two-tank direct storage system with a CSP plant is shown in Figure 2-2 (a). In this configuration, a single HTF is used to collect heat from the generation source and for storage. The HTF uses two large tanks with one kept hot while the other is kept cold.

The HTF is pumped from the cold tank to the power tower collector to receive heat from the heat source and is then pumped into the hot storage tank. For mass balance, the mass flow out of the cold tank must equal the mass flow into the hot tank and is based on the heat generator rate in the power tower collector. The HTF is also pumped from the hot tank through the steam generator back into the cold tank to exchange heat to the power cycle. For mass balance, the mass flow out of the hot tank must equal the mass flow into

the cold tank and is based on the power need for the power cycle. Therefore, the hot and cold tank outlet flow rates can be controlled independently to meet power balance with the heat source and the power cycle.

Charging of the TES occurs when the heat generation rate of the power tower collector is greater than the demand of the steam cycle. This requires a greater mass flow rate out of the cold tank into the hot tank than out of the hot tank into the cold tank. This causes the level of the hot tank to increase over time. Conversely, this causes the level of the cold tank to decrease over time to achieve mass conservation. Discharging of the TES occurs when the heat generation rate of the power tower collector is less than the demand of the steam cycle. To meet the required demand in the steam cycle, the hot tank is required to discharge, and this causes the level of the hot tank to decrease over time.

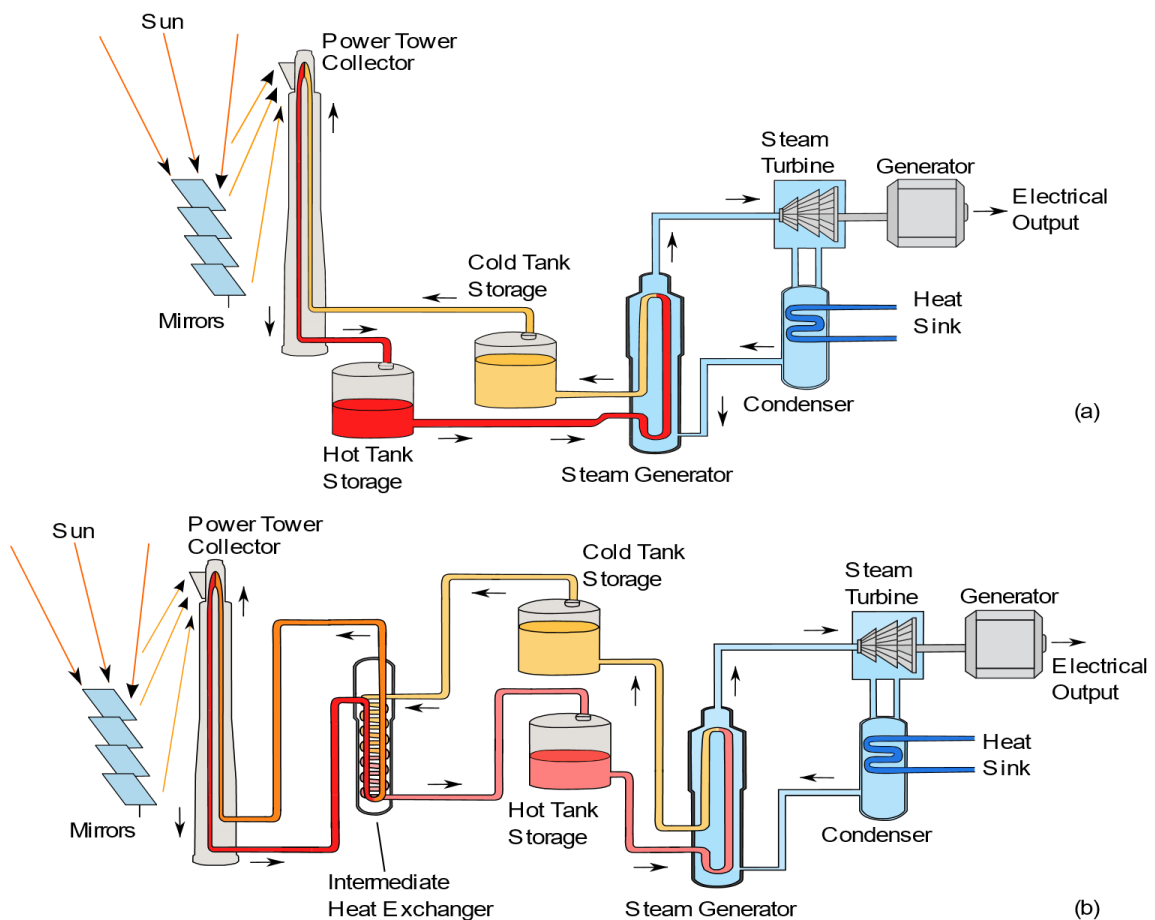


**Figure 2-2 (a) Thermal solar power plant with two-tank direct and (b) Two-tank indirect thermal energy storage**

**Two-Tank Indirect.** An example of a two-tank direct storage system with a CSP plant is shown in Figure 2-2 (b). The difference as compared to the two-tank direct system is there are two separate HTF loops [26]. The primary HTF collects heat from the source and transfers heat to the storage HTF through the intermediate heat exchanger. Like the direct configuration, the mass flow rate out of the hot and cold tanks can be independently adjusted, but the tanks are in the intermediate loop in this configuration. The difference compared to the direct configuration is the required hot tank inlet flow rate is based on the heat exchange rate across the intermediate heat exchanger. The charging and discharging processes are the same as for the direct configuration.

**Single Thermocline Tank.** A single tank thermocline system is similar to the two-tank indirect system but instead uses a single tank separated by a thin thermocline region as shown in Figure 2-3. These systems rely on thermal buoyancy to maintain thermal stratification and discrete hot and cold thermal regions of the TES system. Similar to the two tank configurations, the charging and discharging are controlled independently through adjusting the flow rates in and out of the hot region of the storage tank.

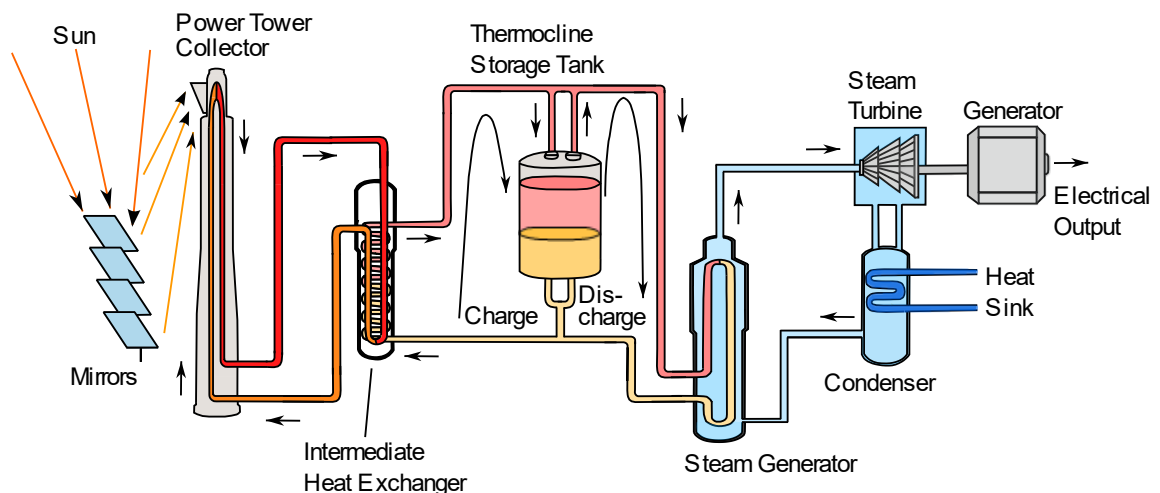


**Figure 2-3 Thermal solar power plant with thermocline thermal energy storage system**

## 2.3 Considerations for SMR Integration into Microgrids

SMRs must be technically and economically viable to be able to integrate them into microgrids for off-grid communities.

### **Technical Considerations of SMRs**

On-grid NPPs are large units that consistently operate in baseload mode at their maximum output and do not routinely adjust their power levels. A measure of the amount of actual power produced from an NPP compared to the maximum power production capacity is defined as the unit capacity factor. In some very special cases, traditional on-grid NPPs can still adjust output power to meet the demands of the grid in load-following modes [28]. Load-following reactors can either operate in frequency control mode to provide grid services through fine adjustments within the order of seconds, typically within  $\pm 2\%$  of the rated power, or can follow a pre-set variable load pattern with one or two power changes in a 24-hour period [28].

To operate within safe operating ranges, there are limits to the allowable rate, magnitude, and frequency of changing the reactor power in load-following mode. For example, the European Utilities Requirements (EUR) set limits on planned load-following, including allowable ramp rates to be less than 5% of the rated power per minute between 50-100% of full power [28]. The number of power maneuvers is limited to no more than 2 per day, 5 per week, and 200 cumulatively per year [28]. Any finer adjustments required for the grid power balance must be accomplished by other generating sources [28].

When performing a power maneuver, power balance is required between the core primary loop and the power cycle loops of the NPP. Currently, these power maneuvers are done by modifying the reactivity within the core through control rods or neutron absorbers in the reactor [29]. A required change in plant power level is accomplished by first changing either the core heat production rate or the steam heat load, which then requires adjustments to the other systems to meet the power balance. The methods used to achieve this power balance can be either (1) maintaining a constant average temperature in the primary loop, with the saturation temperature and steam pressure

varying with the reactor power, or (2) maintaining constant pressure in the secondary loop, with the average temperature in the primary loop varying with the reactor power [28]. However, load-following through these methods can cause thermo-mechanical stresses on components in the core and neutron flux instabilities.

Some proposed SMRs are designed to be able to offer more flexibilities defined in terms of the limits to the allowable rate, magnitude, and frequency of changing reactor power in the load-following mode. However, these SMRs are still limited by the thermo-mechanical stresses and neutron flux instabilities in the core.

### **Economic Considerations of SMRs**

NPP costs are primarily capital costs, with very low relative fuel costs, which incentivize plants to operate at the maximum power output in the baseload mode. However, operating in flexible modes is required within a microgrid. Current load-following methods can waste generation potential when de-rating the reactor. The NPP capital costs can be much higher compared to other generation sources, so minimizing these capital costs and increasing plant capacity factors can improve the economic viability of SMRs.

In relation to SMR cost estimates, there is large uncertainty and even more so for off-grid SMRs. There is no strong literature basis to assess SMR costs for these categories, and only certain vendors have made their estimates public, and they do not include breakdowns of their costs [30]. There is significant uncertainty in the methodology to assess these costs and the most significant aspect is the capital costs. It is unclear how much economies of scale will apply to SMRs, and how much innovative designs and construction techniques have the potential to reduce costs.

There are several studies that estimate SMRs costs compared to that of the current diesel systems. One study [31] estimates that the cost of a 10 MW SMR can be comparable and even less than a 10 MW diesel generator. Another study [32] similarly concludes that a range of SMR designs under development have the potential to be cost comparable with diesel generators. However, another study [33] has the opposite conclusions and state that

SMR costs will be much higher than diesel generators, but is acknowledged as a rough first estimate.

The uncertainty in the estimated costs is based on the uncertainty in how the cost of current nuclear plants compare to new smaller and innovative designs. The most used estimate for small nuclear plants is the power law model, which derives the cost from those of large reactors when there is no empirical experience [31], [33]. However, this comparison assumes that everything is the same between a large scale NPP and a smaller plant except for their size [34]. It does not take any of the innovative design and construction features into account. The capital cost of an off-grid SMR  $C_{SMR}$  with power rating of  $P_{SMR}$ , is scaled by the capital costs of a large scale NPP defined as  $C_{NPP}$  that has a power rating of  $P_{NPP}$ . The SMR capital cost is correlated based on an exponent defined as  $s$  that is estimated between 0.5 and 0.7 [56]. The power law correlates the SMR and NPP costs by:

$$C_{SMR} = C_{NPP} * \left( \frac{P_{SMR}}{P_{NPP}} \right)^s \quad (2.3)$$

Without any actual construction experience and uncertainty in the design of current SMRs, it is difficult to accurately estimate the cost of SMRs for off-grid communities. For this reason, SMR cost estimates will not be made in this work. Rather, arguments will be made about the change in SMR cost based on the sizing and the addition of TES.

### **Potential for Alternative Configurations and Operation of SMRs within Microgrids**

Methods to use SMRs in microgrids as a main controllable source are under development. Current load-following methods for on-grid NPPs are not effective for SMRs in microgrids. Instead, SMRs should utilize their enhanced flexibility. However, when this is done, further issues are introduced. Significant power maneuvering can cause problems including neutronic instabilities and thermal stresses on core components and has technical limitations on the allowable rates. Further, reducing the SMR capacity factor through load-following can reduce their economic effectiveness.

There are other potential alternatives to reactor core power maneuvering for load-following to reduce the problems described above. This can be done by integrating a thermal energy storage device with the SMR. This integration can allow the reactor core to operate at constant power to eliminate any thermal or neutronic issues induced by transients. Storing energy during low demand and releasing this stored energy during periods of high demand can maintain a higher overall capacity factor. Further, integrating thermal energy storage can allow for peaking output power above the nominal rating that has the potential to reduce the required SMR core power rating.

## 2.4 Integration of SMRs with TES

### **Development of SMRs with TES**

Thermal energy storage has been proposed for integration with nuclear power plants [4]. So far, this has mainly been considered for on-grid light-water reactors (LWR) to increase the economic competitiveness and allow for integration of renewables over long time horizons. At times of high renewable generation during the day, the TES system can store excess power production from the LWR core while electricity costs are low, and then sell the extra electricity at later times at high electricity prices [35]. TES systems have also been proposed for some advanced nuclear reactors currently under development. Molten salt intermediate storage loops are proposed for sodium-cooled fast reactors by TerraPower, for advanced solid fuel with salt coolants by Kairos Power, for several molten salt reactors including Moltex and Terrestrial Energy, and for off-grid High-temperature Gas-cooled Reactors (HTGR) including the Global First Power Micro Modular Reactor (MMR) [4].

As an example, Moltex Energy proposes a 300 MW Molten Salt Reactor (MSR) based on a “Grid Reserve” molten salt tank storage [36]. An example configuration uses two 300 MW turbines and 3 GWh of storage for 4 hours of peaking of 600 MW [36]. During the rest of the 20 hours, the reactor charges the storage while outputting 240 MW [36]. The turbine and storage can be sized differently for different output profiles. A similar configuration is proposed for the off-grid Global First Power MMR, but there is little design information available in public domain.

## Existing Work Related to SMR Modelling and Integration of TES

Cogeneration of heat and electricity, and TES configurations have been proposed to couple to the power cycle of LWRs. These reactors have outlet temperatures below 350 °C that limit heat usage and storage applications. Typically, steam is extracted from the main steam header, and can be re-directed to an external heat load or can be stored in the TES. Dynamic models have been created to understand the dynamic behaviours of these systems along with control system design.

An example of a cogeneration configuration of an LWR is shown in Figure 2-4 that uses a flexible heat load to extract steam as a means of load-following [37]. The flexible load is described based on the rate of heat consumption and is established through power balance of the steam across the flexible load. The heat consumption rate of the flexible load is defined as [37]:

$$Q_{fl} = \dot{m}_{fl} * \Delta h \quad (2.4)$$

where  $Q_{fl}$  is the heat consumption rate of the flexible load in kW<sub>th</sub>,  $\dot{m}_{fl}$  is the steam mass flow rate delivered from the steam header to the flexible load in kg/s, and  $\Delta h$  is the steam enthalpy change from the inlet to the outlet of the flexible load in kJ/kg.

In this configuration, the reactor core can operate at constant power while varying the mass flow rate to the variable load. This system can perform load-following by adjusting the steam mass flow rate to the turbine by modifying the bypass flow to the flexible load. It is shown through a dynamical model that the reactor core can continue to operate at constant power and at constant outlet temperature, while maintaining steam pressure near the desired value with only small variations [37]. This work demonstrates that adjusting the steam flow rate to the turbine can be used to perform load-following while maintaining a constant steam pressure and temperature.

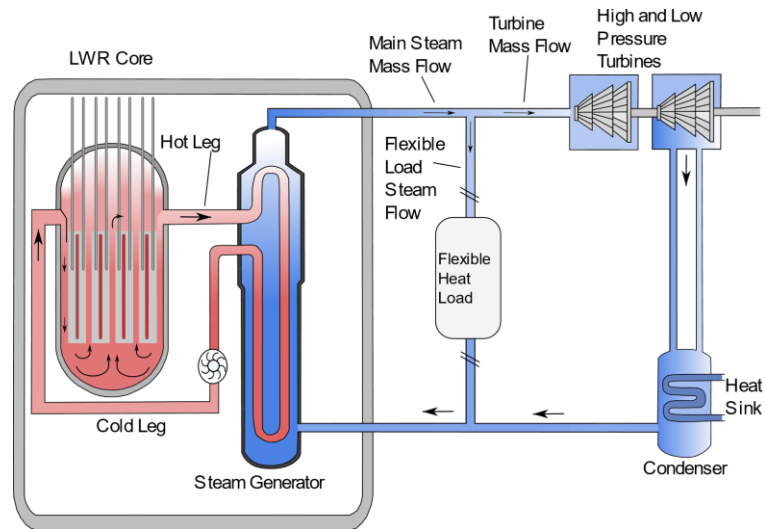


**Figure 2-4 LWR system configuration for load-following through by-passing steam from the main steam header**

Another LWR configuration can add storage of by-passed steam that can be re-introduced to the turbine as shown in Figure 2-5 [38], [39]. A two-tank thermal oil loop can receive heat through a heat exchanger from by-pass steam, that is charged from the cold tank into the hot tank. To produce the peaking output, the hot tank can discharge through a second heat exchanger into the steam driving the low-pressure turbine. The purpose of this configuration is to integrate with renewable generation by smoothing the combined output by adjusting the SMR output accordingly. In this configuration, the hot tank temperature is limited to approximately saturation temperature of the steam source, and the bypass flow is limited to approximately 45% of the nominal steam flow. This configuration can lead to reduced variations in reactor power, primary coolant temperatures, and tank temperatures, while primarily varying the by-pass flow and TES flow rates. These works demonstrate that the steam flow rate to the turbine can be adjusted to control the electrical output, while maintaining the rest of the system at constant steam pressure and temperature. The TES system can re-introduce stored steam back into the turbine while maintaining a constant reactor core power level.

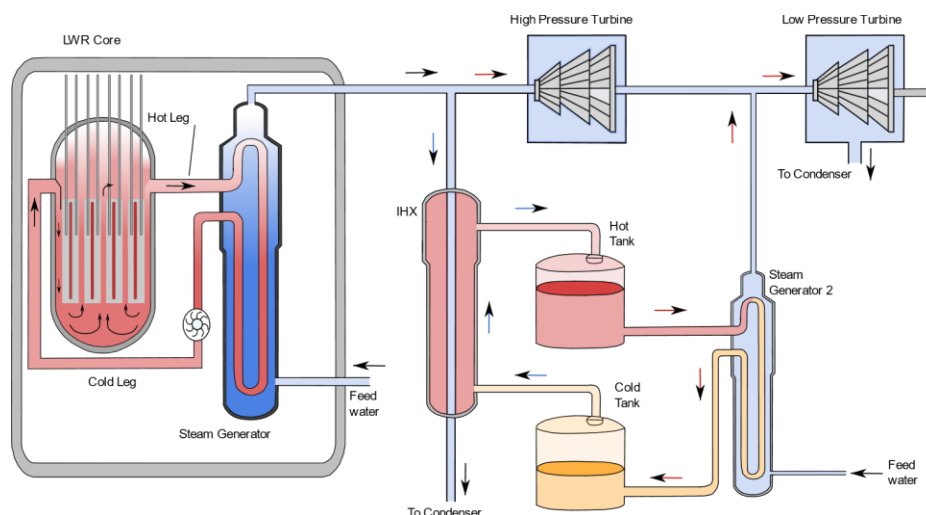


**Figure 2-5 LWR system configuration with TES integrated within the steam cycle**

### **Justification for Analysis of SMRs with TES for Microgrid**

Currently, TES have mainly been proposed for on-grid NPPs as a means for long-term power shaping and have not yet been demonstrated in practice. Many of the reactors identified above are still in their design stages, and very little information is available on the design and operation of the TES systems. Most importantly, SMRs with TES have not been proposed as a means of effectively integrating in microgrids for off-grid communities. In these off-grid communities, the SMRs would be required to rapidly and frequently adjust their power levels to account for load and renewable fluctuations. By storing energy, the effective capacity factor of the SMR can be increased. Integrating TES allows for the load-following to be done with the BOP and TES systems and limit the fluctuations in the core. The ability to produce the peaking output can also allow a reduction in the SMR core power rating that can be economically favorable.

It must be determined: (1) how an SMR can fit into a microgrid, (2) what type and configuration of SMR and TES is to be used, (3) how this system will operate, and (4) suitable sizes of different components in this configuration.

## 2.5 Selection and Description of SMR Type

The purpose of this section is to describe what type of SMR is suited for the given scenario to meet the needs of an off-grid community. SMRs for off-grid applications are currently at the earliest stage of development, and there are still a lot of uncertainties regarding requirements for SMRs to operate in these environments as well as reactor designs and development specifically for Canada. There are several advanced SMR types under development for off-grid applications in Canada as shown in Table 2-6 [40]. The most common reactor type herein is the HTGR that can be advantageous over Lead-Cooled Fast Reactors (LFRs) and Heat Pipe Reactors (HPR) based on (1) a higher TRL for a near-term deployment and (2) higher operating temperature and larger temperature range across the reactor core that can allow for more efficient thermal energy storage.

**Table 2-6 Off-grid SMR designs under development in Canada**

SMR Type	Vendor and Name	Rating (MW <sub>th</sub> /MW <sub>e</sub> )	Core Inlet and Outlet Temperatures (°C)	Refuelling Cycle (yrs)	Source
HPR	Westinghouse eVinci	7-12 / 2-3.5	-/-	3	[41]
LFR	LeadCold Sealer	8/3	432/390	30	[42]
HTGR	USNC MMR	15/5	300/630	20	[40]
HTGR	Starcore	35 / 14	280/750	5	[40]
HTGR	Urenco U-Battery	10 / 4	250/750	5	[43]

### High-Temperature Gas-Cooled Reactor

There is a substantial operating history of gas-cooled reactors around the world that can be leveraged in the current development for off-grid applications. HTGRs use helium coolant and a graphite moderator. They can couple to either a direct or indirect Brayton gas power cycle, or an indirect Rankine steam power cycle. A diagram of a generic HTGR coupled with a steam cycle is shown in Figure 2-6.

There are two types of core designs: the prismatic core or the pebble bed core. Both use TRISO fuels, which contains micro spherical kernels of oxide or carbide fuels that are coated with layers of carbon. Helium is used as the coolant because it is chemically and neutronically inert with respect to the fuel and other structural materials in the core, and it

does not undergo any phase change. The graphite moderator has low neutron absorption, high thermal conductivity, and high heat capacity.

- The prismatic design uses a block of graphite moderator with channels for the fuel and the coolant [44]. The TRISO fuel particles are pressed into cylindrical fuel blocks which are placed in the channels within the moderator. Designs can either have separate fuel and coolant channels, or the coolant can flow concentrically around the fuel channels.
- The pebble bed design uses spherical TRISO particles approximately the size of tennis balls which are placed into a vessel where the helium coolant flows around the pebbles [44]. The moderator is typically in a central cylinder and around the reactor vessel as a reflector.
- The significant differences between the two type are that the pebble bed types allow for online refueling, but the prismatic type has a higher available outlet temperature [44], [45].

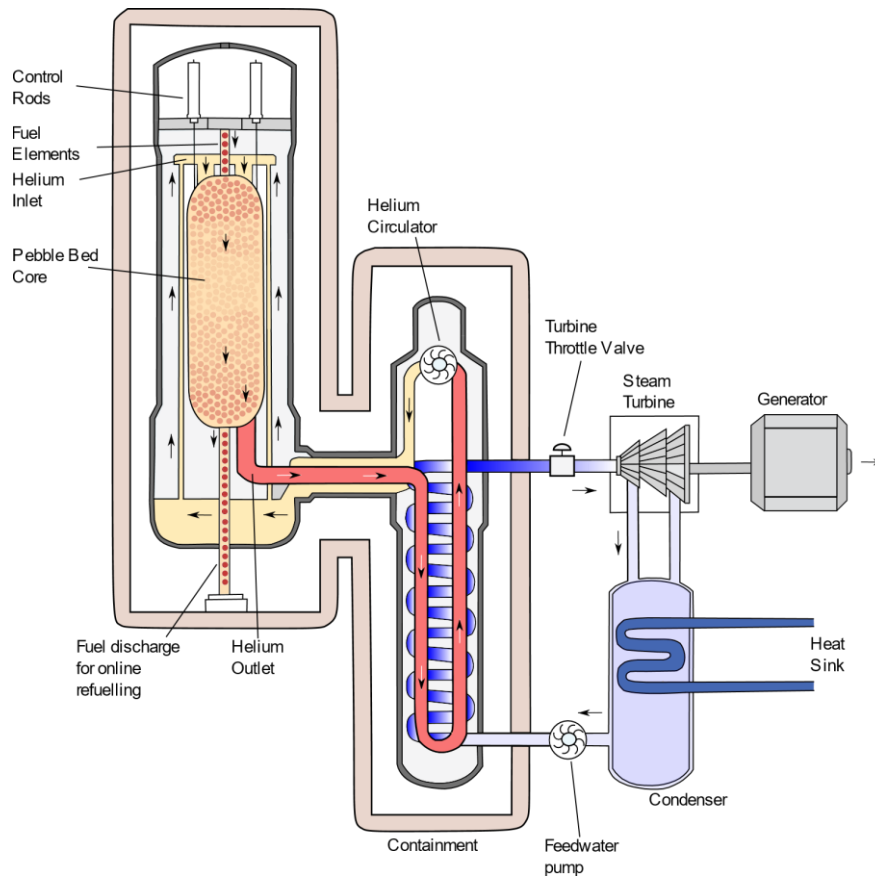


**Figure 2-6 Diagram of High Temperature Gas-cooled Reactor with a steam cycle**

The most significant advantage of HTGRs over other reactor types is:

- High outlet temperature and a large temperature difference across the core due to the use of TRISO fuel, graphite core structure, and helium coolant.
- Higher TRL meaning shorter time to deployment as compared to other reactor types.
- High allowable flexibility and ramp rates based on fuel and coolant characteristics, and no significant fuel limitations during power maneuvering (such as pellet-cladding interaction issues) because of the fully ceramic TRISO fuel.

- Increased safety due to the high operating temperature range of the fuel (which can withstand 2,200 °C during an accident without causing a radioactive release), large negative temperature coefficient, no hydrogen production risk, and the core can withstand accident conditions without relying on active safety systems but only on core conduction and radiation.
- High core outlet temperatures of 600-950 °C can provide high temperature heat for many applications including industrial plants, hydrogen production, and heat storage, while also producing electricity.

### **HTGR Designs**

The IAEA has compiled a survey on all SMR design developments that include current HTGR designs [41]. Some vendors have also made some of their design data available. In this section, reactors with adequate information available are selected and described. They are used as references for design parameters and operation. The selected HTGR designs with important parameters are summarized in Table 2-7. Currently, there is only detailed information available for the GFP MMR-5 and HTR-10 for off-grid HTGRs. The on-grid Xe-100 and HTR-PM are also included for reference and comparison purposes.

The GFP MMR is currently the furthest along in the Canadian Nuclear Safety Commission (CNSC) vendor design review for off-grid reactors, and is planned for use in a demonstration project at Chalk River, Canada [46]. The MMR design is planned to have a molten salt intermediate loop with a two tank thermal energy storage and a tertiary steam power cycle loop. The solar salt in the hot tank located in the intermediate loop will be stored at 560 °C and 100 kPa [47]. However, there are no design details regarding the operation of the intermediate molten salt loop with the storage. The HTR-10 is a Chinese test reactor first operated in 2003. It is used as a reference due to the limited design data available [48].

**Table 2-7 Selected on-grid and off-grid HTGRs under development**

<b>Properties</b>	<b>Xe-100</b> [49], [50]	<b>HTR-PM</b> [51]	<b>MMR</b> [47]	<b>HTR-10</b> [52]
Thermal power/Electric Power (MW)	200/82.5	2x250/210	15/5	10/3
Inlet/Outlet Temperature (°C)	260/750	250/750	300/630	250/700
Helium Pressure (MPa)	6	7	3	3
Helium flow rate (kg/s)	79	88	8.8	4.32
Feedwater/Steam Temperature (°C)	205/565	205/538	-/-	104/440
Secondary Pressure (MPa)	16.5	13.5	-	4
Steam Flow Rate (kg/s)	79	155.4	-	3.49

### 2.5.1.1 HTGR Methods of Operation

Both the Xe-100 and HTR-10 operate in similar ways during load-following operation. In the primary loop, the helium pressure is held constant, while the helium mass flow rate and core inlet and outlet temperatures vary with power levels. Within the secondary loop, the turbine inlet pressure and temperature remain constant, while the turbine and feedwater steam flow rate vary with the reactor power. The variations in these parameters at two different power levels are demonstrated by the HTR-10 design data as summarized in Table 2-8.

**Table 2-8 HTR-10 design data at 100% and 30% full power**

<b>Reactor Parameter</b>	<b>100%</b>	<b>30%</b>	<b>Source</b>
Reactor Thermal Power(MW <sub>th</sub> )	10.0	3.0	[52]
Helium Pressure (MPa)	3.0	3.0	[52]
Helium Flow Rate (kg/s)	4.32	1.29	[52]
Helium Inlet/Outlet Temperature (°C)	250/700	195/645	[52]
Secondary Water/Steam Temperature (°C)	104/440	-/440	[52], [53]
Feedwater Mass Flow Rate (kg/s)	3.49	-	[52]
Steam Pressure (MPa)	4.0	4.0	[53]
Feedwater Pressure of SG (MPa)	6.1	-	[54]

The load-following capabilities have been demonstrated and summarized in Table 2-9, where a Xe-100 reactor uses five manipulated variables for load-following control. While this method is used to control HTGRs during power maneuvering, the design and

operation of an HTGR with TES will be different, which requires different control strategies, but some aspects of this methodology can still be utilized.

**Table 2-9 The manipulated and controlled variables of X Energy Xe-100 during load-following operations [55]**

	<b>Manipulated Variable</b>	<b>Controlled Variable</b>	<b>Explanation</b>
1	Turbine throttle valve position	Electrical output	Through a transient, the fastest way to ramp the power up and down is to manipulate the throttle valve on the turbine
2	Helium circulator speed	Main steam pressure	When the turbine throttle valve is closed to change electrical output to a lower level, steam pressure increases, and the helium circulator speed is manipulated to maintain constant steam pressure
3	Feedwater pump speed	Main steam temperature	The feedwater pump speed is manipulated to maintain a constant steam temperature
4	Turbine extraction steam pressure through turbine extraction steam valve	Secondary feedwater temperature	Manipulating the turbine extraction steam valve controls the pressure which maintains a constant feed water temperature
5	Control rod position	Steam generator inlet temperature	The control rod position is manipulated to maintain a constant reactor outlet temperature

## 2.5.2 High Temperature Gas-Cooled Reactors with TES

As described in the previous section, it is advantageous to use an HTGR over other reactor types, especially for off-grid applications. This reactor design has enhanced safety features, and high allowable flexibility and ramping due to the fuel and coolant characteristics. While this reactor type has good flexibility for power maneuvers, this is not the preferred mode of operation. When integrating thermal energy storage, the high outlet temperature and large temperature differences across the core increase the storage efficiencies. From Eq. (2.2), doubling the hot-to-cold temperature swing of the material

doubles the amount of stored heat per unit mass of the material [4]. The helium and graphite reactor components are also compatible with most storage materials.

HTGRs are a viable type of SMR to be deployed in the near term for off-grid communities. They have very attractive reactor characteristics, and can be efficiently coupled with thermal energy storage to enhance overall microgrid operation.

## Chapter 3

### 3 Configuration and Analysis of Microgrid with SMR and Thermal Energy Storage

The goal of this work is to develop a reliable and cost effective microgrid system to replace diesel generation for off-grid communities in Canada. This solution would utilize an SMR based microgrid incorporating intermittent renewable energy resources in the form of PV power, with thermal energy storage to enable increased flexibility of the SMR.

The configuration of the SMR-TES system must be defined along with descriptions of other system components for the sizing methodology of the microgrid. There are many variables within such a microgrid that are dependent on the components, configurations, and their sizing. The sizing scheme should be based on (1) steady-state analysis considering effects of sizing of components on economic and technical feasibility of the candidate system, and (2) dynamical analysis of the integrated system to determine rates of change and variability of related components. In this work, steady-state modelling and analysis will provide information to determine if a proposed configuration is technically and economically feasible. This will be done through simplified system modelling and establishing system boundaries and state parameters necessary to maintain the power balance. Dynamical modelling will account for rapid variability in load and non-dispatchable sources and will be used to analyze the limitations of SMR load-following capability. Results from this analysis will determine electrical storage requirements and will lead to possible revisions to the sizing from the steady-state analysis.

#### 3.1 Description of System Components

First, a description of the different microgrid components is required. A benchmark community is chosen to represent some common characteristics of off-grid communities. A simplified schematic of the power system for this off-grid community is shown in Figure 3-1. Let  $L[k]$  represent the power required to support this community, where  $k$  is the time indexing variable. This time index is iterated throughout a day in one hour or shorter increments. The power produced by the generation sources are defined as  $P_{SMR}[k]$

for the SMR and  $P_{PV}[k]$  for the PV system. The SMR for this system is flexible enough to meet the load demand by complementing the PV generation. Because the SMR system has finite output ramp rates, an electrical energy storage device is used to balance the remaining power variations due to rapid load fluctuations or renewable energy variations. The electrical energy storage system can either absorb or deliver power to maintain power balance and the power of the EES system is defined as  $P_{EES}[k]$ . In order to analyze this system, a description of each of these component is provided next.

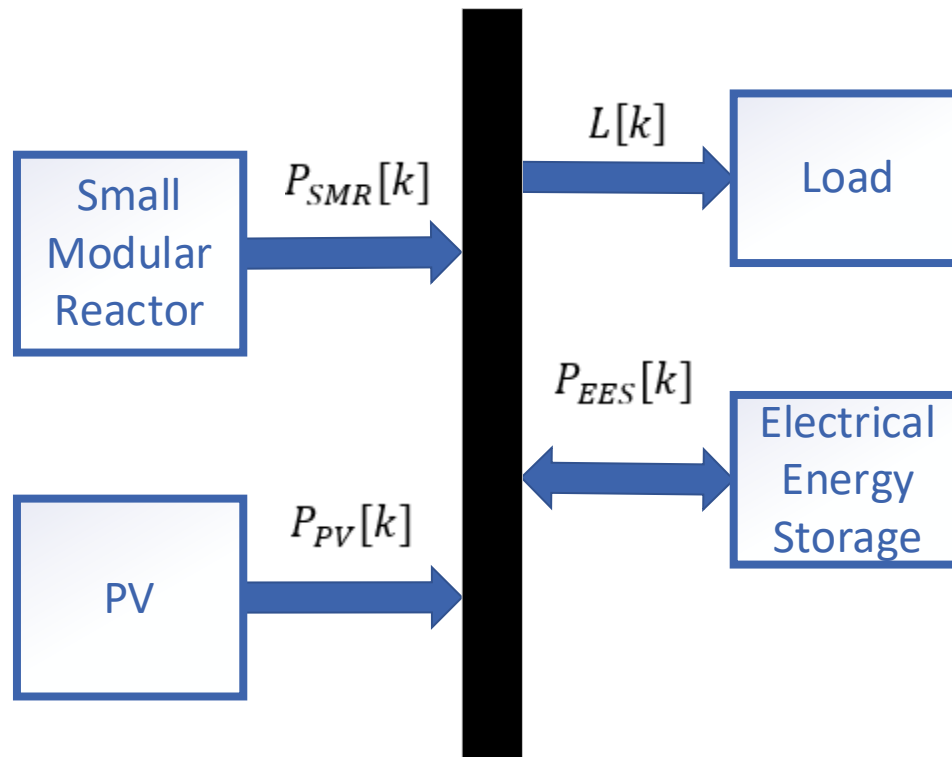


**Figure 3-1 Simplified schematic for off-grid microgrid**

### 3.1.1 Demand Profile

Off-grid communities have unique electrical demand characteristics that can be described by seasonal and daily trends plus variability on hourly or even shorter timescales.

## Demand Limits

This section models the demand profiles and defines the frequency and magnitude of the considered fluctuations. The typical demand profile for the KLFN community over one year [10] is shown in Figure 3-2 (a), where the demand is maximum in the winter months and minimum in the summer months. The four added points can be used to define the extremes of the annual demand, identified as  $L_{S1}$ ,  $L_{S2}$ ,  $L_{W1}$  and  $L_{W2}$  in kW as shown in Figure 3-2 (a).  $L_{W1}$  is defined as the maximum annual demand and  $L_{S1}$  is defined as the minimum daily peak value of the year.  $L_{W2}$  and  $L_{S2}$  are defined as the minimum daily values associated with  $L_{W1}$  and  $L_{S1}$  respectively. The annual minimum demand corresponds to  $L_{S2}$ . For example, this community could have electricity limits defined as:

$$L = \begin{cases} L_{W1} = 850 \text{ kW} \\ L_{W2} = 350 \text{ kW} \\ L_{S1} = 500 \text{ kW} \\ L_{S2} = 200 \text{ kW} \end{cases}$$

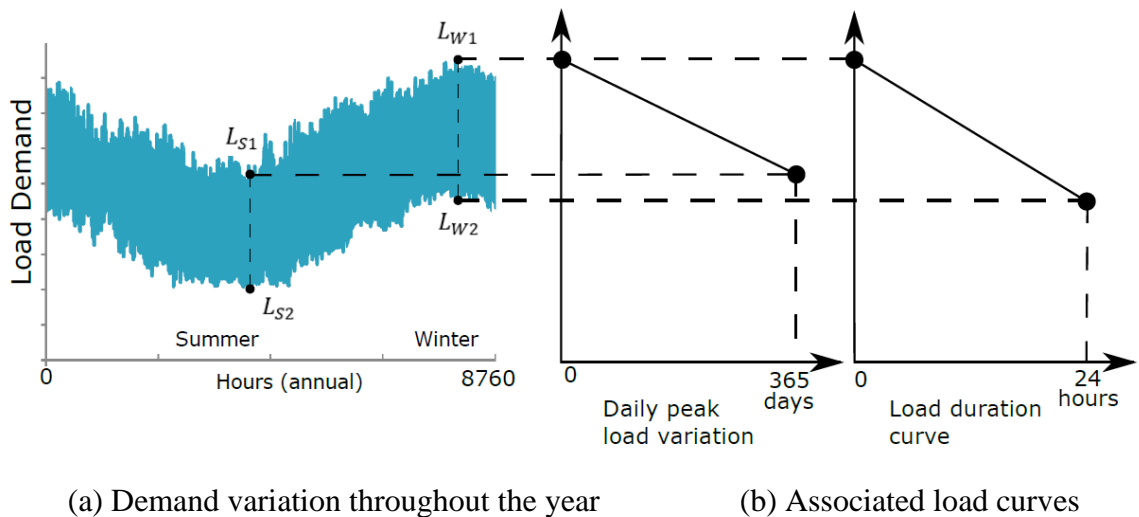


**Figure 3-2 (a) Example of the annual power demand of a remote community and (b) Load curves to define limits on the demand**

The associated load curves of this typical demand profile are shown in Figure 3-2 (b). The daily peak load variation is determined from re-ordered peak demand values from each day in the year in descending order, and describes the ranges of daily peak values. The load duration curve is determined from re-ordered demand values from the hours in

the day in descending order, and describes the ranges in daily demand. Instead of defining the four separate values of the limits of the demand as above, load duration curves can be used to describe the relation between these values more easily.

The timeseries demand can be considered to vary within an interval  $L^I$  with generic lower and upper limits of  $\underline{L}$  and  $\bar{L}$ . The limits can be considered either as the extreme values of the load within a defined time (such as over a year) or can be considered as time varying when considering the behaviour at specific times. In the second case, the time varying lower and upper limits are described as  $\underline{L}[k]$  and  $\bar{L}[k]$ .

The two intervals for the limits of the daily demand throughout the year can be defined as the summer interval  $L_S^I$  with bounds of  $[L_{S2}, L_{S1}]$  and the winter interval  $L_W^I$  can be defined with bounds  $[L_{W2}, L_{W1}]$ . To replace the four values of the limits of the demand with related parameters, three parameters are defined. These defined parameters are first the maximum annual electricity demand  $L_{max}$  in kW. The second parameter defined is the variation in daily peak demand throughout the year  $\sigma_Y$  that corresponds to the daily peak load variation from Figure 3-2 (b). The third parameter defined is the variation in the daily demand  $\sigma_D$  that corresponds to the load duration curve from Figure 3-2 (b). The two variation parameters can be defined from the extreme points as:

$$\sigma_Y = \frac{L_{S1}}{L_{W1}} \quad (3.1)$$

$$\sigma_D = \frac{L_{W2}}{L_{W1}} \quad (3.2)$$

From the example community from above, the variation in daily peak demand throughout the year can be determined from Eq. (3.1) to be 0.6 meaning the daily peak demand can vary up to 60% from the maximum throughout the year. The variation in the daily demand can be determined from Eq. (3.2) to be 0.4 meaning the demand throughout a day can vary up to 40% from the daily maximum.

The summer and winter intervals can then be described in terms of the maximum demand and the variation parameters. By setting  $L_{W1}$  as the maximum annual demand  $L_{Max}$ , and

substituting Eq. (3.2) into the winter limits  $[L_{W1}, L_{W2}]$ , the winter interval can be described as:

$$L_W^l = [\sigma_D * L_{max}, L_{max}] \quad (3.3)$$

By substituting Eq. (3.1) and (3.2) into the summer limit  $[L_{S1}, L_{S2}]$  and defining the summer daily variation as  $L_{S2} = \sigma_D * L_{S1}$ , the summer limits can be described by:

$$L_S^l = [\sigma_Y * \sigma_D * L_{max}, \sigma_Y * L_{max},] \quad (3.4)$$

From this description, any community demand limits can be described by the three defined parameters. For example, another community could be described with a maximum demand of 2,000 kW, a variation in daily peak demand throughout the year of 0.75 and a variation in the daily demand of 0.5. From these parameters, the summer and winter intervals that capture the extremes of the demand can be determined from Eq. (3.3) and Eq. (3.4) to be  $L_W^l = [1000, 2000] \text{ kW}$  and  $L_S^l = [750, 1500] \text{ kW}$ .

### **Demand Profiles and Variability**

The specific demand profiles for a community can vary greatly but there are typical trends to the shape of the demand curves. Demand profiles typically show increases in the morning hours with peaks in the evening, with minimum demand overnight [9], [36], [56], [57].

The daily timeseries demand for a community for a given month can be described as a random process. The timeseries demand each day can be considered as a realization, with a set of realizations for the month (i.e. 30 realizations). Then cross-sections (ensemble average) at regular timesteps result in the description of the mean average timeseries demand for a day [58]. The average timeseries demand for this month can be defined as  $L_{avg}[k]$  in kW that is based on the ensemble averages. The maximum variance in the cross-sections can be defined as the timestep variation parameter  $\sigma_S$  in kW. Then the mean timeseries demand can be considered to be bounded by the upper and the lower demand limits based on the time-step variation parameter. An actual realization of the demand will vary around the average timeseries demand and will be contained within the

upper and lower bounds. This method can be applied to the two seasonal limits of the demand to describe the seasonal and daily variations in the demand.

An illustrative example of this description of the demand is shown in Figure 3-3. The average timeseries demand bounded by the lower bound and upper bound that varies in time. For a specific example from Figure 3-3 at  $k=10$ , a realization of the actual demand of 640 kW varies from the average demand of 670 kW due to random fluctuations. At this timestep, the actual demand will always greater than 540 kW and always less than 800 kW from the upper and lower bounds.

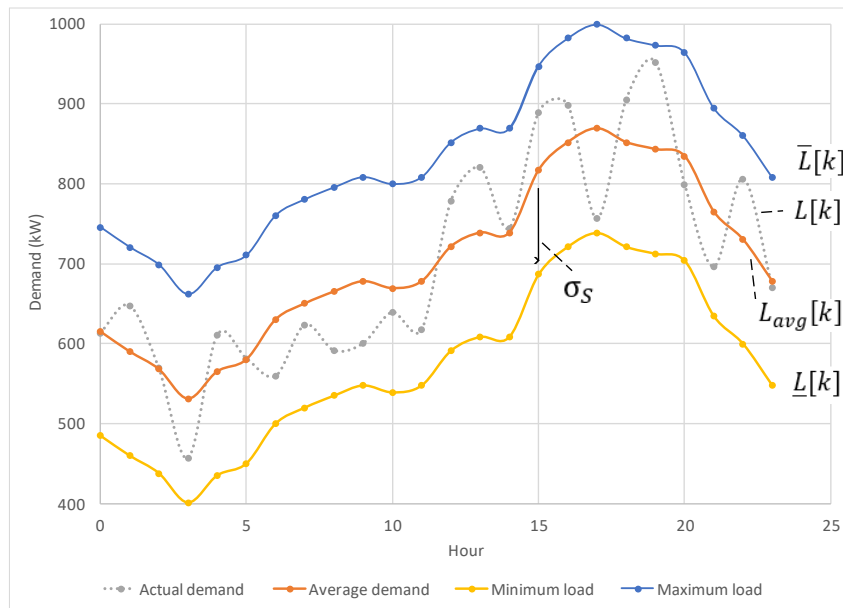


**Figure 3-3 Typical timeseries demand represented by a timeseries mean bounded by variance within lower and upper limits**

In order to describe the demand of a benchmark community without community data, data is generated that contains important characteristics from community demand. This is considered synthetic demand, where the actual demand is composed of the mean demand and stochastic variations. The average demand can be described by a timeseries [59] based on a polynomial function. A stochastic perturbation factor defined as  $\alpha[k]$  can be calculated from a random variable that scales the actual demand to create synthetic variability [59], [60]. The perturbation factor is calculated from a random variable defined as  $\delta_S[k]$  from a normal distribution with mean of zero and standard deviation

equal to the timestep variability parameter ( $\sigma_s$ ) normalized to the maximum demand [59]. The random variable can be described as:

$$\delta_s \sim N\left(0, \frac{\sigma_s}{L_{max}}\right) \quad (3.5)$$

where  $N$  represents the normal distribution described by the mean and standard deviation parameters. The perturbation factor at each timestep is determined from the value of the normal random number drawn at each timestep [59]:

$$\alpha[k] = 1 + \delta_s[k], \forall k \quad (3.6)$$

Limits can be applied to the allowable range of the normal random number based on the number of standard deviations included to set the lower and upper bounds. The timeseries stochastic demand can then be described by the average demand scaled by the perturbation factor from:

$$L[k] = L_{avg}[k] * \alpha[k], \forall k \quad (3.7)$$

The synthetic demand example values from Figure 3-3 can be explained using the above models. The maximum demand is 1,000 kW and the timestep variability parameter is 130 kW that corresponds to a normalized standard deviation of the random variable of 13%. This results in limits on the values of the stochastic perturbation factor within the interval [0.87,1.13] considering limits of one standard deviation. As can be seen from Figure 3-3 at  $k=20$ , the average demand is 834 kW based on a typical demand curve from a polynomial function. The lower limit is 700 kW, and the upper limit is 965 kW at this time based on the ranges of the stochastic perturbation factor. The random number is drawn from (3.5) and in this example run has a value of -0.06. The actual perturbation factor at this timestep is calculated from Eq. (3.6) to be:

$$\alpha[20] = 1 + \delta_s[20] = 1 - 0.06 = 0.96 \quad (3.8)$$

This perturbation factor scales the average demand at this timestep from Eq. (3.7) to calculate the synthetic demand to be 800 kW from:

$$L[20] = L_{avg}[20] * \alpha[20] = 834 \text{ kW} * 0.96 = 800 \text{ kW} \quad (3.9)$$

### 3.1.2 Renewable Generation Characteristics

Renewable generation can be considered as a variable source since its output at any time is uncertain. Within this microgrid, it is desired to maximize the use of the available PV power.

#### **PV Description**

PV panels convert solar irradiance directly into electricity, but the output is dependent on multiple parameters including ambient and cell temperatures and interfacing power electronic characteristics. A simplified description of the output characteristics of a generic PV system will be used in the current study. The correlation of the PV panel power output with the incident solar irradiance  $G[k]$  will be described next.

Solar irradiance has diurnal patterns where the value increases from zero at sunrise to a maximum near midday and then decreases to zero again at sunset. Seasonal variations include longer day light in the summer months with higher peak values, whereas shorter day light and minimal peak values occur in the winter months. Stochastic weather effects, including clouds, reduces incident solar irradiance on the PV panels. Such situations can occur over long periods of time or on very short timeframes.

To evaluate the potential of PV resources and the characteristics of PV output for a benchmark community, NREL's PVWatts calculator [61] can be used to estimate hourly power production from a PV system over one year based on stochastic weather patterns [62]. Solar irradiance potential is assumed to be similar for a common latitude in northern Ontario [9] and the solar irradiances for summer and winter months at a generalized location are summarized in Figure 3-4, where the hourly minimum, maximum, and average values are found from the ensemble data of the month. It is interesting to note that the shapes of the solar irradiance curves are similar between the two seasons from Fig 3-4. However, the area under the curves corresponding to the total energy produced over a day is much greater in the summer due to higher peak values and longer day light hours. Generic parameters were selected within the PVWatts software including 1-axis tracking with  $0^\circ$  tilt,  $180^\circ$  array azimuth, with 10% system losses and 96% inverter

efficiency. They do not represent optimized orientation parameters for a specific community, but rather are used to describe the general characteristics and trends of solar irradiance and PV output in remote northern regions. Detailed site specific data with optimization studies for PV placement is considered beyond the scope of this work. This would be considered as future steps in the refinement of this microgrid system.

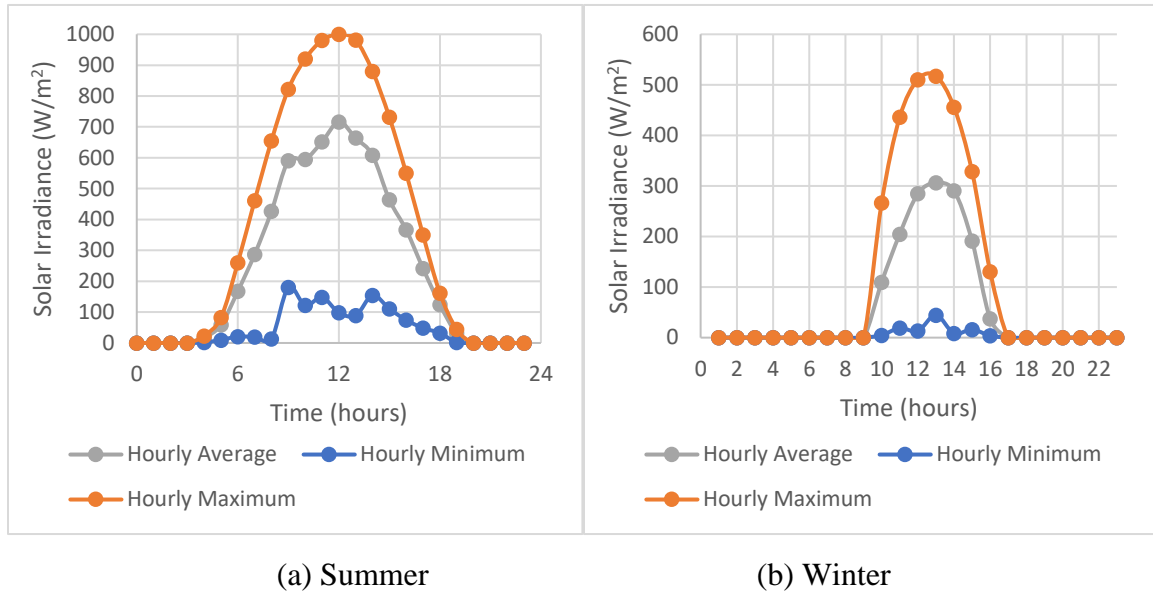


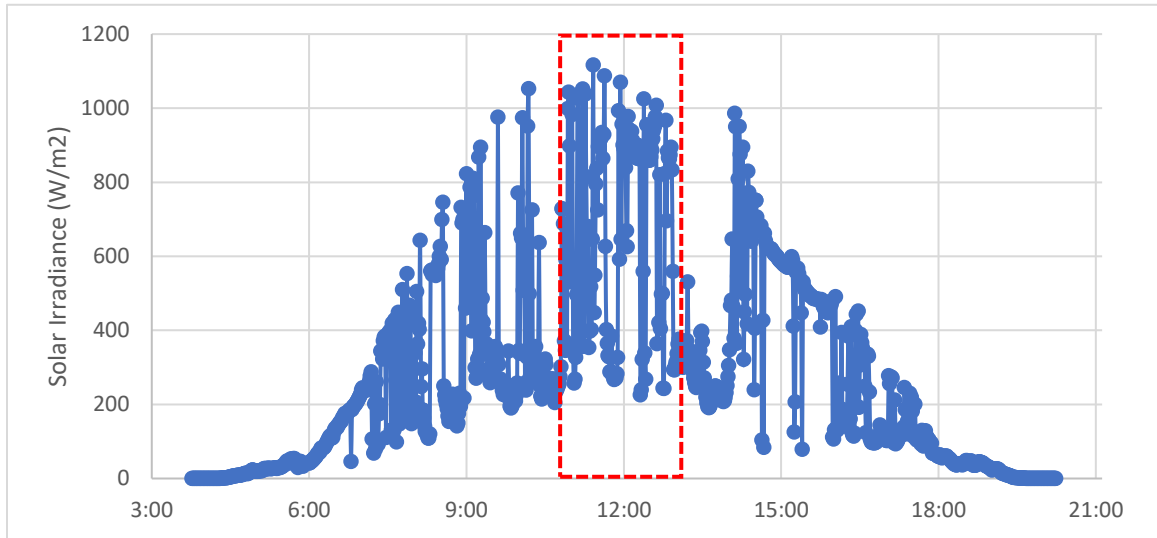
**Figure 3-4 PV potential from PVWatts Calculator showing range of daily trends in summer and winter seasonal limits**

High resolution solar irradiance datasets can provide information on rapid fluctuations in PV output power. A dataset is taken from [63], and is summarized in Figure 3-5. Solar irradiance ramp rates in %/min can be defined as the change in solar irradiance from the beginning to end of a time interval, normalized by the maximum global solar irradiance value, and can be described as:

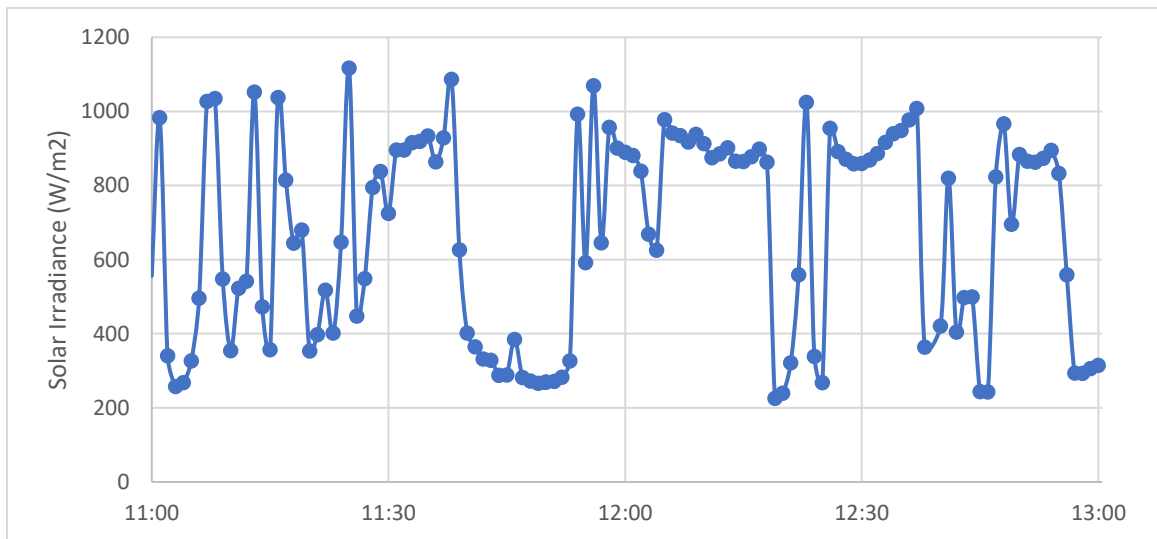
$$RR_{PV} = \frac{1}{G_{max}} * \frac{G[k] - G[k-1]}{\Delta_k} \quad (3.10)$$

where  $G[k]$  and  $G[k - 1]$  is the measured solar irradiance in  $W/m^2$  measured at timestep  $k$  and the previous timestep  $k-1$ ,  $\Delta_k$  is the time duration between timesteps, and  $G_{max}$  is the maximum global solar irradiance value which is typically set at  $1,000 W/m^2$ . It is found from the dataset that the solar irradiance in a volatile day can vary as much as 60%

from the maximum solar irradiance in 1-minute measurements. The frequency of solar irradiance ramp rates is defined as the number of occurrences of ramp rates within a range of values. For example, it was found that the frequency of high ramp rates above 50 %/min are low and many of the ramps occur at rates less than 5 %/min.



(a) Full day



(b) Between 11:00 and 13:00

**Figure 3-5 Solar irradiance dataset measurements for a volatile day**

PV output correlates with solar irradiance. The nominal solar irradiance curve corresponding to the maximum curve from Fig 3-4 can be approximated by a timeseries

that is defined as  $\overline{G}[k]$ . The addition of a component of variability of solar irradiance can exhibit stochastic effects in a similar way to that of the community demand. This variability causes the actual solar irradiance to differ from the nominal solar irradiance. With the assumption that the ratio of the actual PV panel output to the actual solar irradiance is proportional to the ratio of the rated PV output to the maximum solar irradiance, the output power of the PV system can be described by:

$$\frac{P_{PV}[k]}{G[k]} \propto \frac{P_{PV}^{size}}{G_{max}} \rightarrow P_{PV}[k] = P_{PV}^{size} * \frac{G[k]}{1000} * \eta_{PV} \quad (3.11)$$

where  $P_{PV}[k]$  is the actual PV output at timestep  $k$  in kW,  $P_{PV}^{size}$  is the installed PV capacity in kW,  $G[k]$  is the incident solar irradiance at timestep  $k$  in  $\text{W/m}^2$ ,  $G_{max}$  is the maximum solar irradiance and is a constant taken to be  $1,000 \text{ W/m}^2$ , and  $\eta_{PV}$  is the correlating constant corresponding to the system efficiency that represents any losses in the system.

The relation from Eq. (3.11) can be compared with data from the PVWatts calculator. The PVWatts calculator uses a detailed model to calculate solar irradiance from the sun's position and synthetic weather patterns, and accordingly calculates PV panel output [62]. The PVWatts software was used to collect the nominal solar irradiance from a defined location (Lat, Lon: 53.05, -93.3) and the nominal timeseries PV output in the summer for a 1 kW system. The nominal solar irradiance from the PVWatts calculator using generic parameters was then used to calculate the correlated PV output using Eq. (3.11). The two PV power output curves are shown in Figure 3-6 which shows a strong correlation between the calculated output and the reference PVWatts output. The root mean squared error was calculated between the two timeseries and is calculated to be 0.0138 which confirms the correlation between solar irradiance and output power from Eq. (3.11) is sufficient for this analysis.

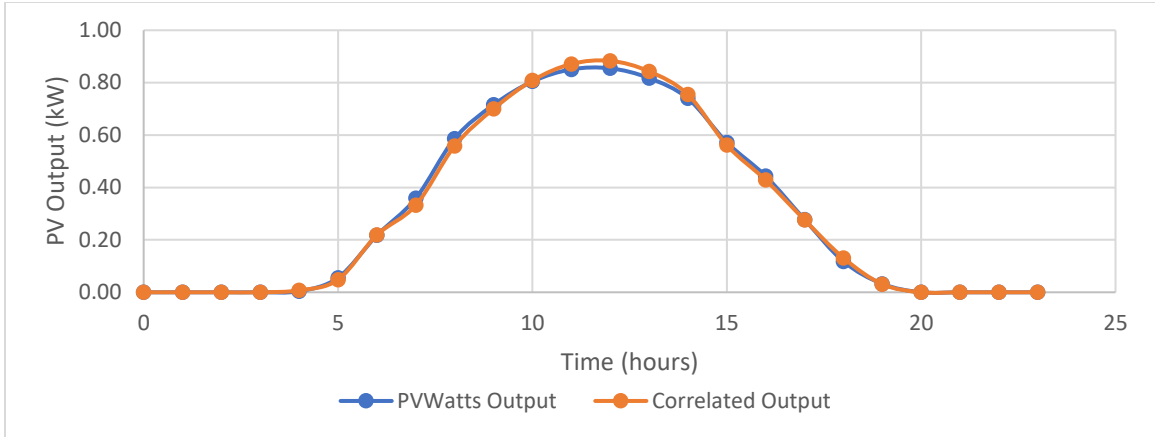


**Figure 3-6 Comparison of PV model with PVWatts calculator**

### 3.1.3 SMR as a Controllable Source

A basic requirement for any power system is to maintain the power balance. At any time, the power from the combined sources and storage should be equal to the load:

$$P_{SMR}[k] + P_{PV}[k] + P_{EES}[k] = L[k], \forall k \quad (3.12)$$

The difference in the power of the load and the renewable source can be defined as the net demand  $P_{net}[k]$  in kW that would have to be met with the SMR and storage:

$$P_{net}[k] = L[k] - P_{PV}[k], \forall k, \quad (3.13)$$

Like the demand, the output power from the PV source is uncertain and it varies within an interval with lower and upper bounds. The PV generation interval is defined as  $P_{PV}^I$  and has generic limits defined as  $[P_{PV}, \overline{P_{PV}}]$ . The intervals of the load and PV generation determine the interval of the net demand defined as  $P_{net}^I$  with bounds defined as  $[P_{net}, \overline{P_{net}}]$ . The upper and lower bounds of the net demand are defined as:

$$\underline{P_{net}} = \underline{L} - \overline{P_{PV}} \quad (3.14)$$

$$\overline{P_{net}} = \overline{L} - \underline{P_{PV}}$$

based on the interval subtraction rules [64]. For an SMR to follow the net demand, the power should span the limits of the net demand:

$$\underline{P_{net}} \leq P_{SMR} \leq \overline{P_{net}} \quad (3.15)$$

As an example, if the load varies within the interval [1,2] kW and the PV output spans [0,0.5] kW, the operating range of the SMR needs to be  $0.5 \text{ kW} \leq P_{SMR} \leq 2 \text{ kW}$ .

### 3.1.4 Electrical Energy Storage

Because of stochastic fluctuations in the load and in PV generation, the SMR may not always be able to respond quickly enough due to limited ramp rates and inertia. This can cause differences in the power generated and the load. Therefore, electrical energy storage is included to provide rapid action for load balancing. EES has rapid response times and can be sized and configured to meet the required energy capacity, power capacity, and charging/discharging speeds. The electrical energy storage device can either charge or discharge depending on the sign of the power. When the power of the EES is positive, the EES is discharging due to deficit power production. When the power of the EES is negative, the EES is charging due to excess power production.

As far as the control is concerned, the rates of change in the net demand from both the demand and PV determine the strategies for the SMR and EES. Two cases can occur based on the change in net demand between timesteps compared to a limiting power difference defined as  $\delta_n$  in kW. The two cases based on the changes in net demand are:

$$\begin{cases} \text{case 1,} & \text{if } |P_{net}[k] - P_{net}[k-1]| \leq \delta_n \\ \text{case 2,} & \text{if } |P_{net}[k] - P_{net}[k-1]| > \delta_n \end{cases} \quad (3.16)$$

Case 1 corresponds to slow changes in the net demand that are less than the limiting values and can be met by only the SMR. Case 2 corresponds to rapid changes in the net demand that are greater than the limiting value. The SMR alone cannot meet these changes and requires the use of the EES. In general, the SMR output may vary between timesteps in both cases, so the operation of the EES can be defined in terms of power as the difference in the load and the power generated from the SMR and PV:

$$P_{EES}[k] = L[k] - (P_{SMR}[k] + P_{PV}[k]), \forall k \quad (3.17)$$

The corresponding amount of electrical energy stored at each timestep in the EES can be determined by:

$$E_{EES}[k] = E_{EES}[k - 1] - P_{EES}[k] * \Delta k * \eta_{EES}, \forall k \quad (3.18)$$

where  $E_{EES}[k]$  is the amount of stored energy in the electrical energy storage systems at timestep  $k$  in kWh,  $E_{EES}[k - 1]$  is the amount of stored energy in the previous timestep,  $\Delta k$  is the time duration between  $k - 1$  and  $k$ , and  $\eta_{EES}$  is a generic electrical energy storage system loss term associated with charging and discharging losses. The electrical energy storage capacity can be normalized by the rated EES capacity, and is defined as the state of charge (*SOC*):

$$SOC[k] = \frac{E_{EES}[k]}{E_{EES}^{size}} * 100\%, \forall k \quad (3.19)$$

where  $E_{EES}^{size}$  is the installed EES capacity in kWh that is selected through the sizing problem. The allowable SOC of an EES system may be limited by lower and upper limits defined by  $\underline{SOC}$  and  $\overline{SOC}$  so that that storage system does not become fully charged or discharged. In this case, there is a constraint on the allowable *SOC* amount defined by:

$$\underline{SOC} \leq SOC[k] \leq \overline{SOC} \quad (3.20)$$

This also ensures that there is adequate margin to allow for power regulation in this system.

### 3.1.5 Integration of TES with SMR

When a thermal energy storage system is added into this microgrid, the earlier system in Figure 3-1 can now be represented in Figure 3-7. The three components associated with the SMR system are defined as (1) the SMR core which produces thermal power, (2) the thermal energy storage system, and (3) the balance of plant system including the steam power cycle which converts the thermal power into electrical power.

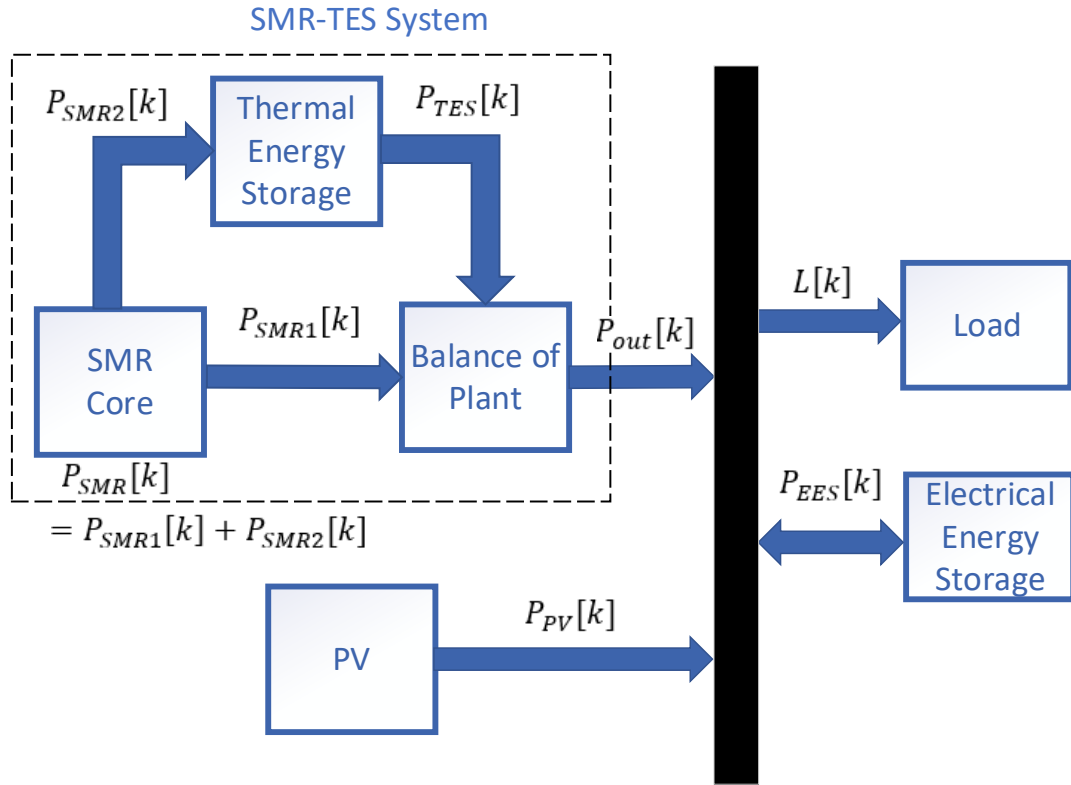


**Figure 3-7 Simplified microgrid schematic including the SMR integrated with thermal energy storage**

The power produced in the SMR core can either be sent to the load through the BOP defined as  $P_{SMR1}[k]$  or can be sent to the thermal energy storage defined as  $P_{SMR2}[k]$  as shown in in Figure 3-7 . In this way, the power of the core is composed of the two components described by:

$$P_{SMR}[k] = P_{SMR1}[k] + P_{SMR2}[k] \quad (3.21)$$

where all power flows as described in Figure 3-7 must be positive. The power into the TES and out of the TES system can be different, which corresponds to charging or discharging of the TES. The combined output of the SMR-TES defined as  $P_{out}$  is comprised of the component from the SMR core and the component of the TES defined as  $P_{TES}$ , and is described by:

$$P_{out}[k] = P_{TES}[k] + P_{SMR1}[k] \quad (3.22)$$

There are then two cases that can occur based on the SMR power level and the required output. The first case occurs when the required output is less than the SMR core power. In this case, the required output is directly from the SMR core through the balance of plant and no power is required to be delivered by the TES. The remaining difference in power from the SMR core not sent to the load is sent to storage. SMR-TES case 1 can be described by:

$$\text{if } P_{out}[k] < P_{SMR}[k] \left\{ \begin{array}{l} P_{SMR1}[k] = P_{out}[k] \\ P_{TES}[k] = 0 \\ P_{SMR2}[k] = P_{SMR}[k] - P_{SMR1}[k] \end{array} \right. \quad (3.23)$$

The second SMR-TES case occurs when the required output is greater than the SMR core power. In this case, all the required power from the SMR core is sent through the balance of plant to the load and no power from the SMR core is sent to storage. The remaining power required to be sent to the load is delivered by the TES. SMR-TES case 2 can be described by:

$$\text{if } P_{out}[k] > P_{SMR}[k] \left\{ \begin{array}{l} P_{SMR1}[k] = P_{SMR}[k] \\ P_{SMR2}[k] = 0 \\ P_{TES}[k] = P_{out}[k] - P_{SMR1}[k] \end{array} \right. \quad (3.24)$$

### 3.2 Determination of TES Configuration and Materials for Integration with HTGR

The coupling of a TES system must ensure the materials and configuration are compatible with the HTGR core and power cycle materials and temperatures [4]. Further, the storage should maintain reasonable economics and efficiencies of the combined SMR-TES system.

#### **Configuration**

Heat storage can couple to either the primary loop of the reactor core, the secondary loop of the power cycle, or to an intermediate loop. Heat storage in the primary loop can have higher efficiencies since it can operate at the core outlet temperature. However, this arrangement may cause coolant variations in the primary loop and requires extra safety considerations. Coupling thermal energy storage within the power cycle has been

proposed [4], including the use of steam accumulators, and packed-bed storage. A significant drawback is that the storage temperature is limited to the steam temperature and does not take advantage of the elevated temperature of the reactor. The third coupling option is to incorporate TES within an intermediate loop between the primary loop and the power cycle loop. This configuration allows the storage to operate near the high core temperature for higher storage efficiency, while allowing for additional flexibility of the complete system. It also reduces impact on the core.

Either an indirect two tank configuration or a thermocline tank system would be compatible in an intermediate loop configuration. The indirect two tank configuration is simpler because it has separate hot and cold tanks. A thermocline system may cost less since it only uses one storage tank. However, it can have operational issues, for example, thermal gradients in the storage tank can cause negative impacts on power output, and mixing of hot and cold salts can reduce storage efficiencies [65]. Therefore, the indirect two tank configuration can be a cost-effective and technically attractive choice to integrate within the HTGR system.

### **Materials in Thermal Energy Storage Systems**

The materials in an intermediate storage loop of an HTGR must be able to operate at high temperatures near 600 °C. In general, sensible heat storage systems are more technologically advanced and can be more cost effective than latent heat storage systems. At these elevated temperatures, water/steam and thermal oils are no longer adequate, but molten salts and liquid metals can be good candidate materials. Hence, molten salts are chosen as the thermal energy storage material in the current investigation.

Molten salts have adequate temperature range and can have very long cycling life and high storage efficiencies. They are also relatively cost effective [4]. Molten salts have good thermal-physical properties including high heat transfer coefficient, high thermal conductivity, and very low vapor pressure. Many of the molten salts reviewed in Table 2-5 have similar properties besides the temperature ranges. These can all be considered candidate materials. A specific salt type should be selected based on the specific reactor properties.

Based on the above factors, an HTGR with a two-tank intermediate storage tank configuration with molten salt and a steam power cycle is a proposed configuration for near-term deployment for off-grid communities. This configuration is shown in Figure 3-8. This specific configuration of the SMR-TES differs from the generic description from Figure 3-7 since there is not a physical direct flow of power from the SMR core through the BOP to the output. However, the general operation described in the previous section remains true with some modifications. In this configuration, the power produced from the core is transferred into the intermediate storage loop, which is adjusted to meet balance with the power cycle. The specific operation of this configuration through state parameters is described in the next section.

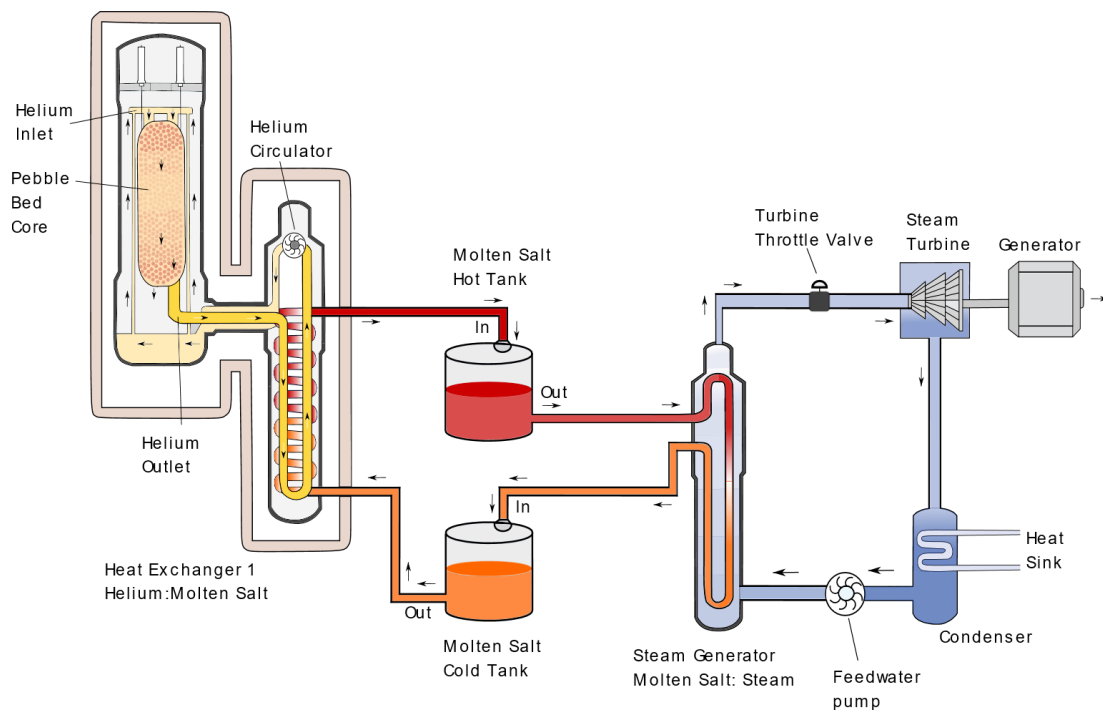


**Figure 3-8. Description of HTGR system configuration with power cycle and thermal energy storage integration into a two-tank indirect intermediate loop**

### 3.3 SMR-TES Design Description and Model

The operation of a reactor with TES will be different from that without TES in the load-following mode. In a traditional load-following reactor without thermal energy storage, the heat generation within the reactor core is controlled to maintain power balance with

the steam cycle. After integrating thermal energy storage, the TES system alone can be modulated to achieve power balance with the power cycle to perform the load-following. As a result, the reactor core can operate at steady state.

A mathematical model of the SMR-TES system is required to perform sizing and operational analysis of this microgrid. This model is simplified to be a lumped parameter model based on quasi-steady state. The configuration of this reactor described in the previous section is shown in Figure 3-9. The three major systems include the SMR core and primary loop, the TES intermediate loop, and the balance of plant with the power cycle loop. The HX1 couples the helium coolant primary loop to the molten salt intermediate loop and the steam generator couples the intermediate loop and the steam power cycle loop.

The important parameters of this configuration are the temperature ( $T$ ) in  $^{\circ}\text{C}$ , pressure ( $p$ ) in MPa, and mass flow rate ( $\dot{m}$ ) in kg/s for the points (a) through (j). Let  $Q$  represent the heat rate in  $\text{kW}_{\text{th}}$ ,  $q$  represents the associate amount of heat per unit mass in  $\text{kJ/kg}$ , and  $w$  represents work in  $\text{kJ/kg}$ .

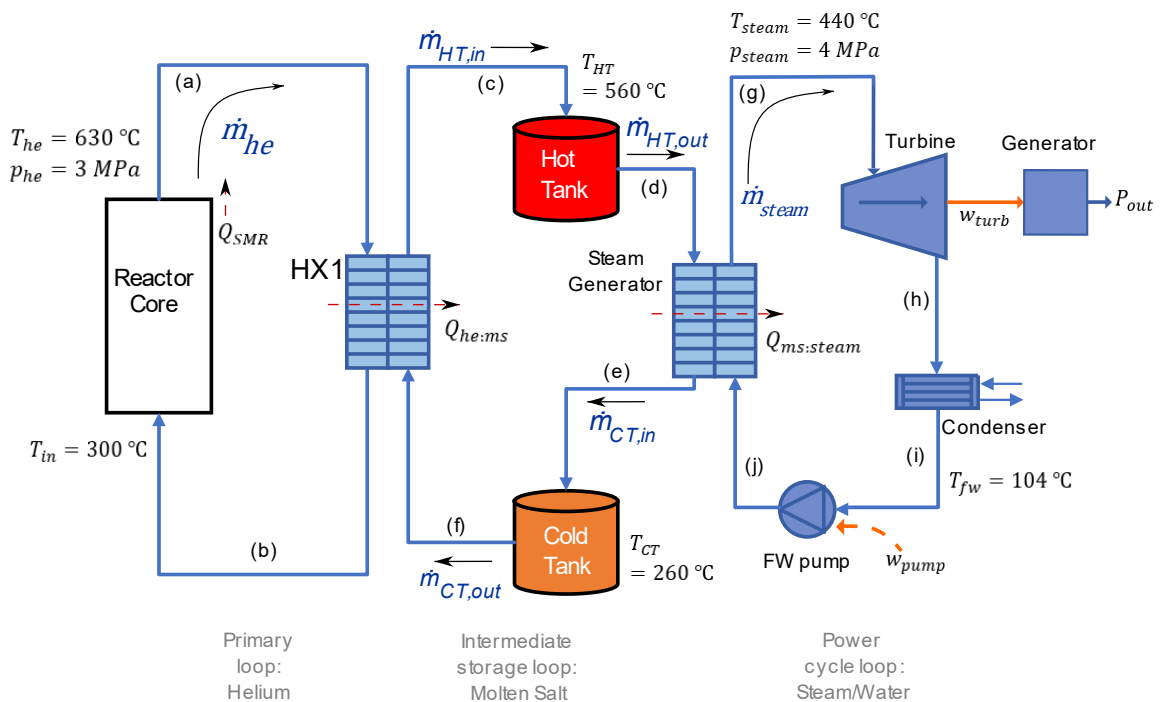


**Figure 3-9 Simplified schematic of SMR-TES model**

### 3.3.1 Description of the System and Key Parameters

#### Reactor Core and Primary Loop

The reactor core produces thermal power defined as  $Q_{SMR}$  in kW<sub>th</sub> that has an equivalent electrical power rating defined as  $P_{SMR}$  in kW. For the sizing problem, the selected size of the SMR core power rating corresponding to  $P_{SMR}$  is defined as  $P_{SMR}^{size}$  in kW. The thermal power in the core is transferred by the coolant (helium) through the reactor core to HX1 at a mass flow rate defined as  $\dot{m}_{he}$  in kg/s. The helium coolant experiences a temperature rise from the reactor inlet defined by  $T_{in}$  in °C to the reactor outlet defined as  $T_{out}$  in °C. The helium pressure in the primary loop defined as  $p_{he}$  in MPa is assumed to be constant.

For this reactor model in the context of the sizing problem, the helium mass flow rate through the core will be considered a calculated variable to maintain the desired inlet and outlet coolant temperatures at a given reactor core power rating. The reference reactor of the GFP MMR has a designed coolant temperature in the range of 300-630 °C at 3.0 MPa. These conditions are selected as the primary loop parameters for this HTGR. The specific values are summarized in Table 3-1. It is assumed that the primary temperatures and pressure remain constant during full power operation.

**Table 3-1 Core and primary loop design parameters**

<b>Parameter</b>	<b>Symbol</b>	<b>Value</b>
Core Heat Production Rate	$Q_{SMR}$	Selected
Helium Inlet Temperature	$T_{in}$	300 °C
Helium Outlet Temperature	$T_{out}$	630 °C
Helium Pressure	$p_{he}$	3.0 MPa
Helium Mass Flow Rate	$\dot{m}_{he}$	Calculated

#### Thermal Energy Storage Loop

The integration of a molten salt intermediate loop should not cause significant changes to the reactor loop, nor the power cycle. The GFP MMR reactor design has a hot tank temperature  $T_{HT}$  of 560 °C and the cold tank temperature  $T_{CT}$  is selected to be 260 °C, as shown in Table 3-2. Solar salt with an operating range of 220-600 °C [26] is compatible with the proposed helium and molten salt temperature range and will be used in this

analysis. Solar salt has a long operating history in CSP plants and has good thermophysical properties. It has lower cost as compared to other molten salts.

The heat transferred from the primary loop into the intermediate storage loop across HX1 is defined as  $Q_{he:ms}$  in kW<sub>th</sub>. For balance, the primary loop heat generation should be transferred across HX1 into the intermediate loop to maintain constant temperatures in both loops. As the helium coolant transfers the heat across HX1 from (a) to (b), there is temperature loss associated with a temperature raise in the molten salt storage material from (f) to (c). The temperature of the molten salt at point (f) is defined as the cold tank temperature  $T_{CT}$  and has an associated mass flow rate  $\dot{m}_{CT,out}$  in kg/s. After HX1 at point (c), the molten salt temperature is assumed to be the same as the hot tank temperature  $T_{HT}$ .

The intermediate loop must also maintain balance with the steam cycle. The heat transferred across the steam generator from the intermediate loop to the steam cycle is defined as  $Q_{ms:steam}$  in kW<sub>th</sub>. The hot tank outlet flow transfers heat across the steam generator into the power cycle loop at the mass flow rate defined as  $\dot{m}_{HT,out}$  in kg/s. After transferring heat across the steam generator, the temperature at point (e) is the cold tank temperature.

The desired operation of the thermal energy storage intermediate loop is to maintain constant temperatures in both the hot tank and cold tank, while varying the cold tank outlet and hot tank outlet mass flow rates during load-following modes. The varying inlet and outlet mass flow rates of the storage tanks are calculated within the SMR-TES models from Table 3-2. However, in order to maintain mass conservation in the intermediate loop, these flow rates are not independent, but are related and must be coordinated. This is described further in the next section.

**Table 3-2 Thermal energy storage intermediate loop design parameters.**

Parameter	Symbol	Value
Hot Tank Temperature	$T_{HT}$	560 °C
Cold Tank Temperature	$T_{CT}$	260 °C
Hot tank inlet and outlet mass flow rates	$\dot{m}_{HT,in}, \dot{m}_{HT,out}$	Calculated timeseries <sup>a</sup>
Cold tank inlet and outlet mass flow rates	$\dot{m}_{CT,in}, \dot{m}_{CT,out}$	Calculated timeseries <sup>a</sup>

<sup>a</sup>The cold and hot tank flow rates are coordinated to ensure mass balance

### Steam Power Cycle

The heat transferred from the molten salt loop across the steam generator produces steam at point (g) at a temperature  $T_{steam}$  in °C and a pressure  $p_{steam}$  in MPa. The steam performs work in the turbine defined as  $w_{turb}$  in kJ/kg, that is determined by the differences in steam enthalpies across the turbine [66]. After the turbine at point (h), the water-steam mixture is condensed and becomes a saturated liquid at point (i) which corresponds to the lowest temperature around the power cycle. The temperature at point (j) is the feedwater temperature defined as  $T_{fw}$  in °C that flows back into the steam generator from the feedwater pump. The feedwater pump consumes work defined as  $w_{pump}$  in kJ/kg.

This power cycle is planned to operate at a constant steam temperature and pressure while also maintaining a constant feedwater temperature with these parameters summarized in Table 3-3. The steam mass flow rate  $\dot{m}_{steam}$  in kg/s is varied in this loop to adjust the amount of electrical power generated in kW. The limit on the amount of the electrical output power ( $P_{out}$ ) is based on the sizing problem for the BOP system and is defined as  $P_{BOP}^{size}$  in kW.

**Table 3-3 Power cycle design parameters**

Parameter	Symbol	Value
Steam Temperature	$T_{steam}$	440 °C
Feedwater Temperature	$T_{fw}$	104 °C
Steam Pressure	$p_{steam}$	4 MPa
Work done in the turbine	$w_{turb}$	Calculated
Work consumed in the pump	$w_{pump}$	Calculated
Steam mass flow rate	$\dot{m}_{steam}$	Calculated timeseries
Output Power	$P_{out}$	Calculated timeseries

### 3.3.2 Design Calculations

#### Reactor Core and Primary Loop

To maintain the desired temperature range of the coolant, the helium flow rate through the core at full power can be calculated from:

$$\dot{m}_{he} = \frac{Q_{SMR}}{c_{p,he} \cdot \Delta T_{he}} \quad (3.25)$$

where  $Q_{SMR}$  is the reactor core heat generation rate in kW<sub>th</sub> that is a selected parameter from the sizing problem. The parameter  $c_{p,he}$  is the specific heat capacity of helium taken to be a constant value of 5.195 kJ/(kg· °C) from [67], and  $\Delta T_{he}$  is the difference in coolant temperature between the inlet and outlet in °C. The value of  $Q_{SMR}$  determines the required helium mass flow rate at full power to maintain the constant helium temperatures.

#### Steam Power Cycle

A detailed explanation of the power cycle can be found in Appendix A. The required electrical output defines the operation of the steam cycle, which accordingly requires balance from the intermediate thermal storage loop. At steady-state with constant temperature and pressure, the work done per unit mass of steam in the turbine is constant. This work is defined as the difference in enthalpy across the turbine and can be determined as:

$$w_{turb} = h_g - h_h = 858 \text{ kJ/kg} \quad (3.26)$$

where  $h_g$  and  $h_h$  are the specific enthalpies of the fluid at points (g) and (h) respectively in kJ/kg. The values of  $h_g$  and  $h_h$  are determined in Appendix A from the cycle states.

The net work done by the power cycle is defined as the difference in the output work done by the power cycle and the work consumed by the power cycle. In this power cycle, the turbine performs work, and the feedwater pump consumes work. The steam generator and condenser transfer heat and are assumed at constant pressure with no work being done [66]. However, the pump work is much smaller than the work of the turbine and can therefore be neglected. The rate of net work done by the cycle through the turbine can be approximated as the electrical power output from the cycle ( $P_{out}$ ), assuming that the turbine and generator are 100% efficient. The electrical output of the power cycle in kW is based on the steam mass flow rate from:

$$P_{out} = \dot{m}_{steam} * w_{turb} \quad (3.27)$$

where  $\dot{m}_{steam}$  is the steam mass flow rate in kg/s and  $w_{turb}$  is the work done in the turbine in kJ/kg. Since  $w_{turb}$  is assumed to be constant under constant temperature and pressure operation, the electrical power production is directly proportional to the steam mass flow rate. This simplification has been used in the literature in SMR modelling including [37]–[39], [68]. In a load-following mode, the steam mass flow rate can be a time-varying function and (3.27) can be revised:

$$P_{out}[k] = \dot{m}_{steam}[k] * w_{turb}, \forall k \quad (3.28)$$

### **Thermal Energy Storage**

Power balance is required across the steam generator as the output power of the power cycle varies according to Eq. (3.28) to perform load-following. At constant temperature and pressure in the power cycle, the specific heat transfer into the steam cycle from the molten salt loop can be described by the differences in steam/water enthalpies from the steam generator inlet and outlet:

$$q_{ms:steam} = h_g - h_j = 2943 \text{ kJ/kg} \quad (3.29)$$

where  $h_g$  and  $h_j$  are the specific enthalpies at points (g) and (j) in kJ/kg. The total heat transfer rate is depended on the steam mass flow rate and is described by:

$$Q_{ms:steam}[k] = q_{ms:steam} * \dot{m}_{steam}[k], \forall k \quad (3.30)$$

This heat transfer rate must be supplied from the flow of molten salt from the hot tank into the cold tank that can described by the heat transfer:

$$Q_{ms:steam}[k] = c_{p,ms} * \Delta T_{ms} * \dot{m}_{HT,out}[k], \forall k \quad (3.31)$$

The relation from Eq. (3.31) can be rearranged to solve for the required hot tank mass flow rate over time based on the required heat transfer rate into the steam cycle:

$$\dot{m}_{HT,out}[k] = \frac{Q_{ms:steam}[k]}{c_{p,ms} * \Delta T_{ms}}, \forall k \quad (3.32)$$

Second, power balance is required across HX1, between the helium coolant and the molten salt that flows out of the cold tank and into the hot tank. The molten salt storage system has a mass flow from the cold tank outlet through HX1 into the hot tank inlet, which is independent of the flow rate from the hot tank outlet into the cold tank inlet.

At full reactor core power operation, the mass flow rate out of the cold tank is maintained constant. This is determined based on the reactor power level through power balance in HX1 across both fluids. The core heat production rate ( $Q_{SMR}$ ) that raises the coolant temperature from  $T_{in}$  to  $T_{out}$  should be the same heat rate that is transferred across HX1 into the molten salt loop. Heat transfer across HX1 can be described between helium and molten salt:

$$Q_{SMR} = \dot{m}_{he} * c_{p,he} * \Delta T_{he} = \dot{m}_{CT,out} * c_{p,ms} * \Delta T_{ms} \quad (3.33)$$

where  $c_{p,he}$  is the specific heat capacity of helium estimated to be 5.195 kJ/(kg·°C) [67],  $c_{p,ms}$  is the specific heat capacity of molten salt estimated to be 1.5 kJ/(kg·°C) from [27] and  $\Delta T_{ms}$  is the temperature change in molten salt between points (f) to (c) estimated to be 300 °C. The heat transfer balance from (3.33) can be rearranged to describe the molten salt mass flow rate based on the helium mass flow rate:

$$\dot{m}_{CT,out} = \dot{m}_{he} * \frac{c_{p,he} * \Delta T_{he}}{c_{p,ms} * \Delta T_{ms}} \quad (3.34)$$

Therefore the required mass flow rate out of the hot tank is dependent on the helium mass flow rate which is dependent on the reactor power level.

It is demonstrated in the above sections that variations in the reactor core and power cycle determine the required changes in the intermediate storage loop to maintain power balance between the three systems. In the storage loop, the molten salt hot tank and cold tank temperatures are assumed constant. The cold tank outlet mass flow rate is set by the reactor power level. The steam mass flow rate varies proportional to the output of the turbine when performing load-following. The hot tank outlet mass flow rate accordingly varies proportional to the steam mass flow rate. For mass conservation in the intermediate storage loop, the requirements for coordination of mass flow rates in the tanks are:

$$\dot{m}_{HT,out}[k] = \dot{m}_{CT,in}[k] \quad (3.35)$$

$$\dot{m}_{CT,out}[k] = \dot{m}_{HT,in}[k]$$

The actual mass in the tanks over time can be determined from:

$$m_{HT}[k] = m_{HT}[k - 1] + (\dot{m}_{HT,in}[k] - \dot{m}_{HT,out}[k]) * \Delta k \quad (3.36)$$

$$m_{CT}[k] = m_{CT}[k - 1] + (\dot{m}_{CT,in}[k] - \dot{m}_{CT,out}[k]) * \Delta k$$

where  $m_{HT}[k]$  and  $m_{HT}[k - 1]$  are the masses of molten salt in the tank at timestep  $k$  and at the previous timestep respectively, and  $\Delta k$  is the time duration between  $k - 1$  and  $k$ .

For the sizing problem, the required thermal energy storage mass is defined as  $m_{TES}^{size}$  in metric tons, that is based on the total mass in both storage tanks.

## 3.4 Methodology of Analysis

### 3.4.1 Modelling and Analysis under Steady-state Conditions

Steady-state simulations and analysis are conducted for this microgrid to determine technical feasibility of candidate configurations. Simulations and calculations are created in Microsoft Excel utilizing simplified models of the system components to meet the power balance. The analysis uses a combination of input selection of sizes for some

system components along with the calculation of sizing of other components. Iterative simulations have been carried out to compare characteristics under different configurations to determine the optimal sizing. A further explanation of the steady-state calculations can be found in Appendix B.

### **Inputs**

The inputs into these simulations are community information in terms of the electrical demand and renewable resource potential. The sizing of the microgrid components is based on the maximum electrical demand for the community. The input for the electrical demand is the maximum annual demand and the upper bound of the demand profile. The input of renewable resource potential is the nominal solar irradiance curve.

### **Sizing Variables**

- SMR system components: Reactor core, balance of plant, thermal energy storage capacity
- Amount of PV generation
- Electrical energy storage (batteries) capacity

The purpose of this analysis is to size the SMR-TES system to be able to operate flexibly to allow the integration of large amounts of PV generation while meeting all demand requirements. Due to high SMR capital costs, the SMR core sizing should be minimized as much as possible by utilizing peaking output through an oversized BOP system and power from TES. The thermal energy storage capacity should be sized to ensure that the peak community demand can be met while also accounting for load and PV variability. Since electrical energy storage can be costly and has limited storage durations, this additional storage should only be utilized to meet quick PV and load demand changes due to its quick response.

## **Analysis Methodology**

The requirement for this microgrid is to continually maintain the power balance between the load and the generation, including the SMR and the PV generation. The hourly PV output is dependent on the input solar irradiance curve which is scaled by the installed PV capacity. At each timestep, the required SMR total system output is determined based on the net demand between the load and the PV generation. The constraint applied is the allowable ramp rates limits of output of the SMR system between timesteps. Any mismatch between the generated power and the load due to limitations in the ramp rates is provided by the electrical energy storage system. The operational characteristics of the total SMR system can be analyzed and compared to determine admissible configurations and to determine appropriate sizing of other components.

The inputs to this simulation and analysis for the SMR systems are the (1) SMR core size and (2) SMR BOP sizing and the installed PV capacity. The operation of the SMR-TES system is based on the model developed in Section 3.3. The required electrical output of the SMR-TES system is set by the net demand and the actual output is limited by the ramp rate constraints. The steam and molten salts mass flow rates are calculated for the load-following process. The variations in the molten salt flow rates determine changes in molten salt storage tank levels. The limits on the tank capacity determine the required TES capacity.

### **3.4.2 Economic Considerations**

#### **Small Modular Reactors with Thermal Energy Storage**

Once a thermal energy storage is integrated with an SMR, the costs will include those of the reactor core, the BOP system and TES system. When including thermal energy storage, the BOP system can be oversized relative to the SMR core sizing. The SMR core is the most significant capital cost component. The relative cost of the BOP is estimated to be 20% of the total SMR capital costs based on the costs from an on-grid HTGR [69]. Therefore, reducing the SMR core power capacity should result in a reduce SMR capital cost.

The added TES costs can be estimated from existing costs of molten salt tank TES systems from CSP plants [70]. The cost data reported in [70] given in \$/kWh is converted into \$/kg of molten salt based on the correlation that 1 kg = 0.125 kWh from (2.2) assuming a heat capacity of 1.5 kJ/(kg· °C) and a temperature change of 300 °C. The total capital cost for the TES system is estimated at 3.27 \$/kg of molten salt material that includes salt and storage tank materials, as shown in Table 3-4. The calculated TES costs can inform on the change in SMR costs when adding this TES system.

**Table 3-4 Breakdown of TES costs**

<b>Component</b>	<b>Capital Cost (\$/kg)</b>
Hot and Cold Tanks (and structures)	1.60
Storage Medium	1.51
Other	0.16
<b>TOTAL</b>	<b>3.27</b>

### 3.4.3 Dynamical Analysis

The second part of the analysis is dynamical analysis during load or PV variations. The purpose of the dynamical analysis is (1) to determine the capability of the SMR-TES system by considering system variabilities, and (2) to determine additional electrical energy storage requirements based on limitations of the SMR-TES system to maintain power balance under rapid load fluctuations or renewable energy variations.

This analysis is conducted in MATLAB Simulink. It considers the terminal characteristics of the system components. Since the performance characteristics of this SMR-TES system are still uncertain, conditions will be set to determine the effect on the total system performance including the required electrical storage capacities. The simulation studies have been conducted for a duration of one day with a description of community demand, PV output, and the SMR-TES system. A detailed description of the dynamical model can be found in Appendix B.

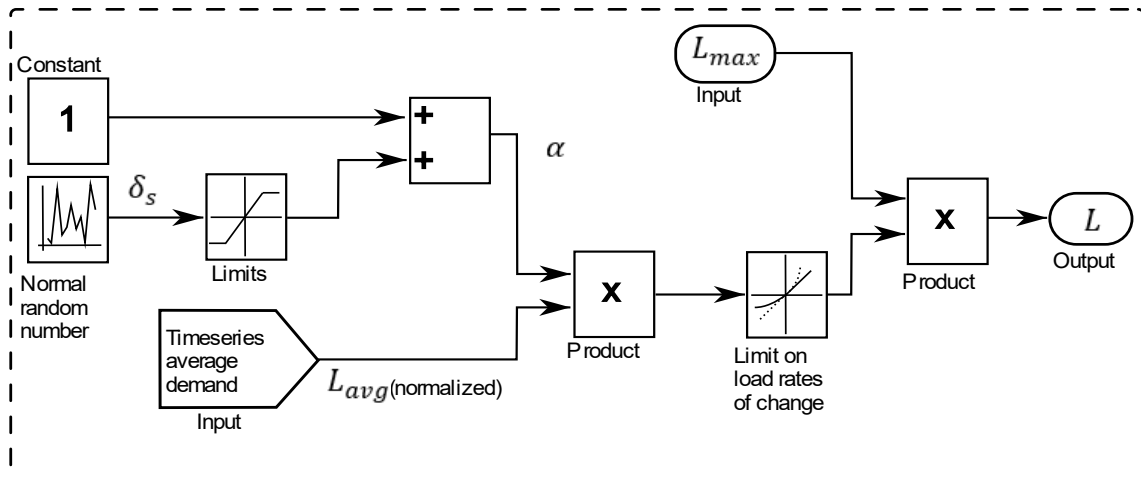
## Demand Model Description

Synthetic community demand is simulated based on the defined community characteristics from Section 3.1.1. A representation of the Simulink function block for creating synthetic demand is shown in Figure 3-10 (a) and represents the synthetic load described by Eq. (3.7).

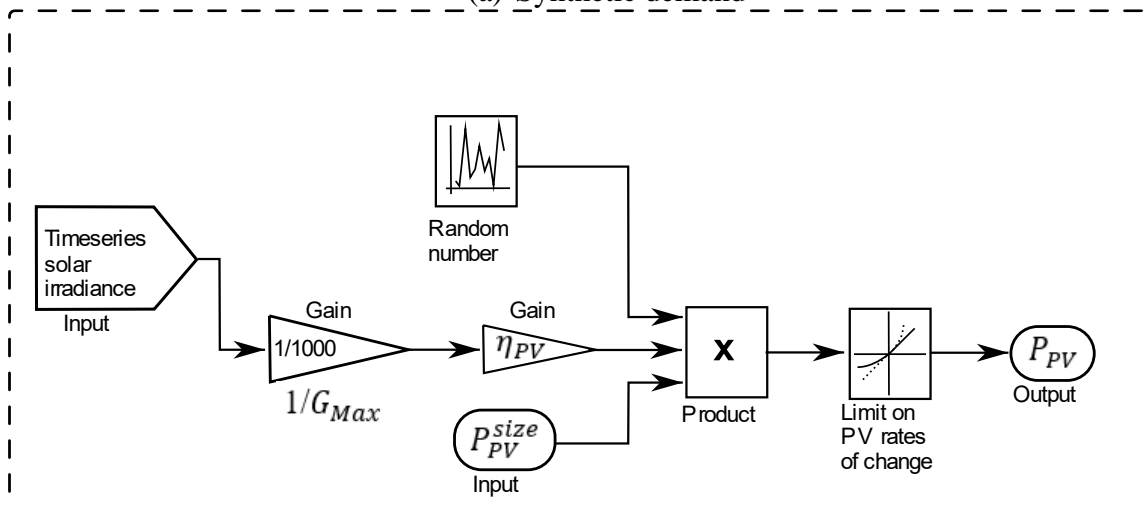
The ‘Timeseries average demand’ represents  $L_{avg}[k]$  and is created as a polynomial function that is normalized as a percentage of the maximum demand. The average demand timeseries has limits based on the seasonal limits from either Eq. (3.3) or (3.4). The average demand is scaled by the perturbation factor from Eq. (3.6) with the normal random number drawn from a normal distribution described by Eq. (3.5). The limits on the normal random number define the bounds around the average demand based on the selected number of standard deviations included. The ‘Limit on load rates of change’ can be varied to select the maximum allowable rates of change of random fluctuations in the demand output.

## PV Model Description

The PV generation model is based on the correlation between PV output and solar irradiance from Eq. (3.11). A representation of the PV generation model from Simulink is shown in Figure 3-10 (b). The input solar irradiance is based on the maximum curves from Figure 3-4 and is calculated from a polynomial fit from the solar irradiance potential of the community. To model PV variability, the PV output is multiplied by a uniform distribution with limits within [0,1] to create synthetic variability of the PV system output that mimics stochastic weather patterns. The rate limiter function limits the allowable variability of the PV output based on the definition of the rising and falling slew rates informed from Section 3.1.2.



(a) Synthetic demand



(b) PV generation

**Figure 3-10 Simulink modelling block diagrams for (a) Demand and (b) PV generation**

The load and PV blocks are used to determine the operation of the SMR-TES and EES systems. The remaining sections of the Simulink model are shown in Figure 3-11.

The net demand from Eq. (3.13) is calculated from in Figure 3-11 (a). The value of the net demand is planned to be met by the size output of the SMR-TES system. However, the actual SMR-TES output has ramp rates limits and may not be able to follow this required signal. The ‘Limit on allowable SMR output rates of change’ can be defined which sets the allowable rates of change in the output.

The combined output of the PV and SMR is defined as the generated power  $P_{gen}[k]$  as shown in Figure 3-11 (b). The difference in the generated power and the load is the required power to be met by the EES system as described in Eq. (3.17).

The associated energy stored in the EES over time is calculated based on the summation of the EES power over time from Eq. (3.18). The required battery power and minimum battery capacity can be determined from the respective output signals. The required capacity can be determined from the difference in minimum and maximum level of the battery energy over the duration of the simulation.

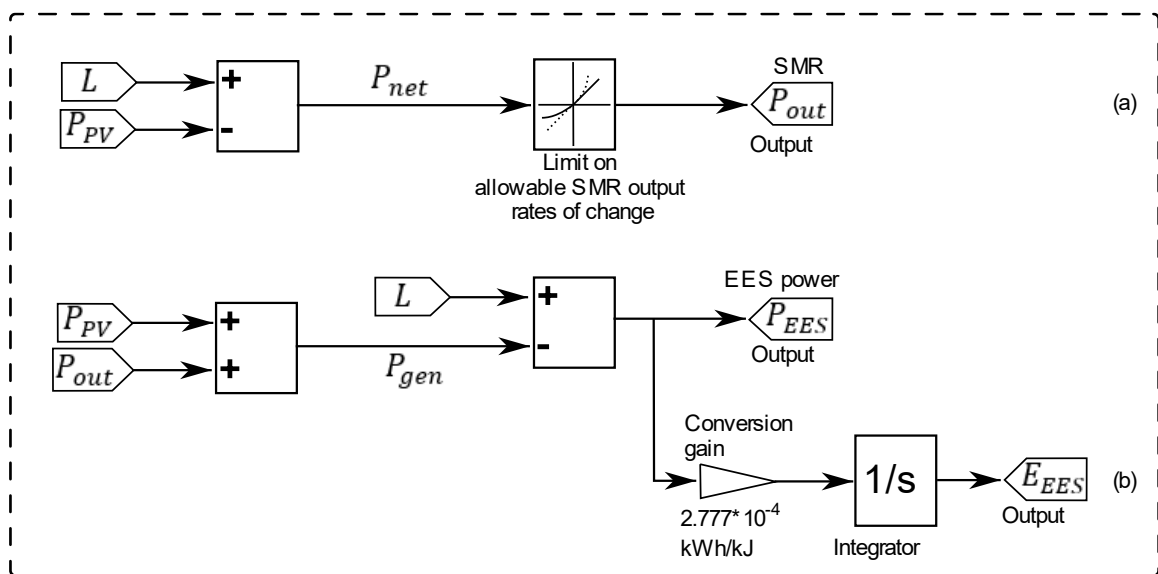


**Figure 3-11 Simulink model for (a) Determination SMR operation based on the net demand, and (b) EES operation to determine EES requirements**

Parameters of the SMR and PV systems can be explored to determine the effect on the EES requirements. Since detailed SMR-TES system response contains some uncertainties, the ramp rate limits can be varied to explore the effects on the microgrid. The results of the requirements of the EES based on the SMR-TES ramp rates can be compared against reasonable behavior from this system to determine the required EES capacity. Similarly, the installed PV capacity can be varied. The results on the EES requirements can determine the amount of PV that should be installed that informs on the

results from the steady-state analysis and can defined the EES storage capacity required. The results of this analysis will be presented in Chapter 4.

## Chapter 4

### 4 Components Sizing Under Different Configurations

The purpose of this chapter is to formulate the sizing problem and develop solution procedures for this microgrid. The desired performance requirements for a controllable source are found under typical load profiles and characteristics of renewable energy resources in an off-grid community. Characteristics of SMRs with and without TES will then be analyzed to determine appropriate sizes for effective operations in such microgrids. This work is carried out using mathematical modelling, interval analysis, and simulations.

#### 4.1 Sizing Problem for the Overall Microgrid

The methodology for sizing different components in this microgrid system is developed and explained in this section.

**Inputs.** The inputs to this analysis are characteristics including demand and renewable resource potential in the community as shown in Table 4-1.

**Table 4-1 Input parameters for the community**

Aspect	Parameters
Community	Peak demand ( $L_{Max}$ ) in kW
	Daily load variation ( $\sigma_D$ ) in %
	Annual load variation ( $\sigma_Y$ ) in %
	Time-step variability ( $\sigma_S$ ) in kW
	Summer and winter typical demand curves ( $\bar{L}[k]$ )
PV Power	Community location that defines resource potential in longitude and latitude
	Summer and winter daily nominal trends of solar irradiance ( $\bar{G}[k]$ )

**Sizing.** The purpose is to size the installed generation capacity for this microgrid, which includes:

- Renewable generation installed power rating:  $P_{PV}^{size}$
- SMR

- SMR core power rating:  $P_{CORE}^{size}$
- Balance of plant/turbine power rating:  $P_{BOP}^{size}$
- Thermal energy storage capacity in terms of the mass of molten salt:

$$m_{TES}^{size}$$

- Electrical energy storage capacity:  $E_{EES}^{size}$

### Technical Considerations and Operational Constraints

1. Power Balance: The total amount of power consumed from the loads must be equal to the sum of power supplied by all generation sources and storage in this system.
2. SMR System Ramp Rate Limits: The ability of the microgrid to respond to variations in the load and the PV generation can be significantly affected by the rate limits of the SMR output. While the SMR should meet the net demand, it must ensure that the SMR system operation is within safe operating limits. The SMR output ramp rate limits in % of full power per minute are set.
3. EES State of Charge Limits and Power Limits: The EES system has state of charge limits that prevent the system from operating below and above its design limits. The EES rates of charge and discharge of the EES power must also be within reasonable limits for its normal operation.
4. TES State of Charge Limits: The thermal energy storage system has state of charge limits similar in principle to those in the EES system to maintain lower and upper storage tank levels.

5. Reserve Capacity: Additional TES and EES capacity can be considered to account for extreme fluctuations in demand and non-dispatchable generation beyond the limits of this analysis.
6. Total System Cost: The system cost is also a constraint for this problem. There are currently large uncertainties in the costs of SMRs. Because of this, a complete cost analysis of the microgrid is not conducted. Instead, arguments are made about the cost of this SMR based microgrid compared to existing diesel generator systems. Further, changes in SMR costs based on sizing and the addition of TES is explored.

## 4.2 Methodology for Component Sizing

The sizing methodology is summarized in the flowchart shown in Figure 4-1.

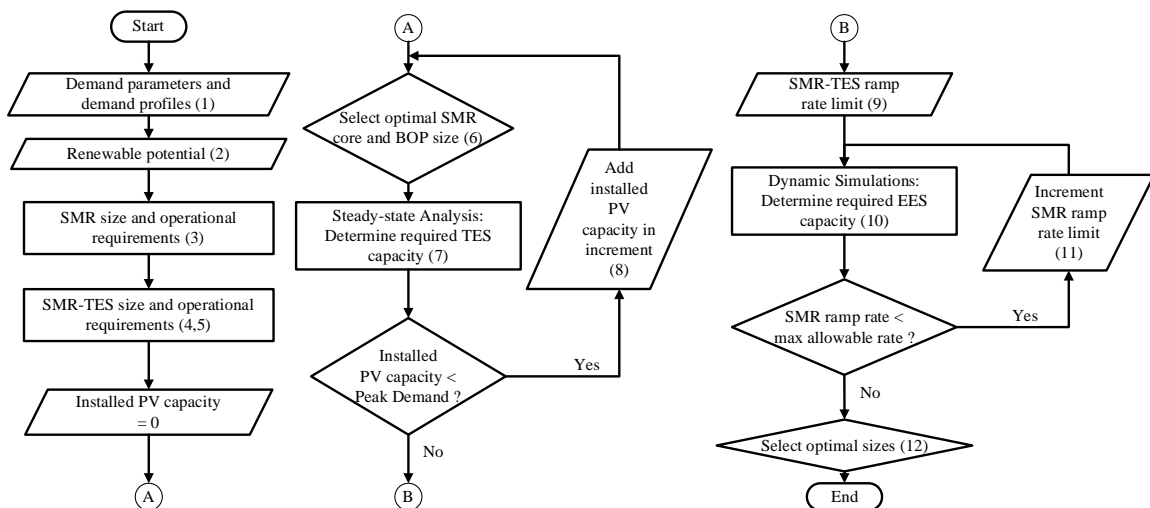


**Figure 4-1 Sizing methodology flowchart**

The sizing methodology steps are:

1. Input community demand characteristics.
2. Input renewable resource potential.

#### Analysis of SMR to fit into microgrid

3. SMR size and operational requirements.

#### Analysis of SMR-TES

4. SMR-TES system size and operational requirements.
5. Determine sizing of SMR-TES system.
  - a. Determine the relation of sizes of SMR core, BOP and TES capacity based on demand profile.
  - b. Determine any changes in sizes from (5a) as a result of introduction of PV generation.

#### Steady-State Simulation and Analysis

6. Select optimal SMR and BOP sizes based on the result of step (5).
7. Perform steady-state simulations to determine the required TES storage mass.
8. Increment installed PV capacity while it is less than the peak demand, and return to step (6). Perform steps (6) and (7) to with updated PV and SMR-TES sizes. The purpose is to determine the relationship between TES storage and PV capacity and the allowable amounts of PV generation that can be accommodated.

#### Dynamics Simulation and Analysis

9. Select minimum SMR-TES system ramp rate limit.
10. Perform dynamical analysis through simulations on the system configurations determined from steady-state analysis. Determine the required electrical energy storage based for the installed PV capacity.

11. Increment SMR-TES ramp rate limits while it is less than the allowable limits, and return to step (10). Perform steps (10) with updated SMR-TES ramp rate limits.
12. Select the candidate configurations meeting the technical considerations and operational constraints. The optimal configuration is determined among the admissible ones that maximizes the PV utilization while minimizing the total system cost.

### 4.3 Analysis of SMR Integrated into a Microgrid

The purpose of this section is to determine the performance of the system and requirements of an SMR as the main controllable source in a microgrid. The section examines the SMR size and operational requirements within the microgrid. This benchmark SMR without TES modulates the steam cycle and balances the heat generation rate in the reactor core. First, terminal effects and the output characteristics of the SMR are defined in terms of the SMR maximum output, and the limit of output power ramp rates (in % of full power/min).

Since the actual demand and output of the PV source are uncertain, their actual values can be described within respective intervals. The net demand the SMR is planned to follow is described by Eq. (3.13). The required overall operating interval of the SMR is determined from Eq. (3.15) with bounds from Eq. (3.14). This demonstrates that the SMR must be able to account for most variations in the load and the PV source. The bounds of the load and PV from Eq. (3.14) are different depending on the span of time that the intervals are identified. Considering the intervals within a year and a day determine the required size of the SMR and the required operational ranges. Considering the intervals on shorter timescales including hourly and sub-hourly scales determines the limits on the required ramp rates of the SMR to account for fluctuations in loads and PV changes that then requires the use of EES devices.

#### **Size Requirements from Load and PV Limits and Trends**

First, the annual limits of the load and PV generation can be used to determine the operating limits of the SMR considering output behaviors from (3.15). The upper bound ( $\bar{L}$ ) is chosen as the maximum annual electricity demand  $L_{Max}$  from Eq. (3.3) and the lower bound ( $\underline{L}$ ) corresponds to the minimum annual load as  $\sigma_Y * \sigma_D * L_{Max}$  from (3.4). The annual PV limits in this interval is  $[0, P_{PV}^{size}]$ . The required annual SMR interval from Eq. (3.14) can be determined as:

$$\begin{aligned} \underline{P}_{SMR} &= \sigma_Y * \sigma_D * L_{Max} - P_{PV}^{rated} \\ \overline{P}_{SMR} &= L_{max} \end{aligned} \quad (4.1)$$

so that the power should span the ranges of the net demand from Eq. (3.15) as:

$$\sigma_Y * \sigma_D * L_{Max} - P_{PV}^{rated} \leq P_{SMR} \leq L_{max} \quad (4.2)$$

This ‘worst case scenario’ of the maximum demand and least PV production set the requirements for the SMR size. This scenario corresponds to the upper bound of the interval in Eq. (4.2). In other words, the SMR must be able to provide sufficient power at the maximum demand in this microgrid.

This SMR would be required to meet the remaining interval through power regulation when performing traditional load-following tasks. While the PV can add additional power to this microgrid, the contributions cannot be guaranteed and therefore cannot be used to reduce the size requirement of an SMR without TES.

## Trends

An illustrative demand curve and representative PV output on a summer day and a winter day are shown in Figure 4-2. The installed PV capacity is at 40% of the maximum demand. These two figures contain the daily trends of the nominal PV output and the daily trends in demand that span the annual limits. It is seen from Figure 4-2 that there is higher PV output in the summer from greater peak PV potential with longer daylight hours combined with lower demand compared to the winter. This results in a much lower net demand in the summer compared to the winter. When considering smooth variations

in the demand and PV over long periods of time at relatively low rates of change, the net demand can be met by the SMR with a low ramp rate limit ( $<2\%$  FP/min). However, it can be seen from Figure 4-2 that there are significant total ramps required from the SMR when the PV generation suppresses the net demand.

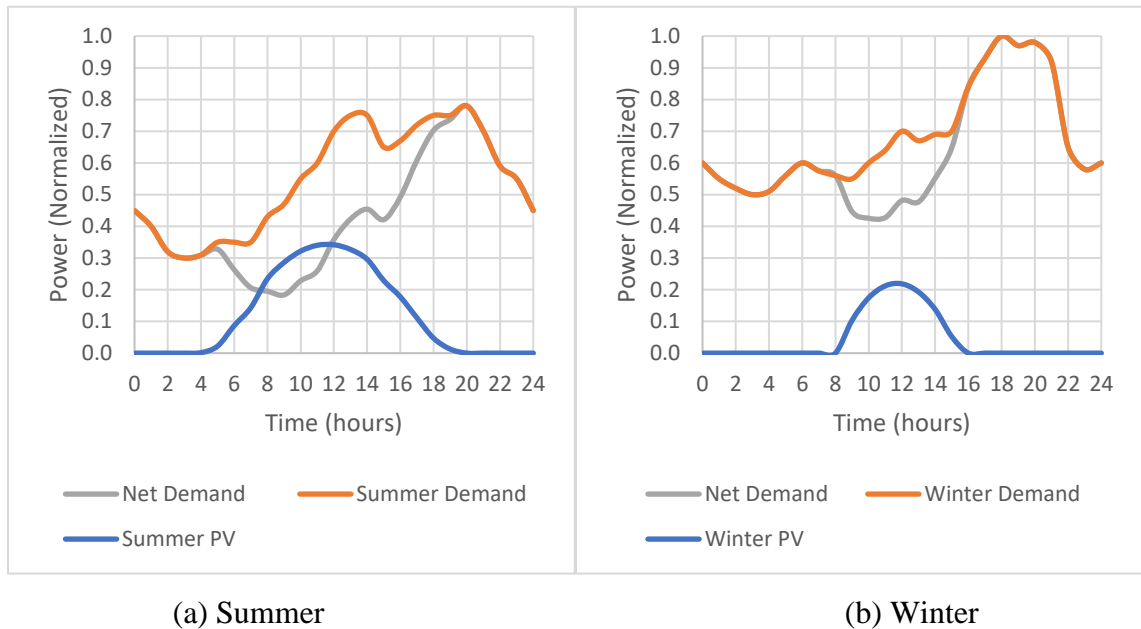


**Figure 4-2 Typical demand and PV production at a remote community with associated net demand for (a) Summer and (b) Winter**

### Variability and Intermittence

Beyond the required ramping of the SMR from smooth variations, rapid changes in the demand and PV output must also be accounted for. The variability from the load is intrinsic to power systems based on the community characteristics (without considering demand response). The variability from PV is also related to the geographic location of the PV system, but the main influencing factor is the size of the PV system. Larger PV systems have the potential for higher magnitudes of variability in response to changes in weather conditions. However, these systems tend to cover a larger area which could reduce overall rates of change if only portions of the PV system were affected at a given time as clouds pass over.

### PV Considerations

It is important to mention that the addition of PV does not enhance the operation of the SMR system, but only affects its capacity factor by de-rating during higher PV output. When the installed PV capacity is increased to large amounts, there can be extended periods when production is higher than demand. In such a case, PV curtailment has to be performed. Further, the magnitude of variability from the PV output increases with the installed capacity.

Based on the typical profiles from in Figure 4-2, the PV power is limited to a maximum of 65% of the peak demand, before it can exceed the instantaneous demand during the summer months. While this is a large fraction of the power, it becomes much less of the total energy. This corresponds to a maximum contribution of solar energy of 35% in the summer and 10% in the winter months compared to the total demand.

### **Considerations of a Load-following SMR in a Microgrid with PV**

The above analysis has identified the following issues for the SMR:

1. This configuration would require continuous load-following with large power ramps which can cause significant thermal and neutronic stresses on the core components. It also increases wear on control elements such as valves and pumps.
2. The capacity factor of an SMR sized at the maximum demand and following the load from Figure 4-2 can be reduced due to the large daily and seasonal variations of load and PV production. For the summer and winter months, the SMR capacity factor would approximately be 55% and 68%, respectively. This capacity factor would further be reduced when the PV capacity increases.

## **4.4 Analysis of SMR-TES Integrated into a Microgrid**

If thermal energy storage is introduced into the microgrid, the methods used in the previous section can be extended to study the behaviour of this new microgrid. This section examines how to determine the size of the SMR core and thermal storage within a microgrid.

The integration of a TES system into a microgrid allows the SMR system to effectively distribute the power produced from the reactor core to match the required variable demand throughout the day. In the previous section, the load-following SMR is found to have a reduced capacity factor due to (1) the required size at least at the maximum demand, while the actual demand is almost always less than the maximum demand, and (2) introducing PV generation further reduces the required SMR operation.

Introducing thermal energy storage can increase the flexibility of the SMR system. The TES system can act as a buffer between the SMR core and the required output of the system (through the BOP). The requirements for this controllable source and the associated sizing and operation of the SMR system will be different when TES is used. When introducing TES, the three components (Core, TES, and BOP) are related and must be sized properly together.

This system can allow the core power generation rate to be dynamically adjusted, but the use of TES can reduce or eliminate frequent adjustments, resulting in a need for only long-term adjustments (e.g. daily). Depending on the net demand and the SMR core power production, the TES and BOP can be adjusted so that the combined output meets the required net demand.

Compared to the conclusions from the previous section, the SMR-TES system has the potential to reduce the reactor core size below the maximum demand by utilizing peaking output by an oversized BOP system and TES. This can lead to a higher capacity factor. The excess power can be stored and used whenever needed. Such a system has the potential to integrate with PV by further utilizing the TES system.

### **System Operation**

Using the same demand and PV profiles as in the previous sections from Figure 4-2, the operation of the SMR-TES system can be analyzed. The following steps and corresponding calculations are explained for the operation of the SMR-TES:

- As the total SMR-TES output is required to follow the net demand, the steam mass flow rate in the power cycle can be varied in constant temperature and pressure mode from Eq. (3.28).
- Then for the TES intermediate loop to achieve power balance across the steam generator, the hot tank outlet mass flow rate can be adjusted accordingly based on Eq. (3.32), to match the required heat transfer rate from Eq. (3.30).
- When the SMR core operates at constant full power, the cold tank outlet mass flow rate will also be constant as defined by Eq. (3.34).
- To main mass conservation within the intermediate loop, the coordination described by Eq. (3.35) between the inlet and outlet mass flow rates of the hot and cold tanks is required.
- The quantities of molten salt in the hot and cold tanks vary over time described by Eq. (3.36) as the steam cycle is varied to follow the net demand.

### **Component Sizing and Operational Considerations (without PV)**

The size requirement remains the same that the controllable sources must have adequate capability and controllability to meet the peak load demand. Specifically for this configuration, the output of the SMR-TES system must be guaranteed to meet this peak demand. After adding TES, the storage of energy makes it possible for this configuration to produce a peaking output above the nominal rating of the SMR core. With storage and an oversized BOP, the combined system can produce more than the nominal core rating for extended periods of time (as the TES discharges) to meet the peak demand. This can effectively allow for a SMR with a smaller power rating as compared to that of the previous section. Therefore, the sizing problem for the SMR-TES system considers the question of by what amount the SMR core power level can be reduced, and what the associated requirements for TES and BOP size would be.

First, the analysis considers demand without any contribution from PV. This is defined as the ‘worst case scenario’. If the required load interval for the SMR-TES system to meet

the demand is  $[\underline{L}, \bar{L}]$  and the SMR core generates a constant power, the relation between the power of the thermal energy storage and SMR core is within this interval, and can be found as:

$$\begin{aligned} P_{TES}^I &= [\underline{L}, \bar{L}] - P_{SMR} \\ &= [\underline{L} - P_{SMR}, \bar{L} - P_{SMR}] \end{aligned} \quad (4.3)$$

Under the assumption that the demand generally varies around the middle of the interval, the SMR core is sized for this middle. This would result in equal amounts of charging and discharging for the TES system. If the BOP system is sized at the maximum demand to ensure that this demand can be met, the difference in the SMR core sizing and maximum load would be the required peaking capacity of this SMR-TES system. The maximum amount of energy storage in the TES system over one day determines the required storage capacity.

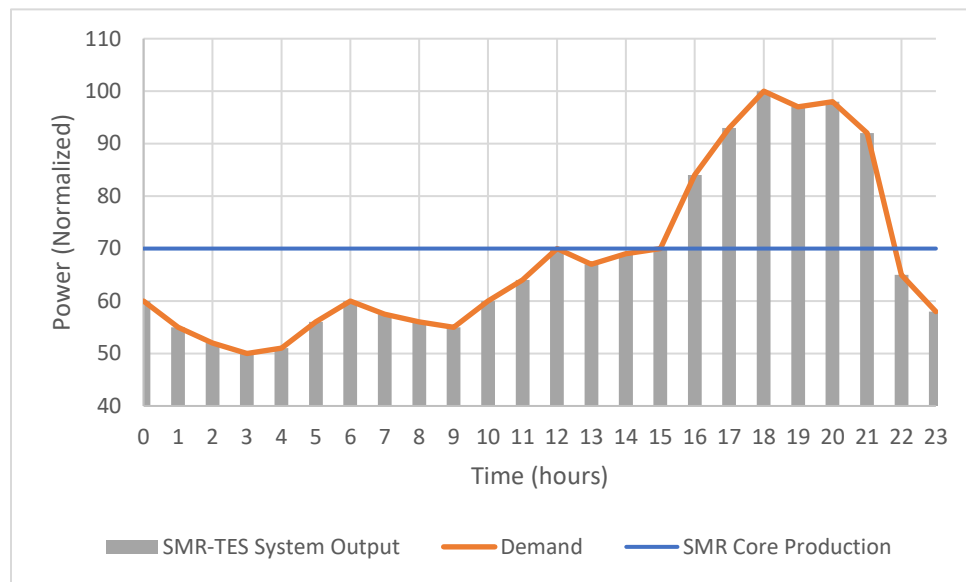
#### 4.4.1 SMR-TES Simulations for Sizing Assessment of TES

Steady-state simulations have been performed for power balance between the SMR-TES system and a typical demand curve over the period of one day as shown in Figure 4-3. The TES power is calculated as the difference in the net demand and the SMR core power. The TES energy is calculated as the sum of the TES power over time.

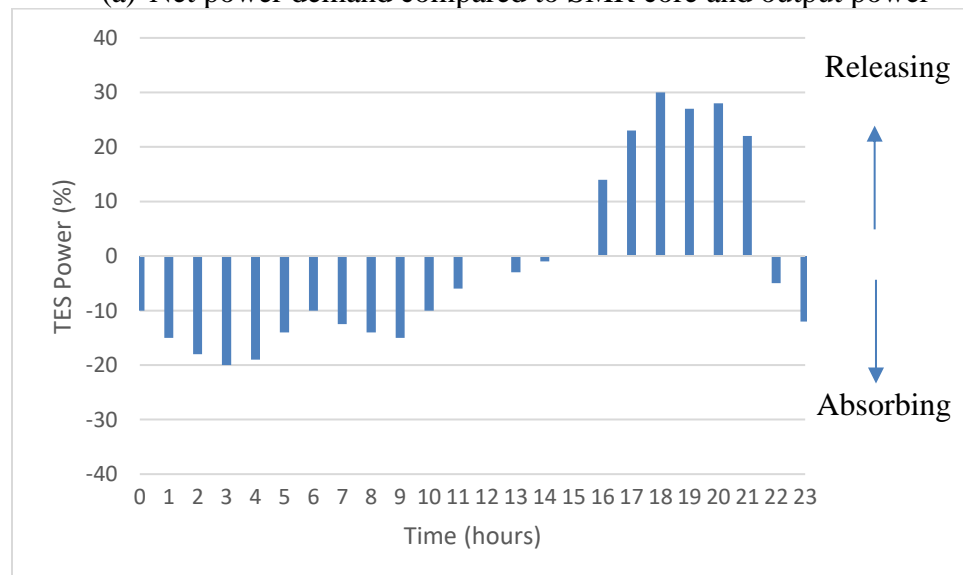
The demand varies between 50% and 100%, normalized with respect to the maximum demand. The SMR core can be sized at the average demand and the BOP is sized at the maximum demand over this period.

The power output of the SMR-TES system to follow the demand is shown in Figure 4-3 (a). The total system output varies while the SMR operates at a constant full power. The difference in the SMR core power production and the power demand must be met by the TES system by either absorbing or delivering power as shown in Figure 4-3 (b). Negative values of the TES correspond to power absorbed in the TES when the demand is less than the SMR core production. Positive values of the TES correspond to power delivered by the TES to the load during periods of high demand. As the power of the TES varies, the stored energy in the TES varies as shown in Figure 4-3 (c). The required TES storage

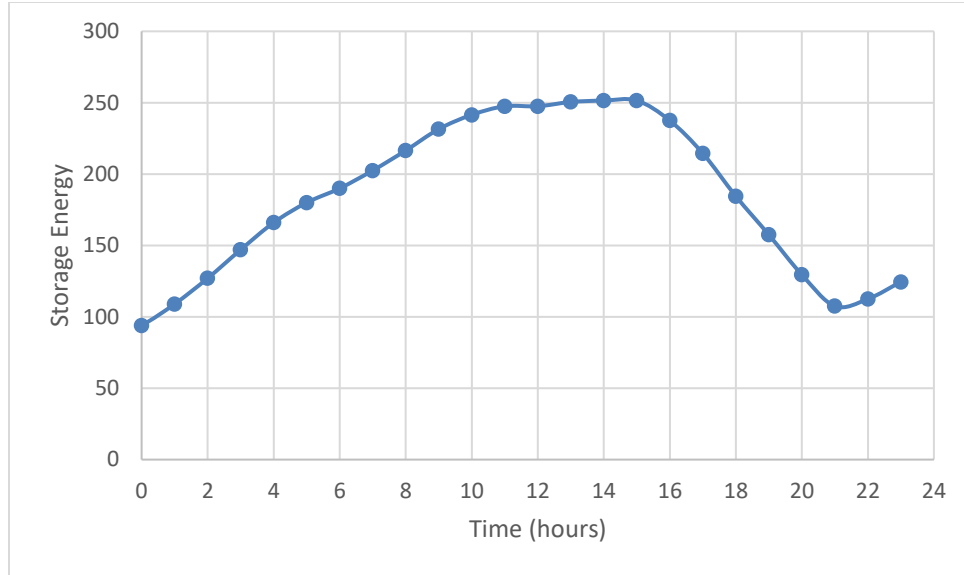
capacity can be determined based on the difference in the minimum and maximum values of the TES capacity in this simulation. The results from Figure 4-3 (c) are normalized to this maximum TES capacity within the upper and the lower SOC limits. The results of the simulation determine the desired TES capacity for the selected SMR core and BOP size for a given demand profile. It is important to not from Figure 4-3 (c) that the amount of energy stored in the TES from the start of the day to the end of the day is very similar, which demonstrates that this system can continue to operate day after day without issue.



(a) Net power demand compared to SMR core and output power



(b) TES power to perform load-following



(c) Amount of energy stored in the TES

**Figure 4-3 Performance of SMR-TES system to follow demand based on power and energy calculations with (a) Demand and SMR power, (b) TES power and (c) TES energy**

The first step in the sizing solution is to set the SMR core output in kW to the average of the demand profile that is defined as:

$$P_{CORE}^{size} = average(\bar{L}[k]), \forall k \quad (4.4)$$

where the *average* function represents the timeseries average of the demand over the period of the day. This demand profile should represent the maximum to align with the ‘worst case scenario’. The size of the balance of plant/turbine in kW is set at the maximum demand defined as:

$$P_{BOP}^{size} = max(\bar{L}[k]), \forall k \quad (4.5)$$

where the *max* function represents the selected maximum value of the timeseries demand over the period of the day. The results of the simulation determine the required storage mass ( $m_{TES}^{size}$ ).

Simulations like that in Figure 4-3 are repeated to determine the effect of the SMR core size between the ranges of the minimum and the maximum demand on the TES system.

The results are summarized in Table 4-2. Five different SMR core sizes selected between the minimum demand (50%) through to the maximum demand (100%) have been considered. The simulations determine the required TES storage capacity along with the maximum required charging and discharging power. The net energy of the TES in Table 4-2 is the calculated net amount of energy that is charged or discharged through the TES over the day.

The simulation studies have found that sizing the reactor core at the average demand will minimize the required storage capacity. When the SMR core is sized below the average demand, the TES system is required to discharge more power to account for the prolonged periods when the demand is above the core production rate. This could create operational problems when the SMR core is sized too small, which can cause the TES to continually discharge and risk running empty. More specifically, if the SMR is the only controllable source in this microgrid, there is no guarantee that the TES can be properly re-charged while the SMR is preoccupied with load-following. Conversely, sizing the SMR core above the net demand does not utilize the strengths of the added TES system to reduce the SMR core size. Sizing this SMR core at the average demand reduces the core sizing while also minimizing the required TES storage capacity.

**Table 4-2 Relationship between core sizing and TES characteristics**

<b>Input SMR Core Size (%)</b>	<b>Calculated Maximum Discharge Power (%)</b>	<b>Calculated Maximum Charge Power (%)</b>	<b>Required Storage Capacity</b>	<b>Net Energy of TES</b>
50 (min demand)	50	0	880	440 (net discharge)
59	41	9	520	224 (net discharge)
68 (avg demand)	32	18	320	0
84	16	34	780	370 (net charge)
100 (max demand)	0	50	1520	760 (net charge)

### **Component Sizing and Operational Consideration with PV**

When PV is brought into the microgrid at a given SMR core power level, the added PV will decrease the net demand required for the SMR and will result in increased periods for charging the TES. While PV cannot be used to offset the sizing of the SMR load-following without TES, it has potential to reduce the core size in an SMR with TES absorbing the PV variability.

The variable nature of PV output makes it difficult to account for using this source to reduce the size of SMR. By considering the daily energy production from PV as a random variable, it can be considered that the actual PV energy output for a day will vary around the mean based on a uniform distribution. Given that the PV daily energy generation varies uniformly around the average (such that the average is  $\frac{1}{2}$  of the maximum power), the core size of the SMR can be reduced by the average PV power output, provided that additional storage is available to compensate. A modification can be made to the size of the SMR core:

$$P_{Core}^{size} = average(\bar{L}[k]) - \frac{1}{2} * average(\overline{P_{pv}}[k]), \forall k \quad (4.6)$$

where  $\overline{P_{pv}}[k]$  represents the nominal timeseries PV output over the day. The modification from Eq. (4.4) is that the SMR core is reduce by the average PV output. The sizing of the BOP remains the same to ensure that the maximum demand can still be met. The required TES storage capacity when adding PV can be calculated through the simulations.

#### 4.4.2 Methodology for Sizing SMR-TES System

This section expands on the previous section and explains the methodology for how the SMR-TES system can be sized for a typical demand profile with the SMR-TES model through an example simulation. The SMR-TES system sizing is based on modelling, simulation and analysis under steady-state conditions. A description of the calculations for these simulations can be found in Appendix B. The generic demand curve from the previous sections was scaled with a peak demand of 2,000 kW that represents  $\bar{L}[k]$  as the maximum winter demand. Here the demand varies between 1000-2000 kW. The demand curve is shown in in Figure 4-4 (a).

#### **Sizing of Balance of Plant**

Building upon the requirements for sizing of the benchmark SMR, the BOP and turbine power rating ( $P_{BOP}^{Size}$ ) is sized at least for the peak demand from Eq. (4.5), that in this case is 2,000 kW.

### **Sizing of Reactor Core**

To effectively utilize the additional power brought by the TES, the SMR core power rating should be sized around the average demand. Given this selection, the core electrical power level can be determined from (4.4). In this case, the SMR core power rating is sized at the average demand of 1,375 kW from:

$$P_{Core}^{Size} = average(\bar{L}[k]) = 1,375 \text{ kW} \quad (4.7)$$

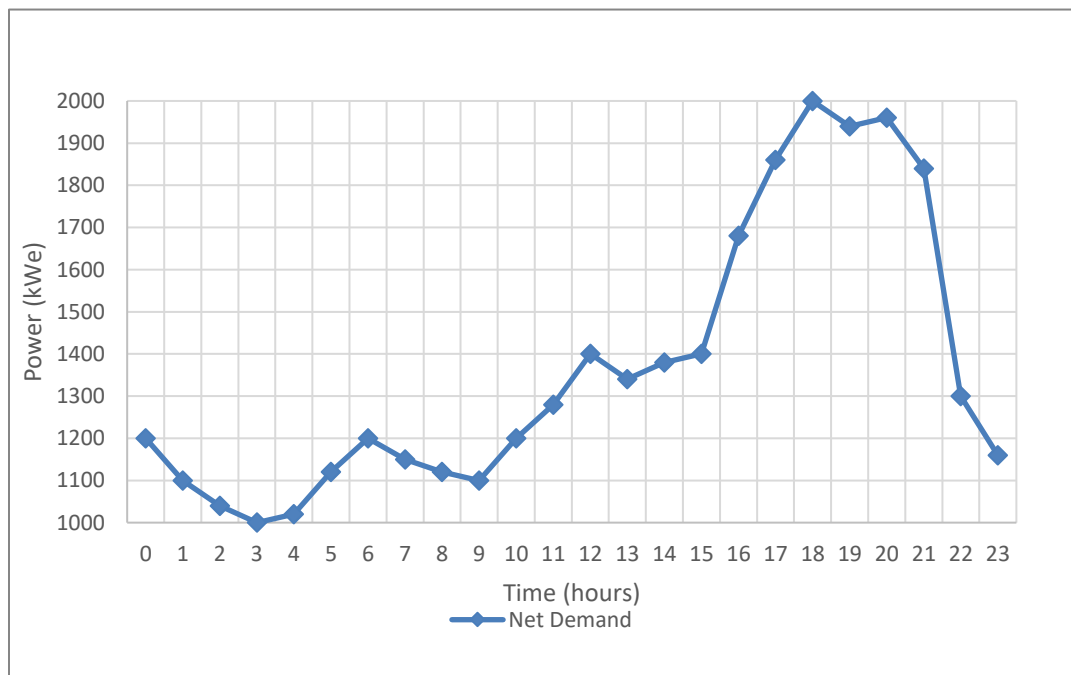
### **Sizing of Thermal Energy Storage**

The sizing of the TES is dependent on the specific size of the reactor core and that of the BOP relative to the specific demand profiles. The SMR model from Section 3.3 is used to calculate the SMR state parameters at each time step, specifically the helium, molten salt, and steam mass flow rates. These calculations are summarized in Appendix B. Through simulations, the quantities of mass in the storage tanks can be determined. From these quantities, the required mass of molten salt as the required TES storage capacity can be determined.

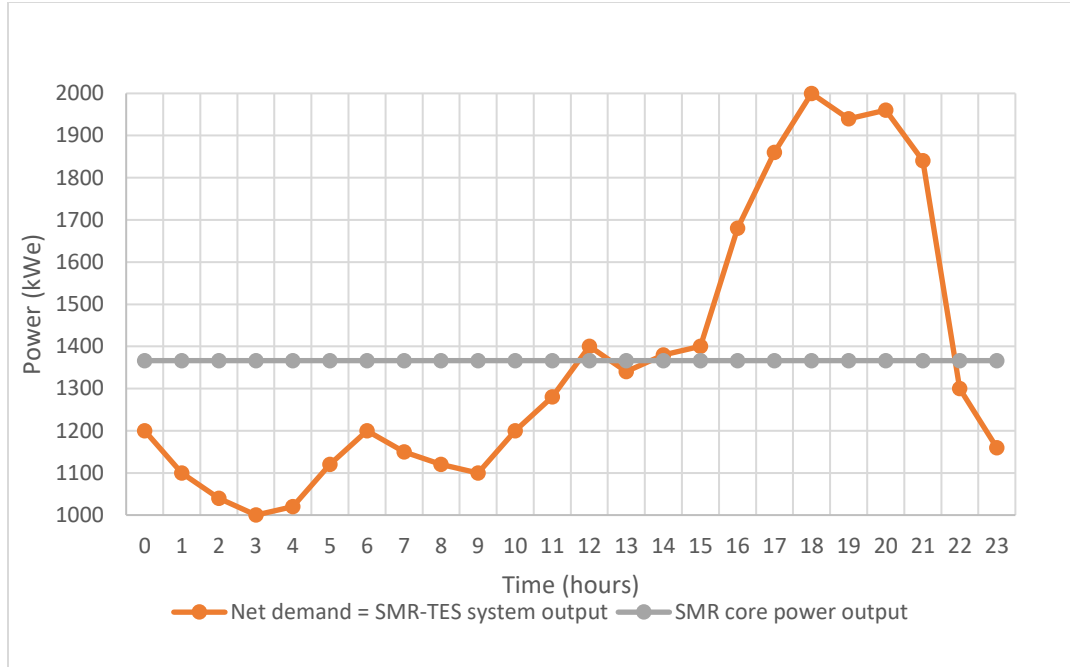
### **Simulation Results (without PV)**

The results from this simulation are presented in Figure 4-4. The demand curve is shown in Figure 4-4 (a). The output power of the SMR-TES over time to follow the demand versus the core power is shown in Figure 4-4 (b). To perform load-following studies, the steam flow rate through the turbine varies to produce the electrical power output as shown in Figure 4-4 (c). The actual steam flow rate is compared to the nominal steam flow rate corresponding to the size of the SMR core and the maximum steam mass flow rate limit that is based on the size of the BOP. The mass flow rates of the molten salts in the intermediate loop are accordingly adjusted based on the variations in steam mass flow and the core power level. The mass flow rates out of the hot and cold tank are shown in

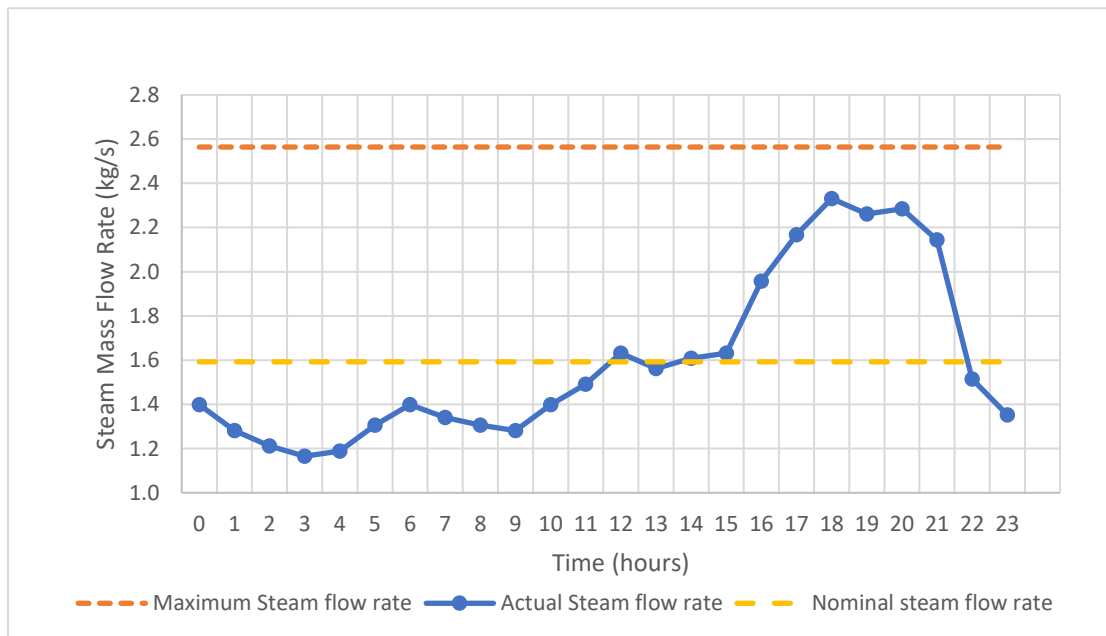
Figure 4-4 (d) that also correspond to the mass flow rates into the cold and hot tank respectively. The hot tank outlet mass flow varies proportionally to the steam flow, whereas the hot tank inlet flow is kept constant for constant power output. The variations in mass flow rates in and out of the storage tanks results in variations in the tank levels as shown in Figure 4-4 (e). In the above simulation, the maximum variation in the storage tank levels is 82 metric tons of storage salt. To avoid exceeding 25% lower and upper SOC limits, the required salt mass capacity ( $m_{TES}^{size}$ ) is determined to be 165 metric tons of solar salt. By sizing the SMR core at the average demand and ensuring SOC limits of the TES are maintained, the complete system can be ensured to have adequate capacity for continuous power regulation.



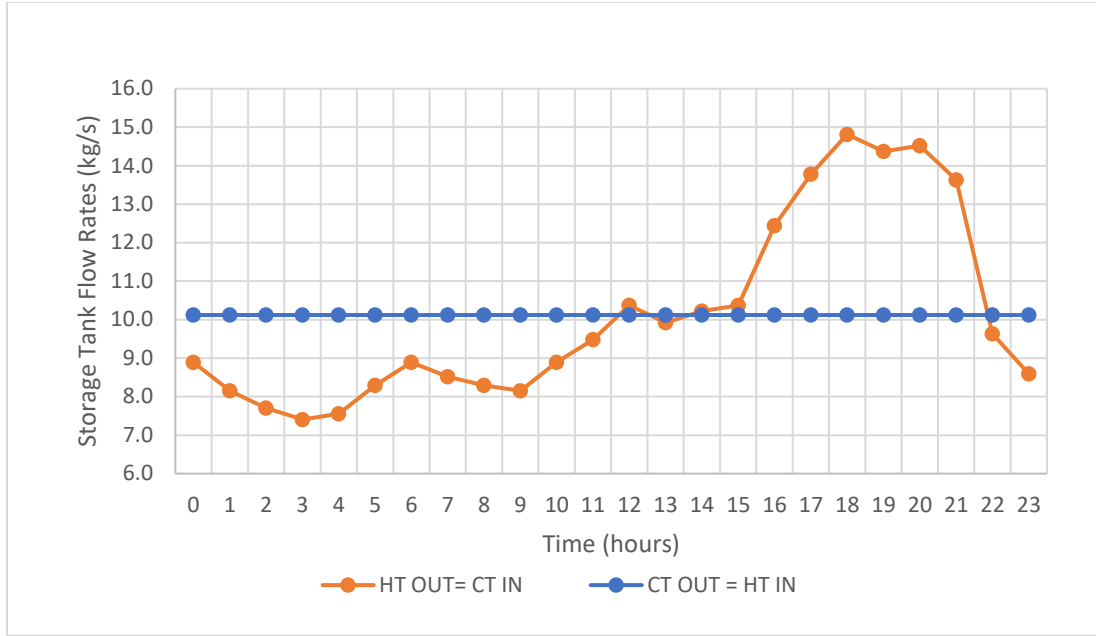
(a) Demand



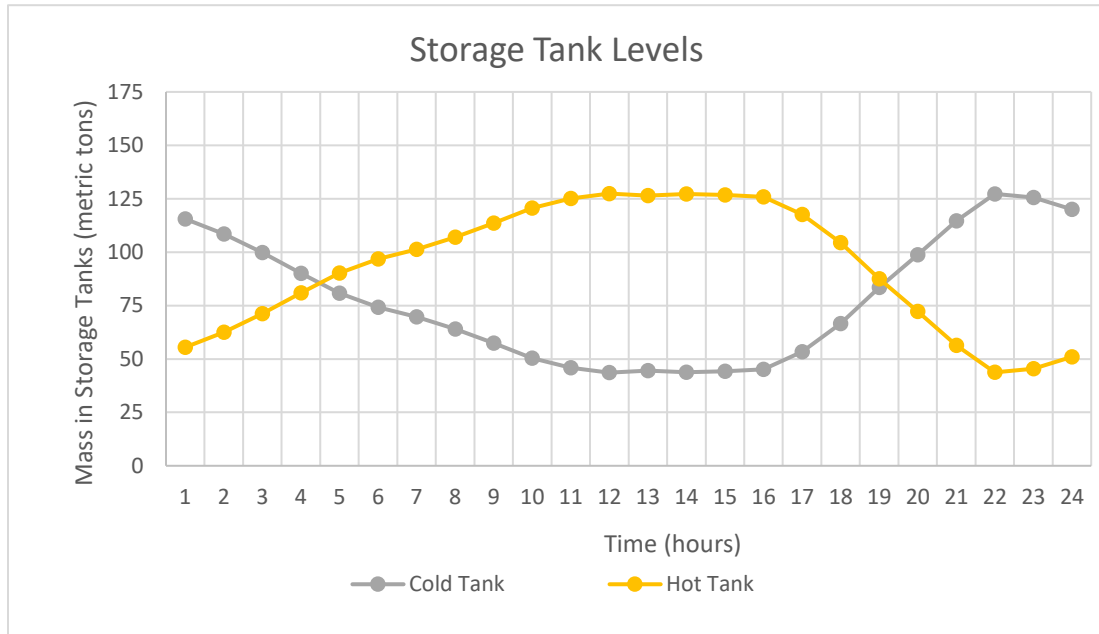
(b) SMR-TES output following the net demand compared to SMR core power



(c) Power cycle steam flow rate compared to the nominal and maximum limit



(d) Inlet and outlet mass flow rates of the hot and cold storage tanks



(e) Mass in the hot and cold tanks

**Figure 4-4 SMR-TES system operation from SMR core and BOP sizing to determine system operation and required TES storage capacity with (a) demand, (b) SMR core and SMR-TES output, (c) steam mass flow rate, (d) hot and cold tank mass flow rates and (e) hot and cold tank storage levels.**

### Simulation Results (PV)

The steady-state simulations and analysis from above can be modified to include PV generation. The SMR-TES sizing will be affected when PV is introduced since the variations and intermittence of PV must be accounted for by the rest of the system. It is demonstrated that the SMR core size can be reduced by the average PV generation during the winter season. As an example, adding 1,000 kW of PV to this microgrid, the SMR core size can be revised based on Eq. (4.6). The SMR core size without PV is selected from Eq. (4.7) to be 1,375 kW. With the average PV power output in the winter month of 57 kW, this results in the revised SMR core size as 1,318 kW calculated from Eq. (4.6):

$$P_{CORE}^{size} = 1,375 - 57 = 1,318 \text{ kW} \quad (4.8)$$

By reducing the SMR core size when adding PV, additional storage capacity is required to account for variations in PV since the maximum output of the PV system cannot be guaranteed. Performing the same simulations from above with the installed PV capacity ( $P_{PV}^{size}$ ) of 1,000 kW. The required TES storage capacity ( $m_{TES}^{size}$ ) is 250 tons, up from the original 165 tons without PV.

### Economic Evaluation

An inferred economic evaluation can be performed to compare the costs of the benchmark SMR against the SMR-TES system.

First, the benchmark SMR without TES is sized at the maximum demand of 2,000 kW. Second, the change in costs when adding TES can be estimated. Here the SMR core size is reduced to 1,375 kW, with the BOP being at 2,000 kW, and the storage capacity being 165 metric tons. It is estimated that the SMR core capital costs will be lowered when the core power rating is reduced from 2,000 kW to 1,375 kW. The added TES costs can be estimated based on the findings in Section 3.4.2. The TES costs can be estimated from the storage capacity and the unit costs:

$$C_{TES,cap} = 165 \text{ tons} * 3.26 \frac{\$}{kg} * \frac{1000 \text{ kg}}{1 \text{ ton}} * \frac{1 \text{ M\$}}{10^6 \$} = 0.54 \text{ M\$} \quad (4.13)$$

The added costs from the TES system are relatively small and should be more than accounted for by the savings from the SMR core capital costs. SMR capital costs are the most significant portion of the expenses, so reducing the required SMR core size results in a reduced total cost. The added costs of the TES can be easily off-set by the savings from the reduced SMR core size it helps to reduce. One can therefore conclude that integrating TES will reduce the total cost of the system without jeopardizing any performance.

The third case involves the addition of 1,000 kW PV. It results in a slight reduction in the SMR core size to 1,313 kW. The required TES capacity in this case is 250 metric tons of solar salt. This TES cost is estimated at 0.82 M\$ which remains a small added cost. In all cases, the cost of added TES are much smaller than the cost savings when reducing the SMR core sizing.

### **Dynamical Simulations**

Dynamical analysis can then be conducted to explore system behaviour under rapid variations in load and PV. Such analysis can further explore the ability of the SMR-TES system during load-following, and to determine additional energy storage requirements. This complete sizing problem will be described in Chapter 5 in the form of a case study.

## Chapter 5

### 5 A Case Study

A case study is conducted using the data from a large sized community in northern Ontario. The system configuration, design and analysis methodologies developed in previous chapters are utilized to select the desirable size of components for this microgrid.

First, steady-state analysis is conducted. The sizing methodologies from previous chapters are used to size the SMR-TES system for the benchmark community that includes analysis and simulations. The effect of adding PV to the microgrid is explored to determine the effect on SMR-TES sizing, and to determine any upper limit on the PV size. Second, dynamical analysis is conducted. The operation of the microgrid and the requirements of the EES is determined based on SMR-TES ramp rate limits and the amount of PV included. Limits on the amount of PV that can be accommodated is informed from the steady-state simulations. From the results of the steady-state and dynamical analysis, the solution to the sizing problem is made to select the size of the SMR-TES system and the components, the size of PV, and the amount of EES required.

#### 5.1 Community Electricity Profile

Community information includes the definition of electrical demand characteristics and renewable resource potential for PV based generation. Community electrical demand and solar resources exhibit seasonal and daily trends as well as variability on the different time scales. The community load demand characteristics are used to determine the required microgrid size.

##### **Electrical Demand**

This benchmark community has a peak demand of 4,500 kW. The sizing methodology is dependent on the maximum demand and the defined maximum daily demand profile representative of the maximal consumption month, which is December, as shown in Figure 5-1. The actual daily demand profiles for this month are assumed to vary within

the upper and lower bounds. The parameters in Table 5-1 describe the variations in the demand. The daily load variation is approximated to be 40%, the annual load variation is estimated to be 60%, and the time-step variability is chosen as 500 kW. Based on these parameters, the maximum demand occurs in December. The seasonal maximum demand varies between 1,800 kW and 4,500 kW. The minimum demand occurs in June. The seasonal minimum demand varies between 1,080 kW and 2,700 kW. It is assumed that the summer and winter demand profiles are similar in shape.

**Table 5-1 Electricity profile of a community**

Benchmark Community Input Parameters	Value
Maximum Annual Demand, $L_{Max}$	4,500 kW
Daily Load Variation, $\sigma_D$	$\frac{1830}{4500} = 0.40$
Annual Load Variation, $\sigma_Y$	$\frac{2700}{4500} = 0.60$
Time-step Variability, $\sigma_S$	500 kW

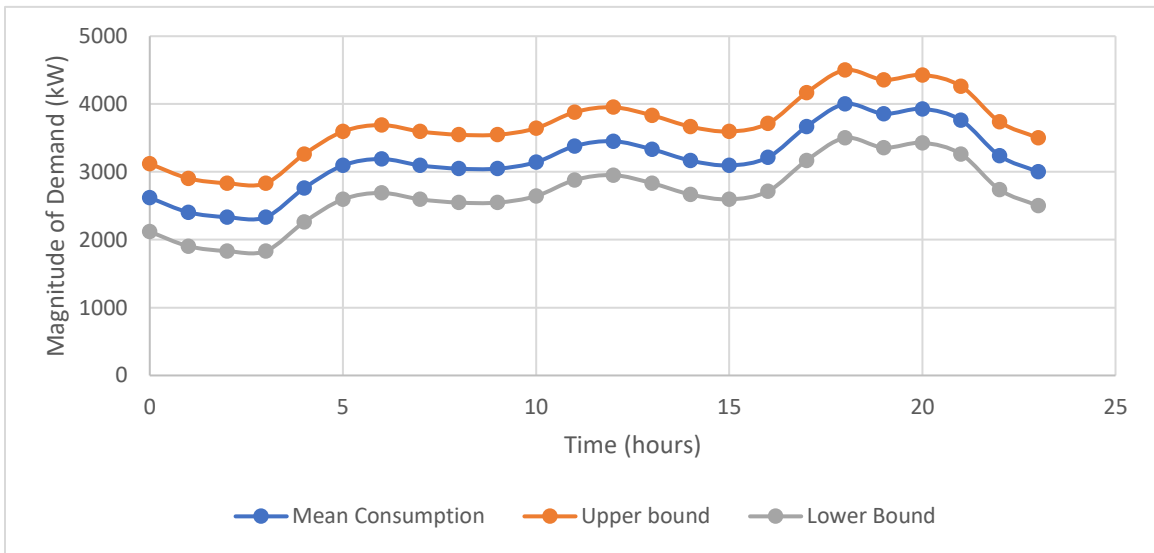
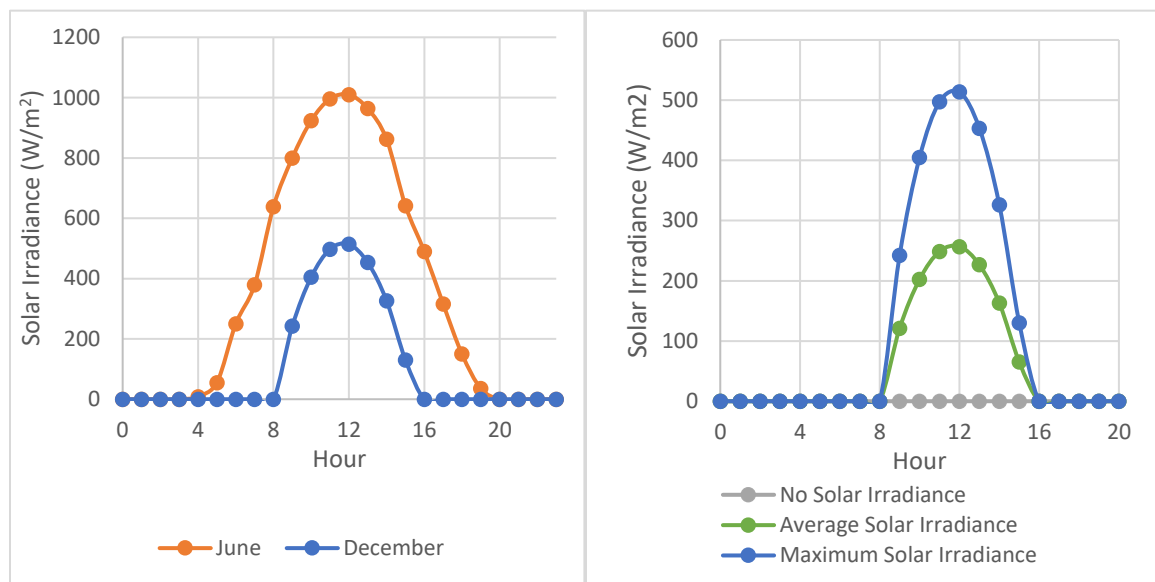


**Figure 5-1 Input community demand profiles in winter month**

**Contributions from Renewable Resources**

The PV generation potential is first estimated using the data from PVWatts Software [44] for the geographical location in northern Ontario (53.05, -93.3). The annual average solar

irradiance is estimated to be 3.99 kWh/(m<sup>2</sup>·day) with large seasonal variations between the peak occurring in June and the minimum occurring in December. The daily nominal trends of the solar irradiance with seasonal variations are shown in Figure 5-2. The annual variation in the peak solar irradiance between the summer and the winter is approximately 50% in this community as shown in Figure 5-2 (a). The actual PV output can deviate based on weather patterns that tend to reduce the actual PV production. The average hourly PV production curve is found to be approximately half of the nominal production for both seasons.



(a) Annual variation in solar irradiance (b) Winter daily variation in solar irradiance

**Figure 5-2 (a) Seasonal variations in the daily PV profiles between summer and winter and (b) Defined range of PV output profiles in the winter month.**

### PV production versus Community Demands

The PV resource potential is maximum in the summer months and minimum in the winter months, which is opposite to the demand characteristics of the community. Not only is the peak solar irradiance reduced in the winter, but the sunshine hours are much shorter in the winter months. The flexibility of the SMR system must account for these large seasonal characteristics along with all shorter timeframe phenomena including daily variations and any intermittence of PV and variability of demand.

## **Size of a Single SMR as a Benchmark**

For comparison purposes, the benchmark SMR is expected to perform traditional load-following to meet most of the needs of this benchmark community, with only small amounts of energy storage devices to account for fluctuations. To meet the sizing requirements, the SMR would have to at least be sized to meet the peak demand of 4,500 kW. To account for community growth this SMR could be sized with a margin to meet increased demand before the future demand growth requires the installation of additional SMR units. Since PV generation is inherently variable, it cannot be guaranteed to meet the peak demand. This fact sets the size requirement for this SMR.

## **5.2 Single SMR Sizing Problem**

The purpose of this section is to demonstrate the solution process for sizing components in this microgrid for the benchmark community. The SMR-TES sizing is completed first without PV and then PV is added to determine the limits of PV for this community.

### **5.2.1 Steady-State Analysis**

#### **Initial Comparison of SMR-TES sizing with benchmark SMR**

The first part of this analysis is through steady-state modelling and simulation. This system sizing is dependent on the maximum demand profile as identified by the upper bound in Figure 5-1. The input for the PV system is the potential curve of the winter months in Figure 5-2 (b).

First, the steady-state simulation is conducted to determine the initial sizing of this SMR-TES system without accounting for contribution from PV for an initial comparison versus the benchmark SMR sizing. The analysis and simulations in Microsoft Excel utilized power balance between the input of the maximum demand curve from Figure 5-1 and the required generation from the SMR-TES system based on SMR-TES models. The detailed process can be found in Appendix B. The inputs for this SMR-TES system are the power ratings of the SMR core and the BOP. The analysis and the calculations determine the required TES capacity for this SMR-TES system to meet the demand.

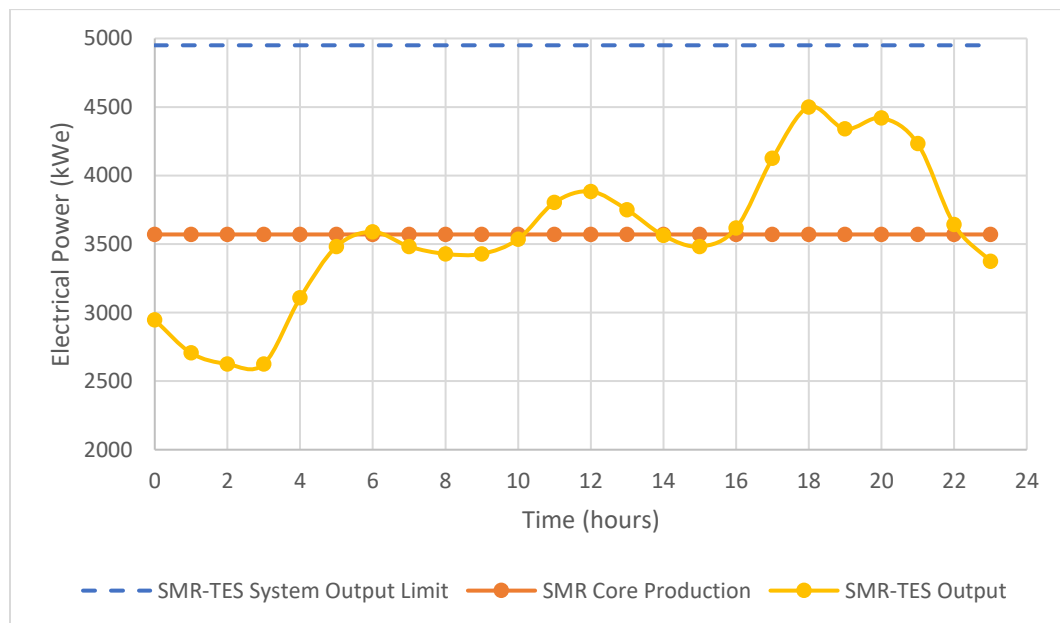
In the simulation and analysis process, the input to this simulation is the SMR core and BOP size. The SMR core is sized as the average of the maximum interval of peak demand and the BOP is oversized to the peak demand plus the margin to allow for this SMR-TES system to meet all demand requirements. The simulation determines the amount of TES capacity that is required to meet the required net demand. The sizing results are summarized as the following:

- $P_{SMR}^{size}$ : The SMR core power rating is sized as the average of the maximum interval of peak demand at 3,570 kW<sub>e</sub>. This corresponds to an equivalent core thermal power of 11,900 kW<sub>th</sub>
- $P_{BOP}^{size}$ : Balance of plant system is sized at the peak demand with margin to ensure that this system can meet the peak demand. To be more specific, this part of the system is sized at 5,000 kW<sub>e</sub> accounting for 10% capacity margin.
- $m_{TES}^{size}$ : The minimum required storage capacity is determined through simulations with the SMR-TES model. It has been found to require at least 241 metric tons of solar salt material.

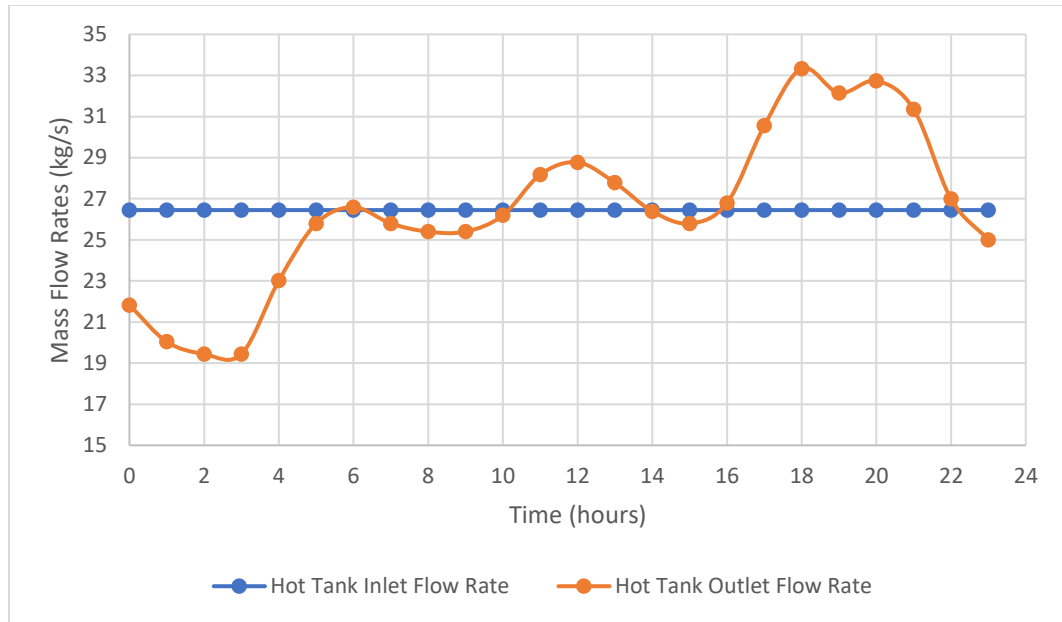
The performance of this system can be demonstrated in Figure 5-3 in terms of the key variables. The SMR-TES output power compared to the core power production is shown in Figure 5-3 (a) with upper limits on the electrical output set by the BOP size. The assumption in this analysis is that the SMR core would operate at full power during the peak demand and the TES and BOP would accordingly modulate power to follow the demand. When the core power production exceeds the required output, the TES system will store this excess power. When the core power production is less than the required output, the TES will contribute additional power to make up the difference. The operation of the TES hot tank is shown in Figure 5-3 (b) showing the inlet and output mass flow rates. The hot tank inlet flow rate is set by the SMR operating power level. When the hot tank outlet flow is greater than the inlet flow rate, the TES system is discharging proportional to the required peaking power within the steam cycle. When the hot tank outlet flow is less than the inlet flow rate, the TES system is being charged in proportion to the excess power produced from the core. The cold tank flow rates operate inversely to

that of the hot tank. The amount of solar salt in the hot and cold tank are shown in Figure 5-3 (c). While 121 metric tons is calculated in the simulations as the maximum change in solar salt capacity in each tank, additional storage material may be required to ensure the SOC lower and upper limits are not exceeded. A total of 241 metric tons is required to maintain 25% margins on the upper and lower levels. This is because there are two storage tanks. If the associated tank volumes were sized for 120 metric tons, both tanks could become completely empty or completely full. This can be avoided by adding additional solar salt as filler in each tank and sizing the tanks to the larger amount. This ensures the both tanks will vary within 25% to 75% of their levels.

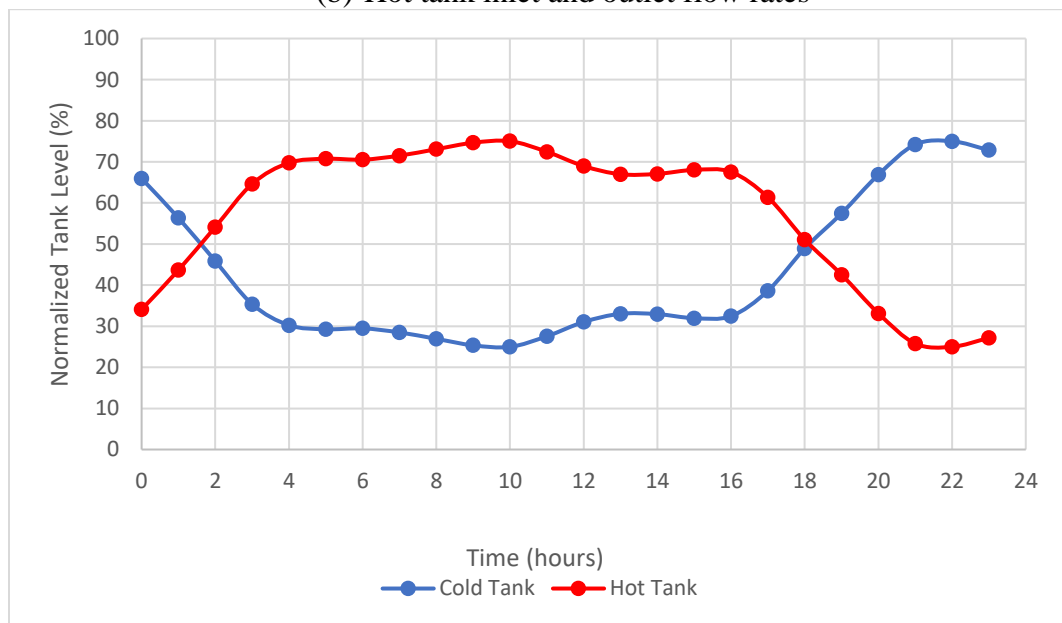
Sizing the SMR core at the average of the upper interval of demand ensures that this system can adequately meet the maximum demands. During periods of maximum demand there are even amounts of charging and discharging of the TES, with nearly constant tank level changes from the start of the day to the end. This can guarantee continual operation for extended periods of peak demand. On days when the demand is less than the maximum, the SMR core can reduce output to the new demand range and the TES can charge and discharge to meet changes in the demand.



(a) SMR-TES output compared to core power production



(b) Hot tank inlet and outlet flow rates



(c) Solar salt levels in hot and cold tank

**Figure 5-3 Key parameters of SMR-TES operation with proper component sizing with (a) SMR output, (b) Hot tank inlet and outlet mass flow and (c) Cold and hot tank levels**

### **Effect of PV on Sizing of SMR-TES System**

The steady-state analysis methodology has been modified to include contributions from PV generation. The purpose is to determine the effects of the SMR core size and required TES capacity from the range of PV outputs and the installed PV capacity. For a given installed PV generation, the steady-state simulations have been conducted in three runs based on the range of actual PV output: (1) maximum PV output, (2) average PV output at 50% the maximum nominal PV output, and (3) zero PV output. These three amounts correspond to the solar irradiance curves in Figure 5-2 (b). These simulation runs have been iterated through the span of PV installed capacity.

Instead of the SMR core sized at the average demand from the previous section, when adding PV, the SMR core can be sized at the average of the net demand from (4.6). This reduction corresponds to the average PV output at 50% the maximum nominal PV output. This will allow for reduction in the SMR core size with the added PV. The TES can then be properly sized with enough capacity to ensure that the required output power can meet the PV variations. This will require additional TES capacity as compared to the case without PV to account for the variation in PV between the lower and upper limits.

The results of the simulations to determine the required TES capacity are summarized in Table 5-2 where the installed PV capacity has been varied between 0 to 5,000 kW. In each simulation the SMR core is sized at the average demand minus the average PV generation.

**Table 5-2 Results of steady-state analysis with integration of PV**

Installed PV Capacity (kW)	SMR Core Size (kW)	Calculated minimum required TES Capacity (Metric tons)		
		(1) No PV	(2) Average PV	(3) Max PV
0	3,570	121	121	121
500	3,542	130	117	123
1,000	3,513	140	115	147
1,500	3,485	150	120	172
2,000	3,457	163	125	196
2,500	3,428	177	131	220
3,000	3,400	190	136	245
3,500	3,371	204	141	269
4,000	3,343	218	147	293
4,500	3,314	224	154	317
5,000	3,286	247	160	342

At all installed PV amounts, the required TES capacity is minimal when the PV output is at the average between the upper and lower limits. For example, when 2,000 kW of PV is installed, the required storage capacity in the case of the average PV output is 125 metric tons. However, when the actual PV output is at the lower and upper bounds, the required TES capacity is 163 and 196 metric tons, respectively.

The variation in the PV output from the average to zero output corresponds to additional required TES capacity. This additional TES capacity can be considered as additional peaking power required from the SMR-TES system to account for the reduced PV output. When the PV output is at a maximum and the SMR core power level is constant, the required SMR-TES system output is less compared to the case of average PV output. The additional TES capacity in this case can be considered as additional stored energy to offset the excess PV generation through the reduced SMR-TES output. The same trend can be observed for all installed PV amounts. The required TES capacity is found to increase as the installed PV capacity increases.

The required TES capacity is minimum in the cases of average PV output because the SMR core is sized based on the average PV output. This results in the balance of the amounts of energy charged and discharged within the TES over the day, which minimizes

the required TES capacity. When the actual PV output varies from the average, the required TES capacity increases due to net charging or discharging of the TES based on the difference in the amount of PV generation compared to the average. The reason for differences in the required storage capacity between the cases of minimum and maximum PV generation is due to differences in the charging and discharging rates of the TES system.

The required TES capacity at a given installed PV capacity should be based on the maximum amount of the three cases. This is found to occur in the case of maximum PV output. In this case, the excess power production from the SMR core at full power is required to be stored in the TES. But under such conditions, the SMR core can de-rate to a lower power level. Hence, it would not be required to store this excess power, which would reduce the storage capacity requirements. For this reason, the required TES capacity can be determined accordingly to the zero PV condition.

While the reduction in the SMR core size with increasing PV is small, it is significant in terms of the cost savings. The cost savings by reducing the SMR core size is greater than the added TES costs. The highest TES cost occurs with 5,000 kW of PV installed, which corresponds to a TES capacity of 247 metric tons. This counts for the added TES cost of 0.81 M\$.

It is seen that this SMR-TES system can accommodate PV generation by operating flexibly with additional thermal energy storage capacity at low cost. Based on this steady-state analysis, there is no limit found on the amount of PV generation that can be accommodated based on long-term PV characteristics.

### **Effects of Seasonal Variations in PV**

However, the seasonal variations in demand and PV generation must be considered, which limit the amount of PV generation to be installed. The above sizing analysis uses the demand and PV generation profiles in the winter months. In the summer, the demand is minimum, and the PV output has a longer duration and a higher output. As the PV installed capacity is increased, the net demand met by the SMR-TES is suppressed. The

net demand can eventually reach zero before becoming negative which represents negative required power as depicted in Figure 5-4. At this point, the SMR-TES would have to operate for extended periods of time only to maintain itself in an off-line state without any power output. For this benchmark community, such scenario occurs in the summer when the PV penetration is above 2,500 kW.

The SMR-TES system has the potential to deal with these situations. This can be done by shutting down the turbine and charging the TES (by allowing flow from the cold tank to the hot tank to achieve energy balance across the primary heat exchanger and to maintain the coolant temperature difference across the core). A second option is to reduce the core power to a lower level or even put it in a safe shutdown state. This may allow for adequate core start-up time by using energy stored in the TES to drive the turbine before the core power is increased to the desired level.

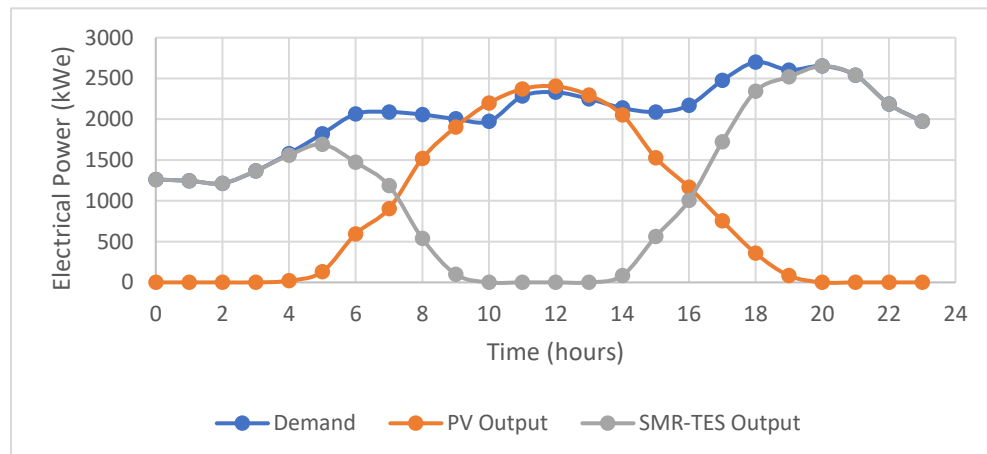


**Figure 5-4 Required SMR operation in summer months when PV output exceeds demand**

## 5.2.2 Dynamical Analysis

Dynamical analysis through simulations is used to determine the requirements and capability of the SMR-TES system by considering system variabilities, and to determine additional energy storage required.

One of the important considerations for a load-following SMR is the allowable ramp rates. Due to the fact that SMRs are still at the early stage of development, such information is not available in the open literature. This analysis considers the output characteristics of the SMR-TES system with the best estimate parameters including maximum ramp rates and range of allowable output values. Specifically, the SMR-TES system maximum ramp rate can be varied to determine the resultant requirements for the electrical energy storage.

The output of the SMR-TES system is planned to follow the net demand between the load and the PV production, but has ramp rates applied to limit the rates of change of this SMR-TES system. The difference in the actual generation of SMR-TES and PV is compensated by the additional electrical energy storage to ensure demands are met. The characteristics of this EES determine the power and capacity requirements.

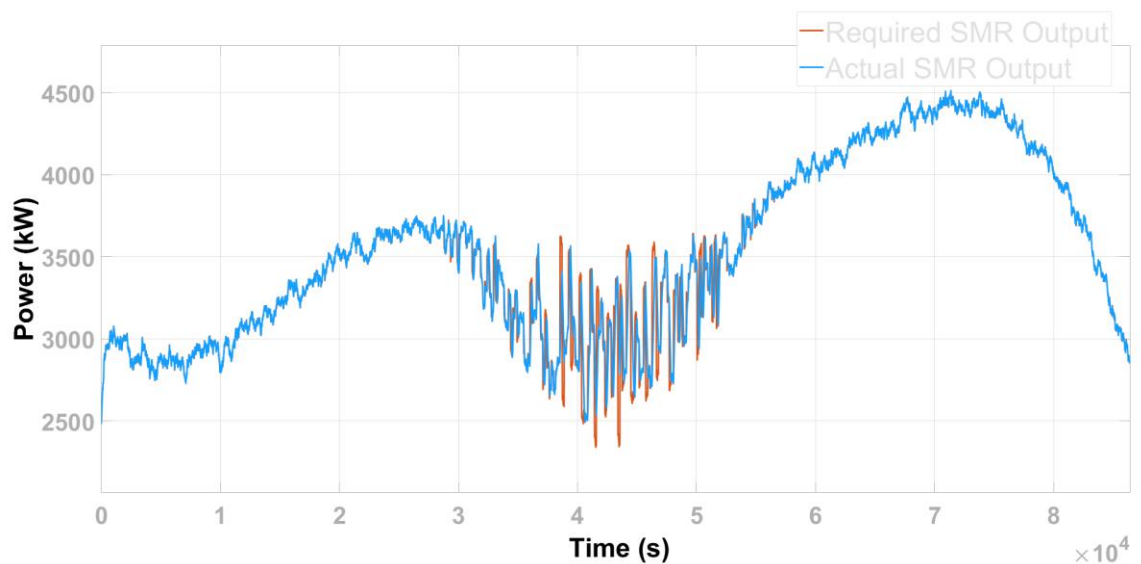
### **Trends of EES Requirements based on SMR Ramp Rates and PV Penetration**

The first set of simulations is based on the input of the maximum winter month with stochastic demand and stochastic PV output. An explanation of the dynamical simulation can be found in Appendix B. The stochastic demand represents the average demand in the winter months that is scaled by the calculated perturbation factor from a random variable that allows the demand to vary within the upper and lower limits. This represents the maximum variability in demand based on this modelling. The ramp rate limit on the rate of change of the demand is selected at 5 %/min. The PV output is based on the maximum demand curve of solar irradiance with variability added. The actual solar irradiance is scaled by the installed PV capacity. Within this simulation, the additional electrical energy storage capacity and the maximum charging and discharging powers are determined.

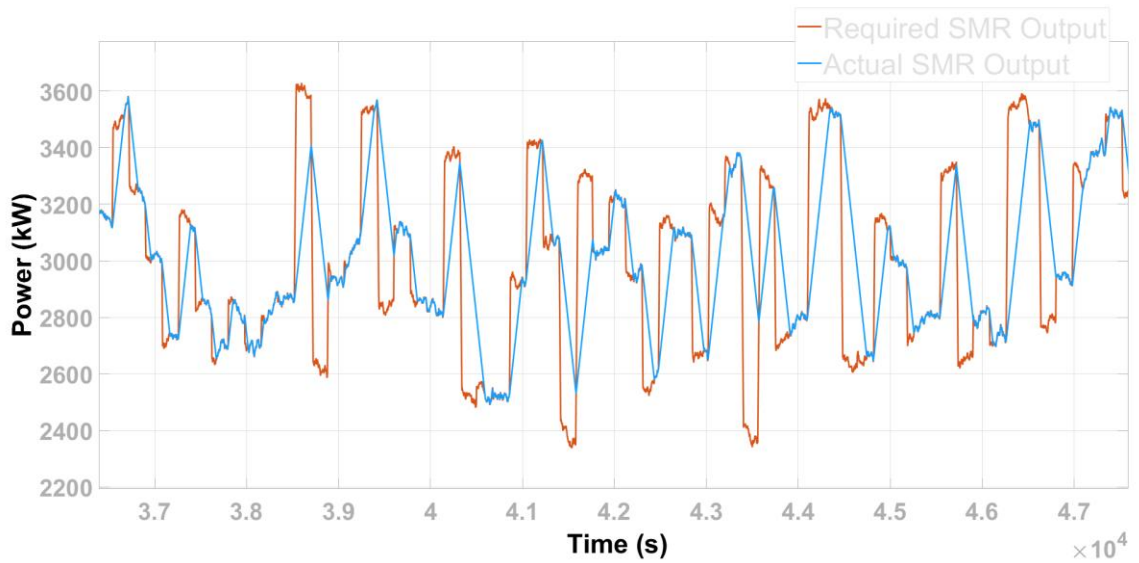
The results of an example simulation are shown in Figure 5-5 at a selected PV capacity of 500 kW for the net demand and the actual SMR-TES output. Differences between the required and actual output of the SMR-TES system occur when the actual ramp rates are kept below maximum rates. The SMR output that accounts for fluctuations in load and the PV is shown in Figure 5-5 (a) over one day. Zoomed sections are shown in Figure 5-5

(b) and (c) for enhancement in a shorter timeframe (from approximately 10AM to 1:30 PM and 11AM to 11:30AM respectively). A ramp event is shown in Figure 5-5 (c) where the required SMR demand sharply increases and 3 minutes later it drops rapidly.

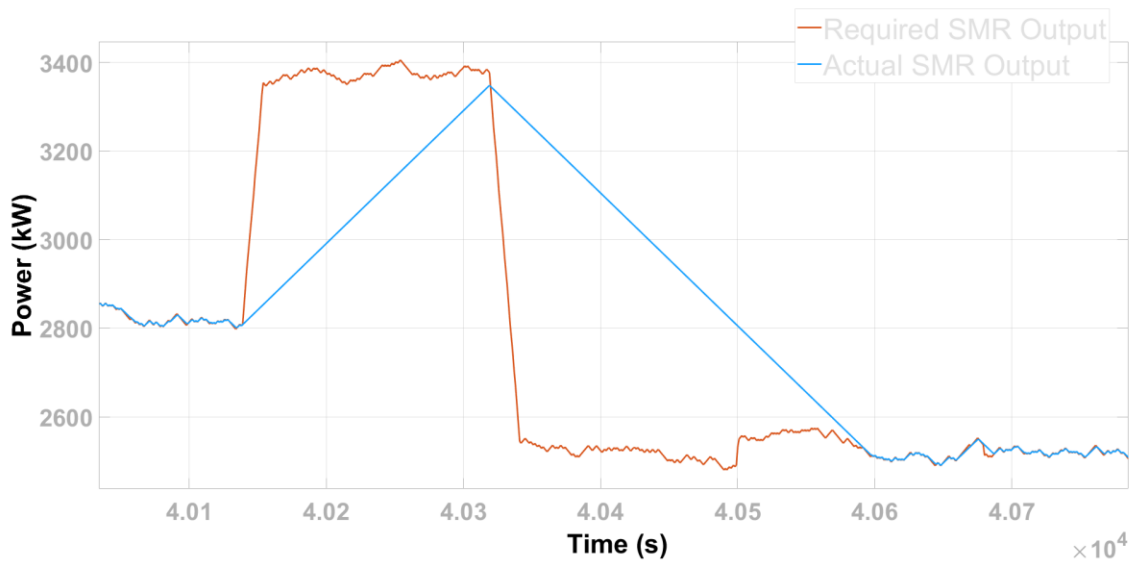
As the ability for the SMR-TES system to follow these variations is limited, the difference between the required and actual system output is required to be met by additional energy storage that has faster response times than the SMR-TES system can offer. The required power to be met by the electrical energy storage, defined as the difference between the demand and generation, is shown in Figure 5-6 (a). This shows the required discharging powers at positive values and required charging powers at negative values. The electrical energy storage system is needed during daylight hours when there is PV power generated. During the daylight hours there are large swings in PV generation that require power to be absorbed or delivered from the EES to maintain power balance in the system. At other times the fluctuations in the load are relatively smaller compared to fluctuations in the PV generation and these can be accounted for by the SMR alone. During these other times, the EES is required to deliver and absorb small variations typically less than 10 kW for balance between the SMR and the load. The associated amount of energy stored in the EES from the powers in Figure 5-6 (a) are shown in Figure 5-6 (b). The required EES energy capacity can be determined from the difference in the minimum and maximum values of the energy levels in Figure 5-6 (b).



(a) SMR actual and required output over one day

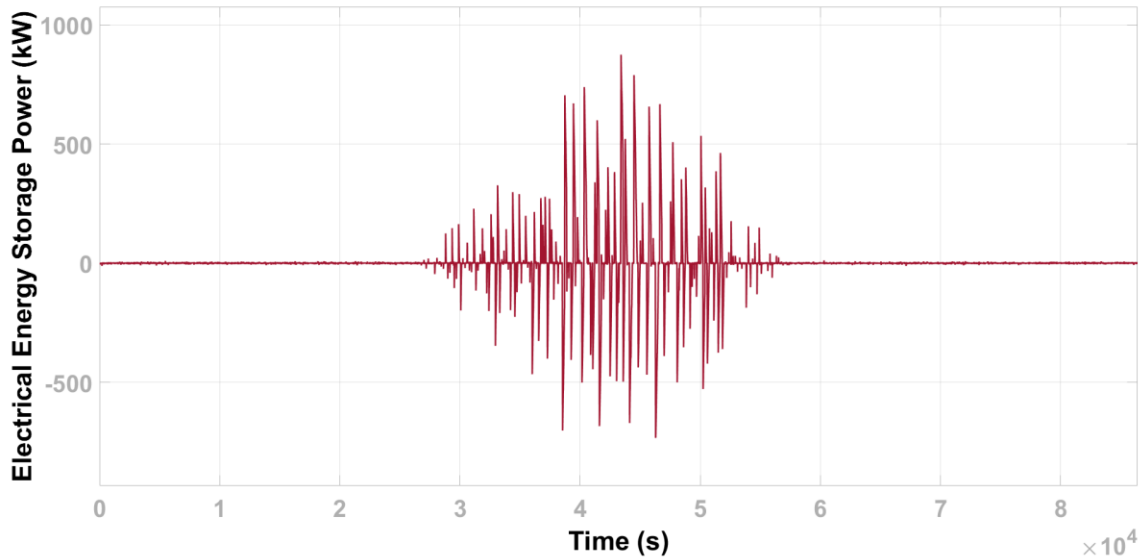


(b) Selected time sequence from (a)

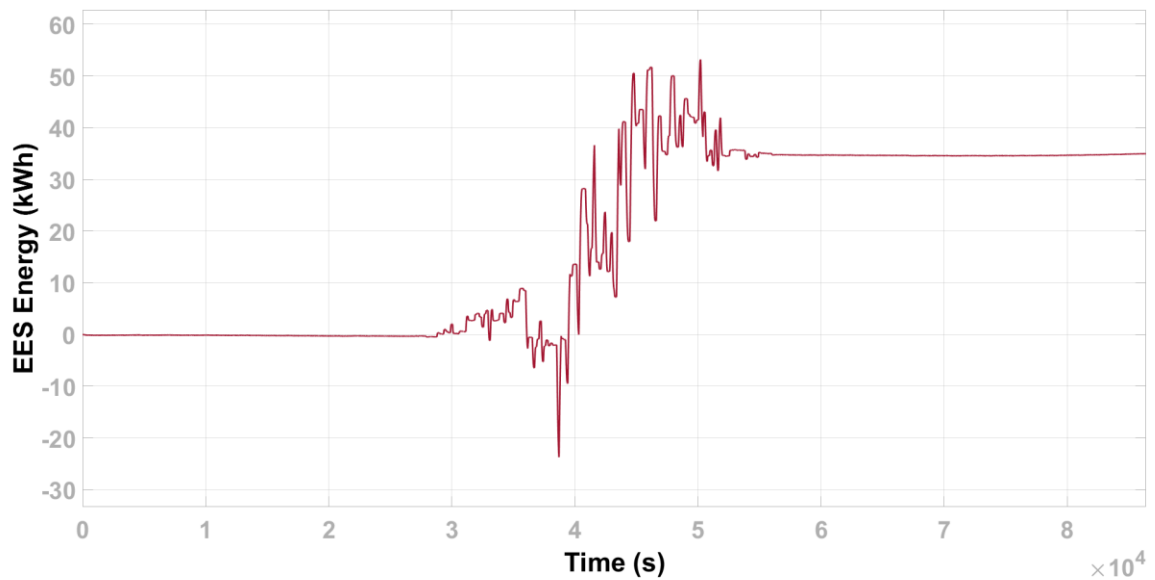


(c) Ramp event from (a)

**Figure 5-5 Simulations of actual and required SMR system response with 500kW installed PV**



(a) Power of the EES



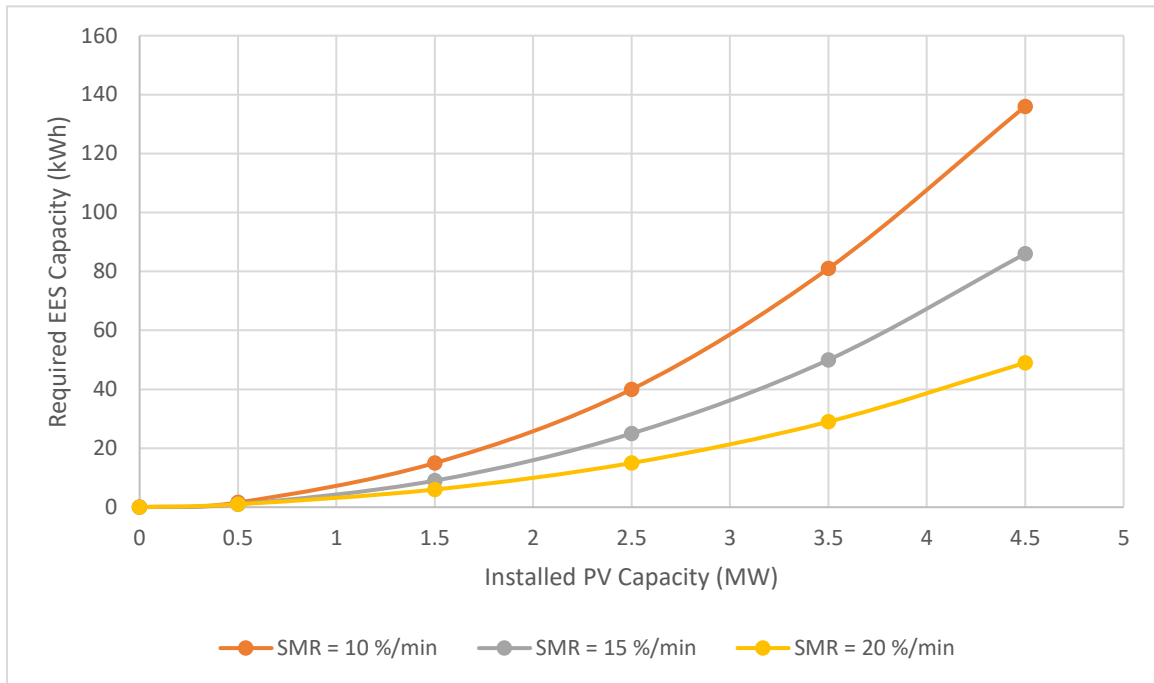
(b) Energy of the EES

**Figure 5-6 (a) Power of EES and (b) Energy capacity of EES for one day with 500kW installed PV**

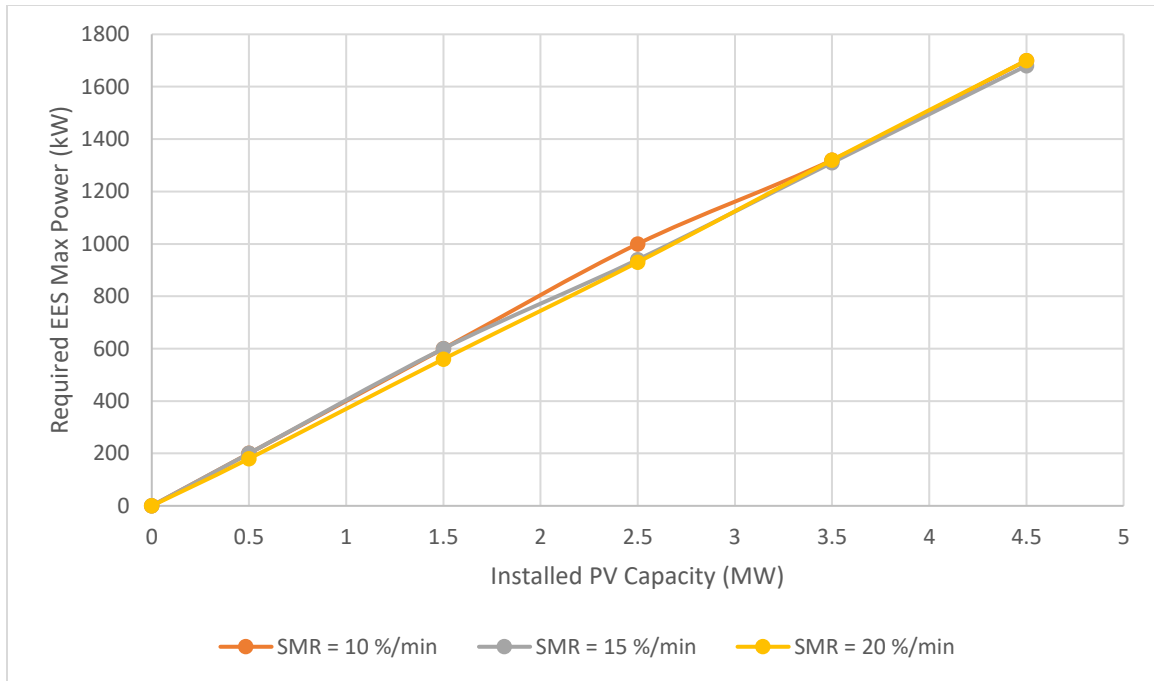
Simulation results based on the above example were collected in runs that varied the installed PV capacity at a selected SMR-TES system ramp rate limit. The characteristics of the EES were found to determine the power and energy requirements. The PV capacity was increased in an increment of 500 kW from 0 to 4,500 kW. The simulations were

repeated for SMR ramp rates limits of 10, 15, and 20 %FP/min while continuously performing load-following without any system delays.

The effect of changing the PV capacity at the three selected SMR-TES ramp rates is shown in Figure 5-7 (a) on the required EES capacity. Increasing the PV capacity can significantly increase the EES capacity requirements, and this becomes more significant at lower SMR-TES system ramp rates limits. The effect on the required maximum instantaneous EES power over the simulation time is shown in Figure 5-7 (b) at a given installed PV capacity. The maximum power required from the EES system increases with installed PV capacity, but were found to be the same for the three runs of different SMR- TES ramp rate limits. This shows that the SMR ramp rate limit affects the total energy difference between the required and actual SMR output while the maximum instantaneous power difference is determined by the amount of PV.



(a) Energy of the EES



(b) Power of the EES

**Figure 5-7 (a) EES capacity requirements and (b) EES maximum power required for different amounts of installed PV capacity and SMR ramp rates**

### Effect of SMR Ramp Rate on EES Requirements

The next set of simulations considers the effect of the SMR-TES ramp rate for a fixed PV installed capacity. This simulation utilizes variable load and PV generation to explore the limits on the requirements for the SMR-TES system. The ramp rate limit of the SMR is varied from very slow values to the limits where the required additional storage capacity approaches zero. This study has been conducted at different installed PV capacities in increments of 1,000 kW. Results from one run are summarized in Table 5-3 where the required EES capacity and maximum power of charging and discharging are determined for an installed PV capacity of 2,500 kW. The SMR-TES ramp rates vary between 0 representing constant output operation and 60 %FP/min. It is concluded that when comparing the results to the previous section, the allowable SMR ramp rates have a greater impact on the required additional EES storage than PV would have.

**Table 5-3 Effect of SMR ramp rates on EES requirements**

<b>SMR Ramp Rate (%/min)</b>	<b>EES Capacity (kWh)</b>	<b>EES Maximum power charging (kW)</b>	<b>EES Maximum power discharging (kW)</b>
0	7500	950	950
0.1	4100	840	800
0.5	370	640	780
1	160	760	820
2	88	860	800
5	77	880	740
10	34	800	810
15	20	740	740
20	14	650	650
25	10	590	580
30	8	510	490
40	4	360	350
50	2	200	190
60	0	0	0

The simulation results for the effect of the SMR-TES ramp rates on the required EES energy capacity at three different PV amounts is shown in Figure 5-8. Beyond a ramp rate limit of 10 %/min, the reduction in the required EES capacity as the SMR-TES ramp rate is increased becomes less significant and is even insignificant above 15 %/min ramp rates. Similarly, the effect of the SMR-TES ramp rates on the maximum charging and discharging power of the EES is shown in Figure 5-9 (a) and (b) respectively. As the SMR-TES ramp rate limits increase, the maximum EES power requirements generally decrease in a linear manner.

An example comparison of the corresponding required power of the EES over time when the SMR-TES ramp rates are 10 %/min and 20 %/min are shown in Figure 5-10 (a) and (b) respectively with 3,500 kW of PV. When increasing the SMR-TES ramp rate limit from 10 %/min to 20 %/min, the maximum delivered power is decreased as well as the total distribution of the required delivered power. This results in a lower required EES capacity.

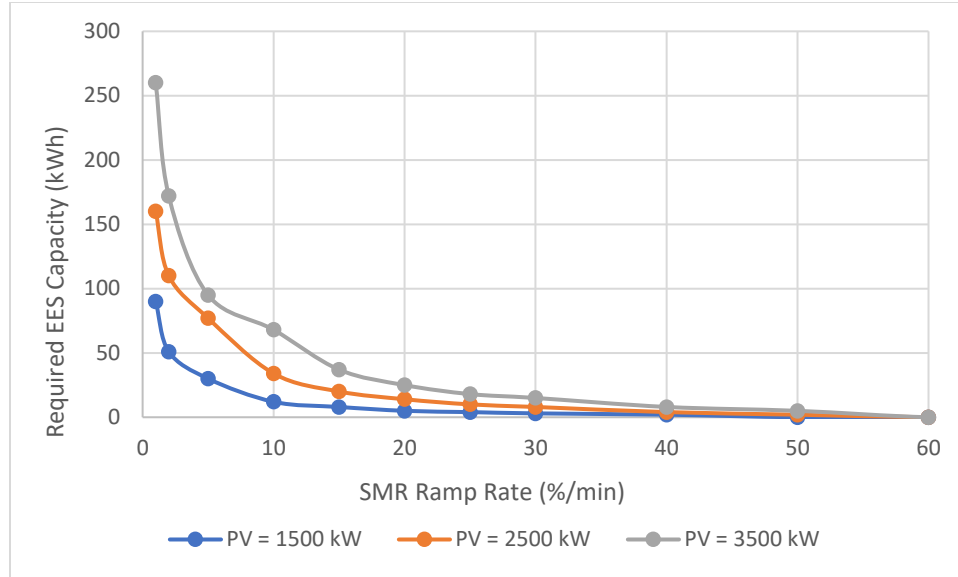
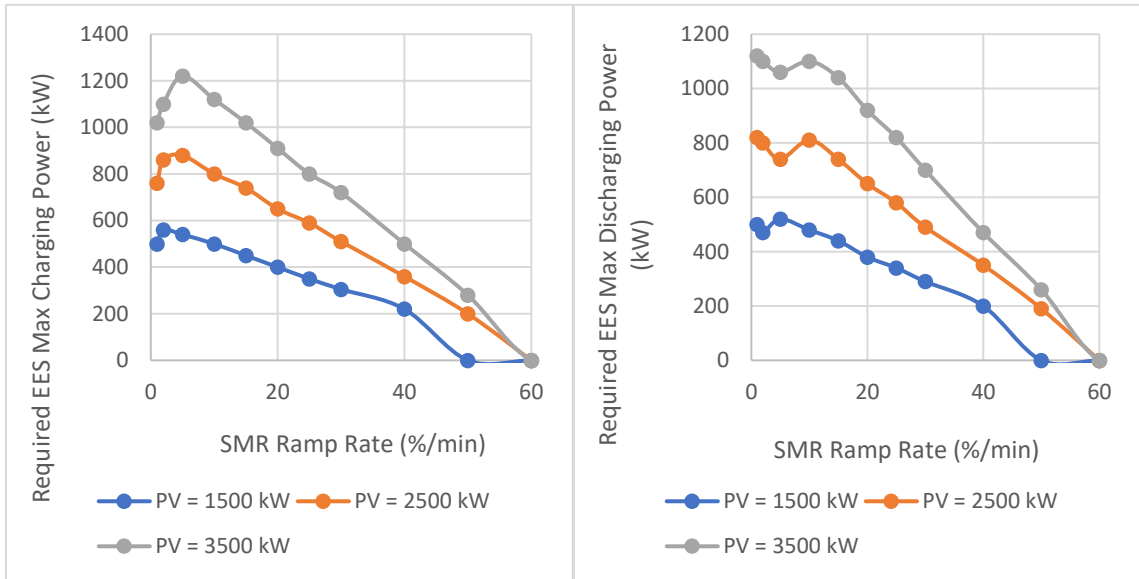


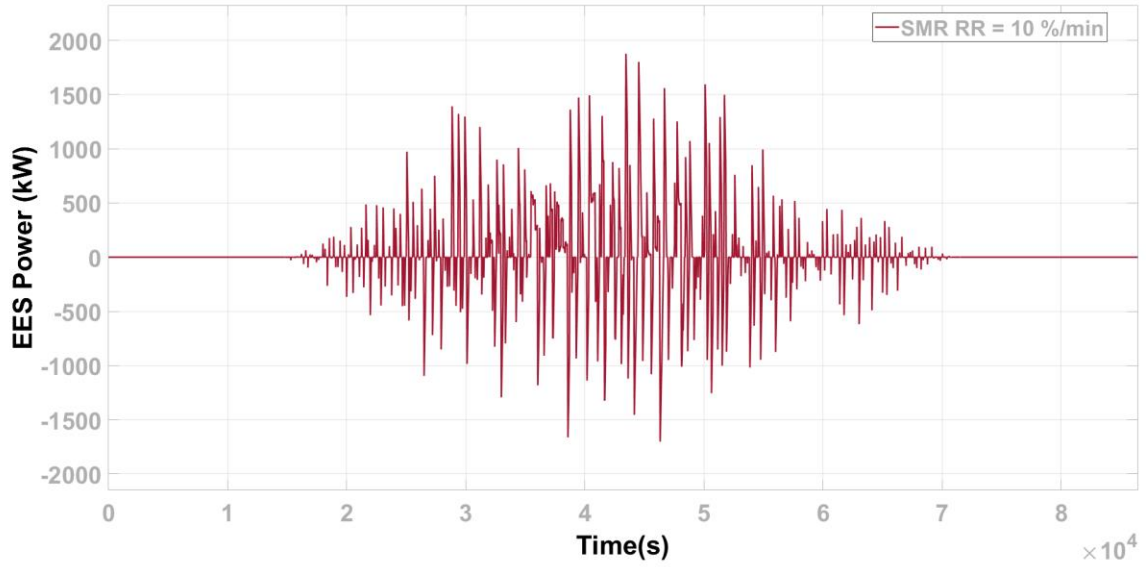
**Figure 5-8 Effect of the required EES capacity from varying the SMR-TES ramp rate under 3 different PV capacities**



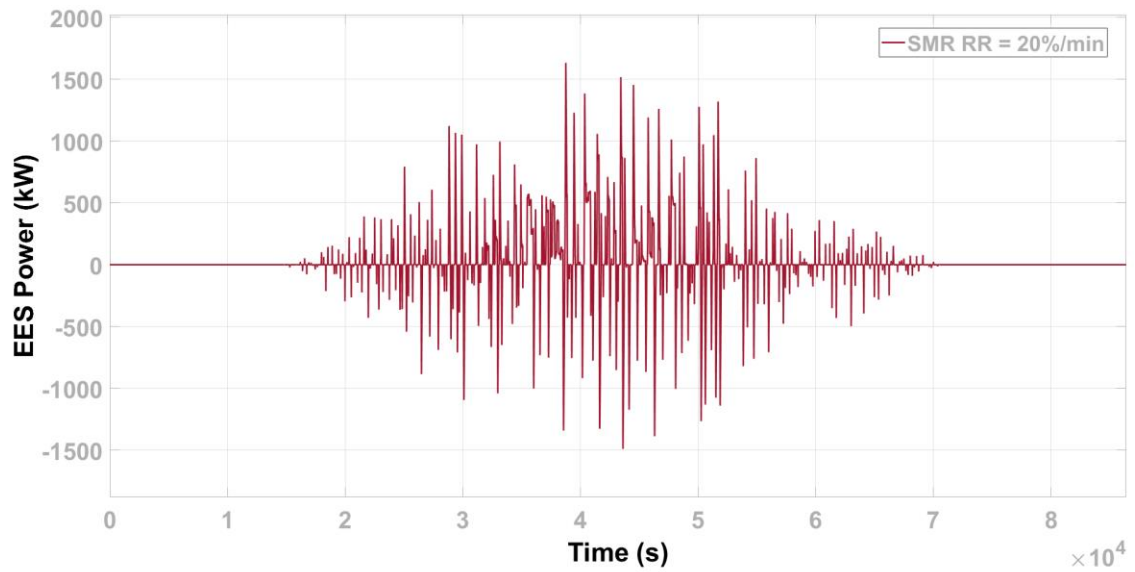
(a) Charging

(b) Discharging

**Figure 5-9 Effect of maximum EES capacity from varying the SMR-TES ramp rate for (a) Charging and (b) Discharging under 3 different PV capacities**



(a) 10%/min



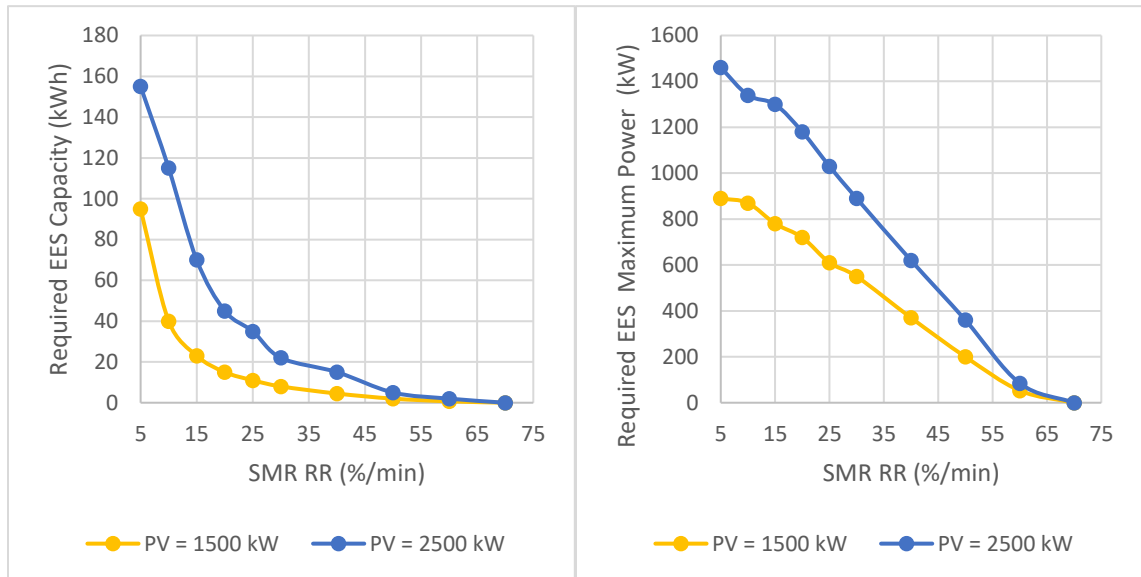
(b) 20%/min

**Figure 5-10 Required EES power with 3,500 kW PV installed at (a) 10%/min and (b) 20%/min SMR ramp rate**

### Effect of PV during summer months

The issue with larger portion of PV generation in the microgrid is that there are more significant seasonal variations. An analysis is also conducted for PV and demand profiles in the summer months since this is when the PV generation is generally maximum, and

the load is minimum. The PV variability becomes more significant when the instantaneous PV generation provides a larger fraction of the instantaneous demand. A third set of simulations have been conducted with the demand input representing the summer months varying between 1,080 kW to 2,700 kW. It is found that the demand is not exceed by PV generation at installed PV capacities less than 2,500 kW. Here, the net demand never becomes negative. The effect on the required EES power and capacity in the summer months with PV capacities of less than 2,500 kW are shown in Figure 5-12. The trends based on varying the SMR-TES ramp rate at a given installed capacity are found to be the same between the summer and winter months. However, the required EES capacity and maximum delivered power is found to be greater in the summer months compared to in the winter months.



(a) EES capacity

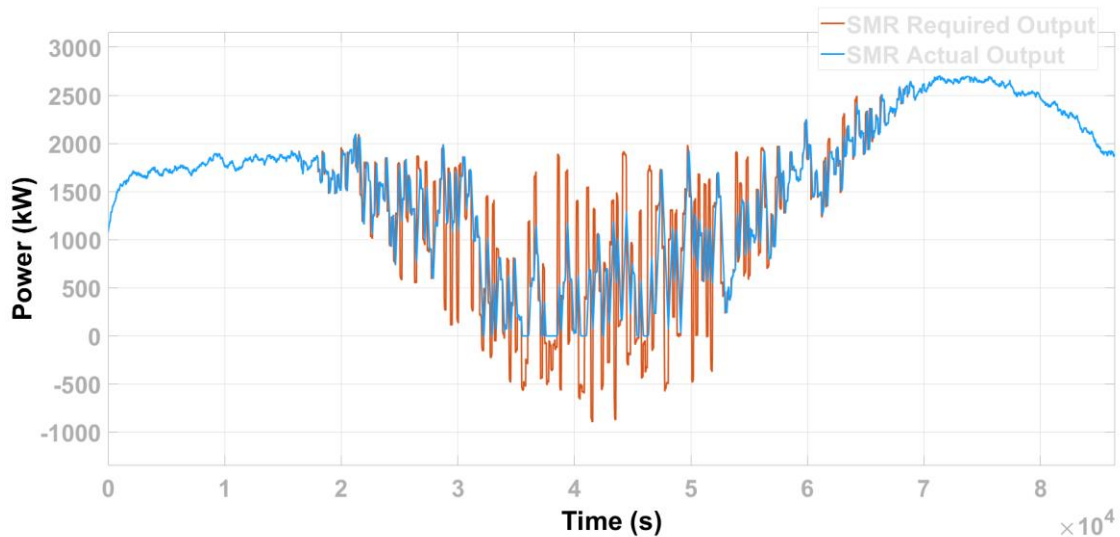
(b) Maximum EES Power

**Figure 5-11 (a) Required EES capacity and (b) Maximum power during summer months when PV output is below demand**

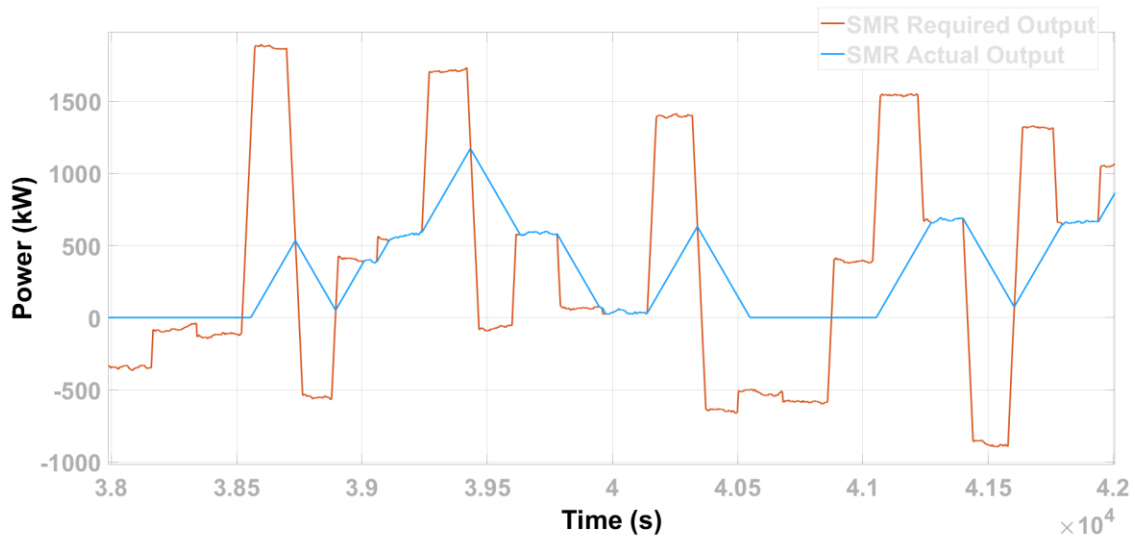
When the PV capacity exceeds this amount of 2,500 kW, PV generation can exceed instantaneous demand as shown as the example in Figure 5-12. During high PV production, the required output from SMR becomes negative. Since the SMR output must be positive, an example output of the SMR during the period of high PV output is zoomed in Figure 5-12 (b). It can be difficult for the SMR-TES system to achieve this

operation and intermittently produce output between periods of no output. This is not a viable operational mode for the system.

During periods of high PV output during the day that exceed demand, the excess PV output needs to be managed. The excess power can either be stored in the EES, or a PV curtailment scheme has to be used. When the net demand of the SMR-TES approaches zero, the SMR core should go into a standby or shutdown mode for extended periods of time. During this time the EES system can complement any variability in the PV output to meet the demand. The excess PV generation above the demand can charge the EES. Therefore, the EES can be thought of as controlling the PV output to effectively load-follow when the SMR is in a shutdown state. However, operational strategies between the SMR core and TES system must be determined. The SMR core takes time to return to full power after a shutdown period, and the power balances between the core, TES and BOP must always be ensured.



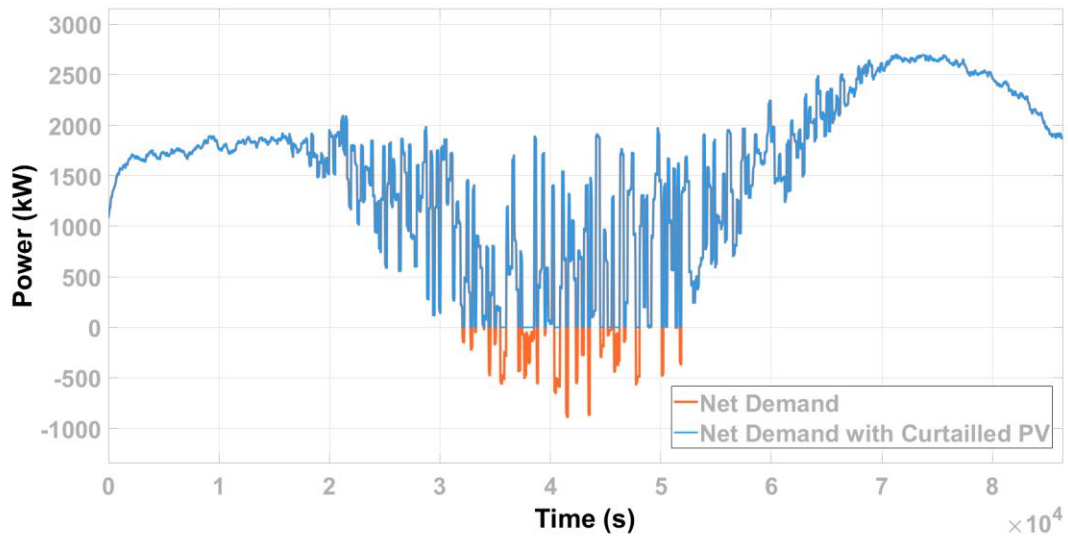
(a)



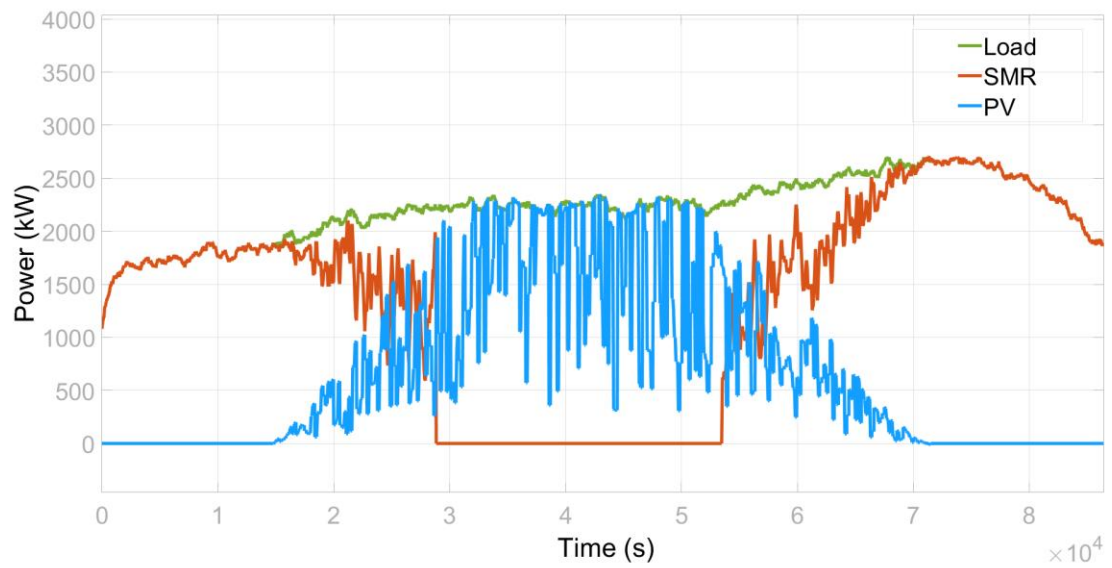
(b) Zoomed between  $3.8 \times 10^4$ s and  $4.2 \times 10^4$ s

**Figure 5-12 (a) SMR actual versus net when instantaneous PV production exceeds instantaneous demand at 3500 kW<sub>e</sub> PV installed and (b) Selected timeframe from (a)**

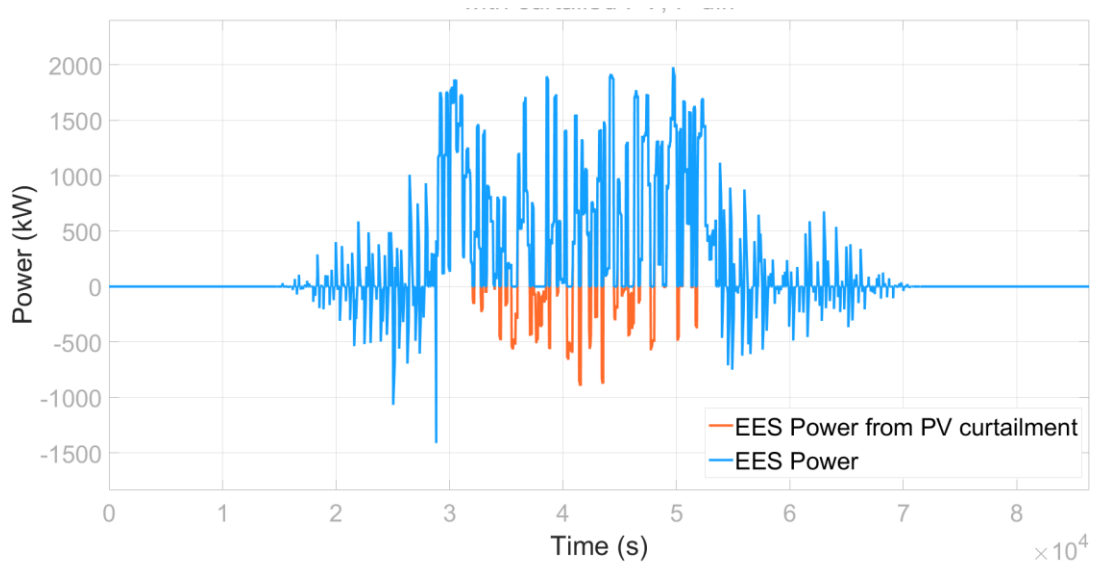
An illustrative example of this operation during a summer day is shown in Figure 5-13 when the PV capacity is 3,500 kW. Here the SMR is set to load-follow at a rate limit of 5 %/min. The net demand between the demand and actual PV output is shown in Figure 5-13 (a). The net demand remains above zero when the PV output is curtailed compared to when it is not curtailed. The output of the SMR and the PV compared to the load is shown in Figure 5-13 (b). The SMR is shown to be shutdown during the periods of high PV output that is curtailed. However, there is still variability in the PV output during this time and PV alone cannot meet the demand. The required power of the EES to compliment the PV is shown in Figure 5-13 (c). The EES is required to rapidly respond to variability in PV to meet the demand. It is shown that the excess PV power above the demand can be stored in the EES.



(a) Net demand compared to net demand with curtailment of PV



(b) Output of SMR and PV compared to load when SMR is shutdown for long period



(c) EES power to compliment PV when SMR is shutdown

**Figure 5-13 Operation of system when PV exceeds load with (a) Net demand, (b) Power of SMR and PV compared to load and (c) Required power from EES**

### 5.2.3 Dynamic PV and SMR Considerations

There are several considerations to be made for this dynamical analysis to determine the PV and EES sizing.

The first case is for the situation where the PV produces more power than the demand. When the PV penetration increases beyond this limit of 2,500 kW, more detailed operational strategies are required between the SMR and EES. Detailed dynamics of the system components and special cases need to be explored further to determine if additional PV capacity can be included in this microgrid. This issue requires further exploration, and is beyond the scope of this thesis analysis.

The next issue to address is the load-following ability of the SMR in terms of ramp rates and response times. This dynamical analysis considers the SMR system to be able to continuously load-follow without considering physical processes in the SMR system. The SMR system has intrinsic inertia in the thermal system (core, TES, and BOP) and in the turbine/generator. There are also delays in responses due to thermal transport delays and

valve actions. The output of the SMR-TES system can be considered to have time delays between the desired and actual output responses due to this inertia.

The simulation model was modified to include a time delay in the output response of the SMR-TES system to represent the system inertia. The duration of the time delay was varied to examine effects on the EES requirements. The results are summarized in Table 5-4, where the time delay was selected as 1 second, 1 minute, and 2 minutes at an SMR ramp rate limit of 5 %/min with an installed PV capacity of 2,500 kW. It is seen that there is an increased storage requirements as the time delay is increased that is small but not negligible.

**Table 5-4 EES requirements based on SMR response delays**

<b>SMR Time Delay (s)</b>	<b>EES Capacity (kWh)</b>	<b>EES Maximum power charging (kW)</b>	<b>EES Maximum power discharging (kW)</b>
0	77	880	740
1	78	880	740
60	87	1000	860
120	94	1050	860

### 5.3 Solutions to Sizing Problem

This section provides solutions to the sizing problems. The following questions will be answered: (1) What is the ‘optimal’ configuration of the SMR with TES? (2) How much PV generation can be accommodated for a certain community? (3) How much electrical energy storage is required? The solutions are summarized in Table 5-5.

**Table 5-5 Sizing solution results**

<b>Parameter</b>	<b>Selection</b>
SMR Core Power Rating	3430 kW
Balance of Plant Power Rating	5000 kW
TES Capacity	370 metric tons
Installed PV Power Rating	2500 kW
EES Capacity	<400 kWh
Maximum EES Power of Charging and Discharging	1,500 kW

**What is the Optimal Configuration of SMR with TES?**

Through this analysis, it is found that the optimal sizing for the SMR-TES system is achieved by sizing the SMR core at the average of the maximum demand interval over the maximum day less the average PV contribution for the day. The BOP system should be sized at least at the peak demand, with a margin that can allow for future growth in demand. A 10% margin results in a BOP sizing of 5,000 kW. The minimum thermal energy storage capacity is dependent on the pattern of the demand and can be determined through steady-state and dynamical simulations. This TES system is able to facilitate the integration of PV generation by adding additional TES capacity to account for variations in PV due to weather or other external influence. In this case, the optimal SMR core sizing is 3,430 kW<sub>e</sub>.

From steady-state simulations, the minimum required TES capacity is calculated to be 177 metric tons of solar salt. The dynamical simulations have found that 181 tons is required when there is no PV production during the period of maximum demand. This confirms that the two types of simulation are in agreement for the calculated TES capacity. Then to ensure 25% of the lower and upper SOC limits are not exceeded, the minimum amount of storage capacity should be 370 metric tons.

### **How much PV generation can be accommodated?**

Through this analysis, the amount of PV generation that can be accommodated in a community is not limited by PV variability if the SMR can follow the load at reasonable ramp rates. The amount of PV generation is limited by large seasonal variations in the demand and PV production in northern communities. The limitation in the amount of PV generation capacity from this analysis is based on when the net demand for the SMR-TES system approaches zero for extended periods of time. For this community, the limit is 2,500 kW of installed PV.

### **How much electrical energy storage is required?**

Electrical energy storage is included to smooth out fluctuations in load and changes in PV generation. It is found that the amount of EES required is strongly dependent on the limit on the SMR-TES system ramp rates. The integration of the TES system offers additional

flexibility and potentially higher ramp rates compared to traditional load-following methods. It is found that an SMR operating continuously at ramp rates of 10 %/min or more of continuous load-following would require less than 200 kWh of electrical energy storage. The actual installed EES capacity should be 400 kWh to ensure that the minimum and the maximum state of charge limits are not exceeded. The maximum charging and discharging power of this EES is found to be at 1,500 kW, and occurs in the summer months.

## Chapter 6

### 6 Conclusions

In this chapter, this work has been summarized and important conclusions are drawn, along with providing suggested future work.

#### 6.1 Summary

To improve upon the current local diesel generator-based power systems for off-grid communities, an SMR based microgrid integrated with renewable energy resources and thermal energy storage systems is analyzed. Steady-state and dynamical simulations and analyses are carried out to determine the system sizing of the various components.

A survey of power requirements and renewable resource potential of a typical off-grid community in northern Canada is used to model load and PV profiles and seasonality in the analysis. The SMR-TES configuration selected is an HTGR reactor and steam power cycle coupled with a thermal energy storage in a two-tank indirect intermediate storage loop. A steady-state model has been developed for this system. The model is then used with a load and PV generation model to perform steady-state simulations for system sizing. It is determined that the SMR core can be sized at the average of the maximum demand interval when integrating thermal energy storage. PV can be integrated into this system and thermal energy storage capacity can account for variability and intermittence of the PV output. Dynamical analysis has also been conducted to analyze rapid variabilities within the system and to determine additional energy storage requirements. Through a case study, the solution methodology using steady-state and dynamical analysis has been demonstrated for sizing of the components in the microgrid for a benchmark community.

#### 6.2 Conclusions

- (1) The HTGR is a preferred reactor choice for near-term deployment for off-grid communities.

- (2) When integrating TES with an SMR in a microgrid, the resulting SMR core sizing can be reduced. This can reduce the total SMR-TES lifecycle cost.
- (3) Operation over the range of load and PV variations can be ensured when the SMR core is sized at the average of the upper demand interval and the BOP is sized at the maximum demand
- (4) Seasonal variations and variability in PV generation in off-grid communities limit the amount of PV generation that can be included. Lower demand coupled with high PV output in the summer can limit the amount of PV that can be included before the net demand on the SMR-TES becomes zero. This can be a relatively high PV power rating but corresponds to a lower energy amount compared to the demand. At this point, more advanced SMR-TES and PV strategies are required.
- (5) The SMR-TES ramp limits has more effect on the required EES capacity than the amount of PV included. At reasonable ramp rates above 10%/min, the SMR-TES can respond to most of the variations in demand and PV, and the required EES capacity is small.
- (6) Both steady-state and dynamical analysis determine the size of microgrid components: Steady-state analysis determines the system sizing and economic viability based on demand and PV trends, while dynamic analysis deals with random fluctuations and is used to determine the additional EES needed to account for fluctuations beyond the ability of the SMR.

## 6.3 Suggestions for Future Work

To improve upon the existing work, four suggestions are provided for future work on SMR integration within microgrids:

- Implement physics-based modelling of SMR-TES system to gain more insights into load-following aspects of the system.
- Explore energy management strategies and the associated control system design within the SMR-TES system, as well as between the SMR and EES, especially at high PV capacities.
- Explore this analysis with multiple SMRs.
- Explore the possibility and technical details of utilizing SMR systems to meet additional community thermal loads in a cogeneration mode. This can enhance the microgrid configuration and can reduce diesel emissions from space heating applications.

## References

- [1] P. R. Bhattarai and S. Thompson, “Optimizing an off-grid electrical system in Brochet, Manitoba, Canada,” *Renewable and Sustainable Energy Reviews*, vol. 53, pp. 709–719, Jan. 2016.
- [2] Natural Resources Canada, “A call to action: A Canadian roadmap for small modular reactors,” Ottawa, ON, Canada, 2018. [Online]. Available: <https://smrroadmap.ca/> (Accessed on 3-June-2021).
- [3] B. Poudel, T. Mcjunkin, N. Kang, and J. T. Reilly, “Small reactors in microgrids: Technical studies guidelines”, Technical Report INL/EXT-21-64616, Idaho National Laboratory, Idaho Falls, ID, USA, 2021.
- [4] C. Forsberg, P. Sabharwall, and H. D. Gougar, “Heat storage coupled to generation IV reactors for variable electricity from base-load reactors: Changing markets, technology, nuclear-renewables integration and synergisms with solar thermal power systems,” INL/EXT-19-54909, Idaho National Laboratory, Idaho Falls, ID, USA, 2019.
- [5] G. Locatelli, A. Fiordaliso, S. Boarin, and M. E. Ricotti, “Cogeneration: An option to facilitate load following in small modular reactors,” *Progress in Nuclear Energy*, vol. 97, pp. 153–161, May 2017.
- [6] D. Michaelson and J. Jiang, “Review of integration of small modular reactors in renewable energy microgrids,” *Renewable and Sustainable Energy Reviews*, vol. 152, p. 111638, Dec. 2021.
- [7] J. Royer, “Status of remote/off-grid communities in Canada,” Ottawa, ON, Canada, 2013. [Online]. Available: <https://www.nrcan.gc.ca/energy/publications/sciences-technology/renewable/smart-grid/11916> (Accessed on 3-June-2021).
- [8] D. Shropshire, G. Black, and K. Araujo, “Global market analysis of

- microreactors,” INL/EXT-21-63214, Idaho National Laboratory, Idaho Falls, ID, USA, 2020.
- [9] M. Arriaga, C. A. Canizares, and M. Kazerani, “Renewable energy alternatives for remote communities in Northern Ontario, Canada,” *IEEE Transactions on Sustainable Energy*, vol. 4, no. 3, pp. 661–670, July 2013.
- [10] D. A. Johnson, “Wind-diesel-storage project at Kasabonika Lake First Nation,” 2009. [Online]. Available: <https://www.pembina institute.org/reports/wind-diesel-2-david-johnson.pdf> (Accessed on 3-June-2021).
- [11] E. Karimi, “A generalized optimal planning platform for microgrids of remote communities considering frequency and voltage regulation constraints,” Ph.D. dissertation, Department of Electrical and Computer Engineering, University of Waterloo, Waterloo, ON, Canada, 2017.
- [12] Natural Resources Canada, “Towards renewable energy integration in remote communities: A summary of electric reliability considerations,” in *Energy and Mines Ministers' Conference*, Iqaluit, NU, Canada, Aug. 2018.
- [13] Fortis Ontario “The Wataynikaneyap Transmission Project,” [Online]. Available: <https://www.fortisontario.com/our-work/wataynikaneyap-transmission-project> (Accessed on 24-August-2022).
- [14] D. Curtis and B. N. Singh, “Northern micro-grid project - A concept,” 2010. [Online]. Available: <https://www.osti.gov/etdweb/servlets/purl/21390264> (Accessed on 13-Oct-2020).
- [15] K. Karanasios and P. Parker, “Recent developments in renewable energy in remote aboriginal communities, Ontario, Canada,” *Papers in Canadian Economic Development*, vol. 16, pp. 82–97, 2016.
- [16] T. Weis and P. Cobb, “Aboriginal energy alternatives,” The Pembina Institute, Calgary, AB, Canada, 2008.

- [17] B. V. Solanki, C. A. Cañizares, and K. Bhattacharya, "Practical energy management systems for isolated microgrids," *IEEE Transactions on Smart Grid*, vol. 10, no. 5, pp. 4762–4775, 2018.
- [18] A. A. Anderson and S. Suryanarayanan, "Review of energy management and planning of islanded microgrids," *CSEE Journal of Power and Energy Systems*, vol. 6, no. 2, pp. 329–343, June 2020.
- [19] J. M. Raya-Armenta, N. Bazmohammadi, J. G. Avina-Cervantes, D. Sáez, J. C. Vasquez, and J. M. Guerrero, "Energy management system optimization in islanded microgrids: An overview and future trends," *Renewable and Sustainable Energy Reviews*, vol. 149, no. February 2020, p. 111327, Oct. 2021.
- [20] E. Karimi and M. Kazerani, "Impact of renewable energy deployment in Canada's remote communities on diesel generation carbon footprint reduction," in *IEEE Canadian Conference on Electrical and Computer Engineering*, Windsor, ON, Canada, 2017.
- [21] M. M. Rahman, M. M. Khan, M. A. Ullah, X. Zhang, and A. Kumar, "A hybrid renewable energy system for a North American off-grid community," *Energy*, vol. 97, pp. 151–160, Feb. 2016.
- [22] V. Kuznetsov, A. Lokhov, R. Cameron, and M. Cometto, "Current status, technical feasibility and economics of small nuclear reactors," Organisation for Economic Co-operation and Development, Washington, DC, USA, 2011.
- [23] Natural Resources Canada, "Canadian SMR Roadmap - Technology Working Group Report," [Online]. Ottawa, ON, Canada, 2018. Available: <https://smrroadmap.ca/wp-content/uploads/2018/12/Technology-WG.pdf?x64773> (Accessed on 3-June-2021).
- [24] J. Coleman, S. Bragg-Sitton, E. Dufek, S. Johnson, J. Rhodes, T. Davidson, and M. E. Webber, "An evaluation of energy storage options for nuclear power," Technical Report INL/EXT-17-42420, Idaho National Laboratory, Idaho Falls, ID,

USA, 2017.

- [25] K. M. Powell and T. F. Edgar, “Modeling and control of a solar thermal power plant with thermal energy storage,” *Chemical Engineering Science*, vol. 71, pp. 138–145, Mar. 2012.
- [26] G. Alva, Y. Lin, and G. Fang, “An overview of thermal energy storage systems,” *Energy*, vol. 144, pp. 341–378, Feb. 2018.
- [27] W. Ding, A. Bonk, J. Gussone, and T. Bauer, “Electrochemical measurement of corrosive impurities in molten chlorides for thermal energy storage,” *Journal of Energy Storage*, vol. 15, pp. 408–414, 2018.
- [28] A. Lokhov, “Technical and economic aspects of load following with nuclear power plants,” Organisation for Economic Co-operation and Development, Washington, DC, USA, 2009.
- [29] G. Locatelli, S. Boarin, F. Pellegrino, and M. E. Ricotti, “Load following with small modular reactors (SMR): A real options analysis,” *Energy*, vol. 80, pp. 41–54, Feb. 2015.
- [30] Natural Resources Canada, “SMR Roadmap - Economic and Finance Working Group Report,” Ottawa, Canada, 2018. [Online]. Available: <https://smrroadmap.ca/wp-content/uploads/2018/12/Economics-Finance-WG.pdf?x64773> (Accessed on 3-June-2021).
- [31] M. Moore, “The economics of very small modular reactors in the north,” in International Technical Meeting on Small Reactors (ITMSR-4), Ottawa, ON, Canada, 2016.
- [32] Hatch, “Feasibility of the potential deployment of small modular reactors (SMRs) in Ontario,” H350381-00000-162-066-0001, Rev. 0, Toronto, Canada, 2016.

- [33] S. Froese, N. C. Kunz, and M. V. Ramana, “Too small to be viable? The potential market for small modular reactors in mining and remote communities in Canada,” *Energy Policy*, vol. 144, p. 111587, 2020.
- [34] G. Locatelli, C. Bingham, and M. Mancini, “Small modular reactors: A comprehensive overview of their economics and strategic aspects,” *Progress in Nuclear Energy*, vol. 73, pp. 75–85, 2014.
- [35] C. Forsberg, “LWR heat storage for peak power and increased revenue,” *Nuclear News*, vol. 62, no. 6, pp. 40-43, May 2019.
- [36] J. Soravilla, S. Martínez, O. Larrosa, D. Taylor, G. Anderson, and R. O’Sullivan, “GridReserve, technical feasibility and economics of a hybrid small modular reactor and thermal energy storage to enable nuclear as peaking plant,” 2021, [Online]. Available: <https://www.moltexenergy.com/wp-content/uploads/Moltex-GridReserve-system-FINAL.pdf> (Accessed on 3-August-2021).
- [37] Q. Ma, X. Wei, J. Qing, W. Jiao, and R. Xu, “Load following of SMR based on a flexible load,” *Energy*, vol. 183, pp. 733–746, Sept. 2019.
- [38] K. Frick, C. T. Misenheimer, J. M. Doster, S. D. Terry, and S. Bragg-Sitton, “Thermal energy storage configurations for small modular reactor load shedding,” *Nuclear Technology*, vol. 202, pp. 53–70, 2018.
- [39] K. Frick, J. M. Doster, and S. Bragg-Sitton, “Design and operation of a sensible heat peaking unit for small modular reactors,” *Nuclear Technology*, vol. 205, no. 3, pp. 415–441, 2019.
- [40] CNSC, “Pre-licensing vendor design review,” 2022. [Online]. Available: <https://nuclearsafety.gc.ca/eng/reactors/power-plants/pre-licensing-vendor-design-review/> (Accessed on 7-Mar-2022).
- [41] IAEA, “Advances in small modular reactor technology developments,” Vienna, Austria, 2020. [Online]. Available: [https://aris.iaea.org/Publications/SMR\\_Book\\_2020.pdf](https://aris.iaea.org/Publications/SMR_Book_2020.pdf) (Accessed on 20-Dec-

2020).

- [42] J. Wallenius, S. Qvist, I. Mickus, S. Bortot, J. Ejenstam, and P. Szalalos, “SEALER: A small lead-cooled reactor for power production in the Canadian Arctic,” in *International Conference on Fast Reactors and Related Fuel Cycles: Next Generation Nuclear Systems for Sustainable Development*, 2017.
- [43] M. Ding, J. L. Kloosterman, T. Kooijman, R. Linsesen, T. Abram, B. Marsden, and T. Wickham, “Design of a U-Battery,” 2011. [Online]. Available: [http://www.janleenkloosterman.nl/reports/ubattery\\_final\\_201111.pdf](http://www.janleenkloosterman.nl/reports/ubattery_final_201111.pdf) (Accessed on 13-Oct-2020).
- [44] D. Chapin, S. Kiffer, and J. Nestell, “The Very High Temperature Reactor: A Technical Summary,” MPR Associates Inc, Alexandria, VA, USA, 2004. [Online]. Available: <http://large.stanford.edu/courses/2013/ph241/kallman1/docs/chapin.pdf> (Accessed on 13-Oct-2020).
- [45] G. Locatelli, M. Mancini, and N. Todeschini, “Generation IV nuclear reactors: Current status and future prospects,” *Energy Policy*, vol. 61, pp. 1503–1520, 2013.
- [46] Canadian Nuclear Laboratories, “Siting Canada’s first SMR,” [Online]. Available: <https://www.cnl.ca/clean-energy/small-modular-reactors/siting-canadas-first-smr/> (Accessed on 3-August-2021).
- [47] Ultra Safe Nuclear, “MMR energy system,” [Online]. Available: <https://usnc.com/mmr-energy-system/> (Accessed on 3-August-2021).
- [48] F. Chen, Y. Dong, and Z. Zhang, “Temperature response of the HTR-10 during the power ascension test,” *Science and Technology of Nuclear Installations*, vol. 2015, 2015.
- [49] H. Bowers, “X-energy Xe-100 reactor: Initial NRC meeting,” X-Energy, Greenbelt, MD, USA, 2018. [Online]. Available: <https://adamswebsearch2.nrc.gov/webSearch2/main.jsp?AccessionNumber=ML18>

253A109 (Accessed on 3-August-2021).

- [50] E. J. Mulder and W. A. Boyes, “Neutronics characteristics of a 165 MWth Xe-100 reactor,” *Nuclear Engineering and Design*, vol. 357, p. 110415, 2020.
- [51] Z. Zhang, Z. Wu, Y. Sun, and F. Li, “Design aspects of the Chinese modular high-temperature gas-cooled reactor HTR-PM,” *Nuclear Engineering and Design*, vol. 236, pp. 485–490, 2006.
- [52] H. Li, X. Huang, and L. Zhang, “A simplified mathematical dynamic model of the HTR-10 high temperature gas-cooled reactor with control system design purposes,” *Annals of Nuclear Energy*, vol. 35, no. 9, pp. 1642–1651, 2008.
- [53] H. Li, X. Huang, and L. Zhang, “A lumped parameter dynamic model of the helical coiled once-through steam generator with movable boundaries,” *Nuclear Engineering and Design*, vol. 238, no. 7, pp. 1657–1663, 2008.
- [54] IAEA, “Evaluation of high-temperature gas cooled reactor performance: Benchmark analysis related to initial testing of the HTTR and HTR-10,” Vienna, Austria, 2003.
- [55] Y. Brits, F. Botha, H. van Antwerpen, and H. W. Chi, “A control approach investigation of the Xe-100 plant to perform load following within the operational range of 100 – 25 – 100%,” *Nuclear Engineering and Design*, vol. 329, pp. 12–19, Apr. 2018.
- [56] M. Brenna, M. Longo, W. Yaici, and T. D. Abegaz, “Simulation and optimization of integration of hybrid renewable energy sources and storages for remote communities electrification,” in 2017 IEEE PES Innovative Smart Grid Technologies Conference Europe (ISGT-Europe), Torino, Italy, Sept. 2017.
- [57] O. Hafez and K. Bhattacharya, “Optimal planning and design of a renewable energy based supply system for microgrids,” *Renewable Energy*, vol. 45, pp. 7–15, Sept. 2012.

- [58] J. Jurasz, M. Guezgouz, P. E. Campana, and A. Kies, “On the impact of load profile data on the optimization results of off-grid energy systems,” *Renewable and Sustainable Energy Reviews*, vol. 159, no, pp. 112199, May 2022.
- [59] Homer Energy, “HOMER Pro Version 3.7 User Manual,” [Online]. Available: <http://www.homerenergy.com/pdf/HOMERHelpManual.pdf> (Accessed on 13-Oct-2020).
- [60] M. Freire-Gormaly and A. M. Bilton, “Optimization of renewable energy power systems for remote communities,” in ASME 2015 International Design Engineering Technical Conferences and Computers and Information in Engineering Conference, Boston, MA, USA, Aug. 2015.
- [61] NREL, “PVWatts Calculator,” [Online]. Available: <https://pvwatts.nrel.gov/> (Accessed on 13-Oct-2020).
- [62] A. P. Dobos, “PVWatts Version 5 Manual,” 2014. [Online]. Available: <https://www.nrel.gov/docs/fy14osti/62641.pdf> (Accessed on 13-Oct-2020).
- [63] A. Gagné, D. Turcotte, N. Goswamy, and Y. Poissant, “High resolution characterisation of solar variability for two sites in eastern Canada,” *Solar Energy*, vol. 137, pp. 46–54, 2016.
- [64] D. Bose, S. Banerjee, M. Kumar, P. P. Marathe, S. Mukhopadhyay, and A. Gupta, “An interval approach to nonlinear controller design for load-following operation of a small modular pressurized water reactor,” *IEEE Transactions on Nuclear Science*, vol. 64, no. 9, pp. 2474–2488, 2017.
- [65] M. Green, P. Sabharwall, M. G. Mckellar, S. Yoon, C. Abel, B. Petrovic, and D. Curtis, “Nuclear hybrid energy system: Molten salt energy storage,” INL/EXT-13-31768, Idaho National Laboratory ,Idaho Falls, ID, USA, 2013.
- [66] Y. Cengel and M. Boles, *Thermodynamics: An Engineering Approach*, 8th ed. New York, USA: McGraw Hill Education, 2015.

- [67] Z. Gao and L. Shi, “Thermal hydraulic calculation of the HTR-10 for the initial and equilibrium core,” *Nuclear Engineering and Design*, vol. 218, no. 1–3, pp. 51–64, 2002.
- [68] B. Poudel, K. Joshi, and R. Gokaraju, “A dynamic model of small modular reactor based nuclear plant for power system studies,” *IEEE Transactions on Energy Conversion*, vol. 35, no. 2, pp. 977–985, 2020.
- [69] A. M. Gandrik, B. W. Wallace, M. W. Patterson, and P. Mills, “Assessment of high temperature gas-cooled reactor (HTGR) capital and operating costs,” TEV-1196, Idaho National Laboratory, Idaho Falls, ID, USA, 2012.
- [70] G. Glatzmaier, “Developing a cost model and methodology to estimate capital costs for thermal energy storage,” NREL/TP-5500-53066, National Renewable Energy Laboratory, Golden, CO, USA, 2011.

## Appendices

### Appendix A: Steam Cycle. This appendix presents the model calculations for the steam power cycle.

This analysis will describe an ideal simple Rankine cycle without reheat. The major components of this steam cycle include four components: steam generator, turbine, condenser, and feedwater pump, and four states between these components shown in Figure A-1. The state of the steam/water and the associated temperature and pressure are summarized in Table A-1.

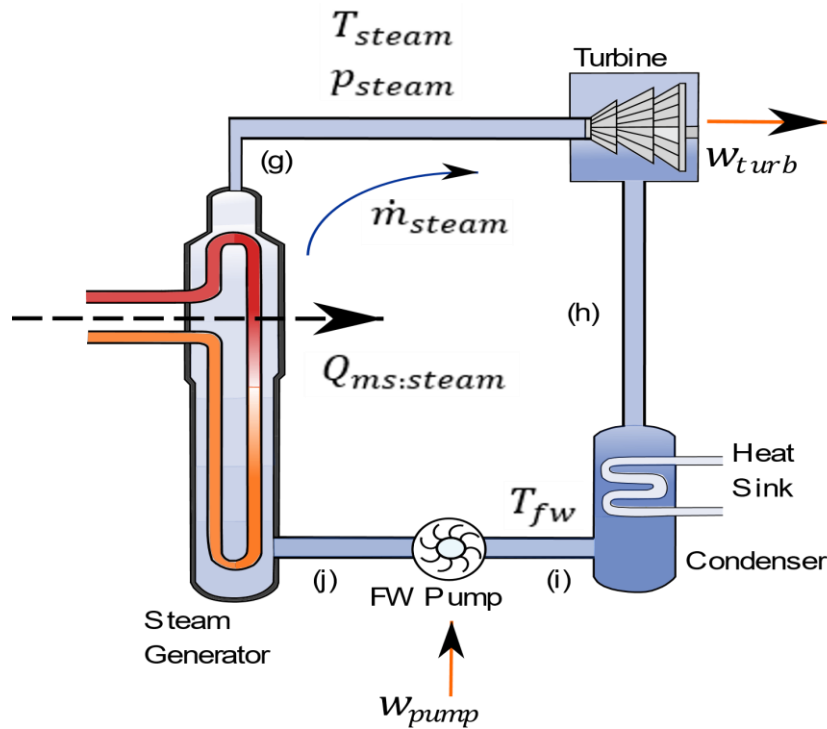


Figure A-1 Steam power cycle schematic

Table A-1 Conditions of steam/water around power cycle

Position	State	Temperature (°C)	Pressure (MPa)
g	Superheated steam	440	4.0
h	Saturated mixture	92	0.075
i	Saturated liquid	92	0.075
j	Compressed liquid	104	4.0

Steady-state thermodynamic parameters at these four points can be calculated for this cycle through energy analysis. This was done following the process from [58]. The assumption is that the steam generator and condenser do not involve any work, and the pump and the turbine are isentropic.

Let  $h$  represent the specific enthalpy in kJ/kg, let  $w$  represent the net work of a component in kJ/kg, let  $q$  represent the heat transfer rate between components in kJ/kg and let  $Q$  represent the heat transfer rate in kW.

First, the enthalpy and entropy at the four points around this power cycle are determined from the process from [58]. The calculated values are summarized in Table A-2 with an explanation explained below.

**Table A-2 Thermodynamic properties at states around power cycle**

Position	Enthalpy (kJ/kg)	Entropy (kJ/(kg· °C))
g	3331.2	6.9386
h	2473.6	6.9386
i	384.44	1.2132
j	388.55	1.2132

### Position g

This state is superheated steam at 440 °C and 4 MPa. The enthalpy  $h_g$  and entropy  $s_g$  from saturated steam tables are the following (Table A-6):

$$g: \begin{cases} h_g = 3331.2 \frac{\text{kJ}}{\text{kg}} \\ s_g = 6.9386 \frac{\text{kJ}}{\text{kg} \cdot \text{K}} \end{cases} \quad (\text{A.1})$$

### Position h

It is assumed that this state is a saturated mixture at pressure  $p_h$  of 0.075 MPa. The enthalpy at point h is the same as point g:

$$s_h = s_g = 6.9386 \frac{\text{kJ}}{\text{kg} \cdot \text{K}} \quad (\text{A.2})$$

The quality of the steam/water mixture at point h is determined from:

$$x_h = \frac{s_h - s_F}{s_{FG}} \quad (\text{A.3})$$

where  $s_F$  is the entropy of saturated liquid with a value of 1.2132 kJ/(kg·K) and  $s_{FG}$  is the entropy of evaporation with a value of 6.2426 kJ/(kg·K) from saturated water table (Table A-4). The quality of the steam/water mixture at this point is:

$$x_h = \frac{6.9386 - 1.2132}{6.2426} = 0.9171 \quad (\text{A.4})$$

The enthalpy at point H is determined from the following based on the steam quality:

$$h_h = h_F + x_h * h_{FG} \quad (\text{A.5})$$

where  $h_F$  is the enthalpy of saturated liquid with a value of 384.44 kJ/kg and  $h_{FG}$  is the enthalpy of evaporation with a value of 2278.0 kJ/kg. The enthalpy at point h is:

$$h_h = 384.44 + (0.9171 * 2278.0) = 2473.6 \frac{\text{kJ}}{\text{kg}} \quad (\text{A.6})$$

### Position i

It is assumed that this state is a saturated liquid with pressure  $p_i$  of 0.075 MPa. This correlates to enthalpy  $h_i$  and entropy  $s_i$  of:

$$\begin{cases} h_g = 384.44 \frac{\text{kJ}}{\text{kg}} \\ s_g = 1.2132 \frac{\text{kJ}}{\text{kg} \cdot \text{K}} \end{cases} \quad (\text{A.7})$$

The specific volume of the saturated liquid  $v_i$  in m<sup>3</sup>/kg at the above conditions is:

$$v_i = 0.001048 \frac{\text{m}^3}{\text{kg}} \quad (\text{A.8})$$

### Position j

The pressure at state j is 4 MPa, and there is no enthalpy change from state i. The enthalpy  $h_j$  is based on the work consumed from the pump  $w_{pump}$  in kJ/kg, which can be calculated as:

$$w_{pump} = v_i(P_j - P_i) \quad (\text{A.9})$$

$$w_{pump} = 0.001048 \frac{\text{m}^3}{\text{kg}} * (4000 - 75) \text{kPa} * \left( \frac{1 \text{kJ}}{1 \text{kPa} \cdot \text{m}^3} \right) = 4.1134 \frac{\text{kJ}}{\text{kg}} \quad (\text{A.10})$$

The enthalpy at point J can be determined from:

$$h_j = h_i + w_{pump} \quad (\text{A.11})$$

$$h_j = (384.44 + 4.1134) \frac{\text{kJ}}{\text{kg}} = 388.55 \frac{\text{kJ}}{\text{kg}} \quad (\text{A.12})$$

## Total Cycle

The heat transfer (into the power cycle) across the steam generator per unit mass can be determined based on the differences in enthalpies across the steam generator:

$$q_{ms:steam} = h_g - h_j = 3331.2 - 388.55 = 2943 \frac{kJ}{kg} \quad (A.13)$$

The heat transfer rejected to the condenser can be determined based on the differences in enthalpies across the condenser:

$$q_{out} = h_h - h_i = 2473.6 - 384.44 = 2089.16 \frac{kJ}{kg} \quad (A.14)$$

The thermal efficiency of the power cycle is based on the difference in heat rates and can be determined by:

$$\eta_{th} = 1 - \frac{q_{out}}{q_{ms:steam}} = 1 - \frac{2089.16}{2942.65} = 0.29 \quad (A.15)$$

## Output

The work done in the turbine  $w_{turb}$  in kJ/kg is described by:

$$w_{turb} = h_g - h_h = 3331.2 - 2473.6 = 858 \text{ kJ/kg} \quad (A.16)$$

The output power by the power cycle  $P_{out}$  in kW is described by:

$$P_{out} = \dot{m}_{steam} * w_{turb} \quad (A.17)$$

## Example

The relationship between the electrical output and core thermal production rate is:

$$\eta_{th} = \frac{P_{out}}{Q_{core}} \quad (A.18)$$

For example, when  $P_{out}$  is 3000 kW, the required core thermal power production From Eq. (A.18) is:

$$Q_{SMR} = \frac{P_{out}}{\eta_{th}} = \frac{3000 \text{ kW}}{0.29} = 10350 \text{ kW}_{th} \quad (A.19)$$

The required steam flow through the turbine can be determined from Eq. (A.17):

$$\dot{m}_{steam} = \frac{P_{out}}{w_{turb}} = \frac{3000 \text{ kW}}{857.6 \frac{kJ}{kg}} = 3.5 \text{ kg/s} \quad (A.20)$$

For verification, given the value of  $q_{ms:steam}$  from Eq. (A.13), the total heat transfer rate across the steam generator can be calculated from:

$$Q_{ms:steam} = q_{ms:steam} * \dot{m}_{steam} = 2942.65 \frac{kJ}{kg} * 3.5 \frac{kg}{s} = 10300 kW \quad (A.21)$$

which is in close agreement with the calculated value of  $Q_{SMR}$  from Eq. (A.19).

**Appendix B: Simulations. This appendix presents the calculations and process for the steady-state and dynamical simulations**

**Steady-State Analysis**

The steady-state analysis is conducted through simulations in Microsoft Excel. The timestep index  $k = 0..23$  is selected over one day at a one-hour timestep for each run of the simulation.

For demand,  $L_{avg}[k]$  is the input timeseries to represent the average daily demand profile that occurs in the winter month corresponding to the maximum demand period. Based on the value of the selected timestep variation parameter  $\sigma_s$ , the lower bound  $\underline{L}[k]$  and upper bounds  $\overline{L}[k]$  around the average demand are determined. The upper bound is selected as the input demand to this analysis.

For PV,  $\overline{G}[k]$  is an input solar irradiance timeseries based on the community location and the associated data from the PVWatts calculator. The nominal solar irradiance curve is the maximum solar irradiance corresponding to the winter month. The size of the PV system  $P_{PV}^{Size}$  in kW is selected for each run of the simulation as well as the PV system efficiency  $\eta_{PV}$ . The nominal output of the PV system at each timestep is calculated from:

$$P_{PV}[k] = P_{PV}^{Size} * \frac{G[k]}{1000} * \eta_{PV}, \forall k \quad (\text{B.1})$$

The net demand between the load and PV is calculated at each timestep by:

$$P_{net}[k] = \overline{L}[k] - P_{PV}[k] \quad (\text{B.2})$$

The SMR-TES system should be able to follow the net demand over long time periods due to sufficient ramp rate limits so that EES is not required in this simulation.

The SMR sizing selections are the SMR core thermal power rating defined as  $Q_{SMR}$  in kW<sub>th</sub> and the BOP size defined as  $P_{BOP}^{Size}$  in kW. The SMR core thermal power rating can be mapped to an equivalent electrical power rating defined as  $P_{SMR}^{Size}$  in kW. The relation can be described by:

$$\eta_{SMR} = \frac{P_{SMR}}{Q_{SMR}} \quad (B.3)$$

where  $\eta_{SMR}$  is the total efficiency of the SMR system including the steam power cycle. When the SMR-TES system follows the net demand, the total output  $P_{out}[k]$  is set as the net demand.

The following equations are calculated at each timestep to describe the operation of the SMR-TES system.

First, assuming that the SMR core will operate at constant power during the period of maximum demand, the helium mass flow rate through the core will be constant and calculated by:

$$\dot{m}_{he} = \frac{Q_{SMR}}{c_{p,he} \Delta T_{he}} \quad (B.4)$$

Within the power cycle, the required steam mass flow at each timestep is calculated by:

$$\dot{m}_{steam}[k] = \frac{P_{out}[k]}{w_{turb}} \quad (B.5)$$

with  $w_{turb} = \Delta h_{turbine} = 858$  kJ/kg. There are upper and lower limits to the steam mass flow rate. The upper limit is based on the turbine rating that is set by:

$$\overline{\dot{m}_{steam}} = \frac{P_{BOP}^{size}}{w_{turb}} \quad (B.6)$$

and the lower limit can be near zero. This sets the allowable limits of the steam flow rate through the simulation as  $0 \leq \dot{m}_{steam}[k] \leq \overline{\dot{m}_{steam}}$ .

With varying power output from the steam cycle, the required heat rate into the steam cycle varies and is calculated by:

$$Q_{ms:steam}[k] = q_{ms:steam} * \dot{m}_{steam}[k] \quad (B.7)$$

with  $q_{ms:steam} = \Delta h_{SG} = 2943$  kJ/kg. This heat transfer rate  $Q_{ms:steam}[k]$  is required from the molten salt intermediate loop and specifically from the hot tank outlet mass flow rate to be calculated by:

$$Q_{ms:steam}[k] = \dot{m}_{HT,out}[k] * c_{p,ms} * \Delta T_{ms} \rightarrow \dot{m}_{HT,out}[k] = \frac{Q_{ms:steam}[k]}{c_{p,ms} * \Delta T_{ms}} \quad (B.8)$$

Between the helium coolant and the molten salt storage loop, the heat transfer rate is described, which can be used to calculate the outlet mass flow rate of the cold tank:

$$\dot{m}_{CT,out} = \dot{m}_{he} * \frac{c_{p,he} * \Delta T_{he}}{c_{p,ms} * \Delta T_{ms}} \quad (B.9)$$

The coordination between the inlet and outlet flows of the hot and cold tank are calculated by:

$$\dot{m}_{HT,out}[k] = \dot{m}_{CT,in}[k] \quad (B.10)$$

$$\dot{m}_{CT,out}[k] = \dot{m}_{HT,in}[k]$$

The mass in the tanks at each timestep is calculated based on the mass in the previous step and the net mass flow rate which is calculated by:

$$m_{HT}[k] = m_{HT}[k-1] + (\dot{m}_{HT,in}[k] - \dot{m}_{HT,out}[k]) * \Delta k \quad (B.11)$$

$$m_{CT}[k] = m_{CT}[k-1] + (\dot{m}_{CT,in}[k] - \dot{m}_{CT,out}[k]) * \Delta k$$

with selected  $m_{HT}[0]$  and  $m_{CT}[0]$  and the condition that  $m_{HT}[k] > 0$  and  $m_{CT}[k] > 0$ .

The required mass  $m_{TES}^{size}$  is calculated from:

$$m_{TES}^{size} = m_{HT}[k] + m_{CT}[k] \quad (B.12)$$

since there is mass conservation in each step. If the SMR cannot meet the net demand, the remaining power is met by the EES system that is calculated by:

$$P_{EES}[k] = L[k] - (P_{SMR}[k] + P_{PV}[k]), \forall k \quad (B.13)$$

### **Dynamical Analysis**

The same community demand and PV characteristics from the steady-state analysis is used in this dynamical analysis.

The timeseries demand polynomial is scaled by a perturbation factor  $\alpha[k]$  that is drawn from a random variable  $\delta_s[k]$  that is described from a normal random variable as:

$$\delta_s \sim N\left(0, \frac{\sigma_s}{L_{Max}}\right)$$

Limits can be applied to the allowable limits on the random number  $\delta_s$  so that the synthetic demand is contained within the desired lower and upper limits.

The perturbation factor is calculated at each timestep as:

$$\alpha[k] = 1 + \delta_s[k], \forall k \quad (\text{B.14})$$

$$L[k] = L_{avg}[k] * \alpha[k], \forall k \quad (\text{B.15})$$

Desired ramp rate limits (in  $\%L_{max}/s$ ) can be applied to the synthetic output  $L[k]$ .

For PV,  $\bar{G}[k]$  is an input solar irradiance timeseries based on the community location and the associated data from the PVWatts calculator that is the same from the steady-state analysis. The nominal solar irradiance is scaled from a uniform distribution that can be described by:

$$\delta_{PV} \sim U(0,1) \quad (\text{B.16})$$

From this, the actual synthetic solar irradiance is scaled by this random variable by:

$$G[k] = \bar{G}[k] * \delta_{PV}[k], \forall k \quad (\text{B.17})$$

Then the synthetic PV output is calculated by:

$$P_{PV}[k] = P_{PV}^{Size} * \frac{G[k]}{1000} * \eta_{PV} \quad (\text{B.18})$$

Desired ramp rate limits (in  $\%P_{PV}^{Size}/s$ ) can be applied to the synthetic output  $P_{PV}$ .

For the operation of the SMR and EES, the net demand is calculated by:

$$P_{net}[k] = L[k] - P_{PV}[k] \quad (\text{B.19})$$

The value is applied to the SMR output ( $P_{out}$ ), but there are ramp rates applied to the allowable rates of change in the SMR output. The combined output from the PV and the actual output of the SMR is defined as  $P_{gen}[k]$  and is defined as:

$$P_{Pv}[k] + P_{out}[k] = P_{gen}[k] \quad (\text{B.20})$$

With the EES power calculated by:

$$P_{EES}[k] = L[k] - P_{gen}[k] \quad (\text{B.21})$$

The energy stored in the EES over time is based on the Simulink integrator function.

## Curriculum Vitae

**Name:** Michael Davis

**Post-secondary Education and Degrees:** University of Western Ontario  
London, Ontario, Canada  
2020-2022 M.E.Sc. (Electrical & Computer Engineering)

University of Ontario Institute of Technology  
Oshawa, Ontario, Canada  
2015-2020 B.Eng. (Nuclear Engineering)

**Honours and Awards:** Hydro One Graduate Scholarship  
2021

Canadian Nuclear Society Graduate Entrance Scholarship  
2020

**Related Work Experience:** Teaching Assistant  
The University of Western Ontario  
2020-2021

Engineering Internship  
Ontario Power Generation  
2018-2019

**Publication:**

M. Davis and J. Jiang, "Configuration and sizing of small modular reactor with thermal energy storage for off-grid communities," Renewable and Sustainable Energy Reviews (Submitted on August 30, 2022).